ABSTRACT

Title of dissertation: STRUCTURAL CHARACTERIZATION OF METAL AND DNA BINDING TO DREAM PROTEIN, A CALCIUM SENSING TRANSCRIPTIONAL REPRESSOR IN PAIN MODULATION

Aswani Kumar Valiveti, Doctor of Philosophy, 2006

Dissertation directed by: Dr. James. B. Ames

Center for Advanced Research in Biotechnology

DREAM (**D**ownstream **R**egulatory **E**lement **A**ntagonistic **M**odulator) is the first reported calcium binding protein that directly binds to DNA and affects gene expression. It belongs to recoverin sub-family of neuronal calcium sensing proteins that form part of EF- hand super-family. Knockout mice, devoid of DREAM protein, exhibit ongoing analgesia due to upregulated expression of the prodynorphin gene. DREAM binds to a specific DNA silencing element in the prodynorphin promoter called Downstream Regulatory Element (DRE) and serves as a transcriptional repressor under basal resting conditions. Neuronal stimulation leads to a rise in nuclear calcium, causing Ca^{++}-bound DREAM to dissociate from DNA and result in derepression of prodynorphin expression.

Thus, DREAM may serve as a potentially specific target for effective pain management. Understanding the structural determinants of metal binding and DNA recognition by DREAM may help in the future rational design of analgesic drugs.

In this thesis, the calcium and magnesium binding properties of DREAM were studied by performing isothermal titration calorimetry (ITC) analysis on wild-type DREAM protein and mutants that have each of the functional EF hands disabled for calcium binding. Our results show that DREAM binds two Ca^{++} ions and one Mg^{++} ion with high affinity. Mg^{++}-bound DREAM is stable as a monomer and Ca^{++}-bound DREAM exists as a dimer. Calcium binding stabilizes the protein structure and promotes dimerization to control calcium-sensitive recognition of DNA targets. Next, we attempted to map the DNA binding residues in DREAM and its oligomerization interface using biophysical and functional characterization of chimeric protein constructs generated by swapping specific EF-hand motifs of DREAM protein with those of recoverin. Nuclear magnetic resonance (NMR), gel-filtration and electrophoretic mobility shift assays were employed for this purpose. The results from this study suggest that both the amino and carboxy terminal halves of the protein are important for DNA binding and dimerization of DREAM protein. All four EF-hands in DREAM appear to participate in the recognition of DNA.

STRUCTURAL CHARACTERIZATION OF METAL AND DNA BINDING TO DREAM PROTEIN, A CALCIUM SENSING TRANSCRIPTIONAL REPRESSOR IN PAIN MODULATION

By

Aswani Kumar Valiveti

Dissertation submitted to the Faculty of the Graduate School of the
University of Maryland, College Park, in partial fulfillment
of the requirements for the degree of
Doctor of Philosophy
2006

Advisory Committee:

Professor. Douglas Julin, Chairman
Dr. James. B. Ames, Advisor
Professor. Sandra Greer, Dean's Representative
Dr. Harold Smith
Dr. Leslie Pick

Dedication

To my mentors during graduate study-

Dr. Masanori Osawa

Dr. Alexandra Dace

Dr. James. B. Ames

Acknowledgements

I would like express my profound gratitude to my advisor Dr. James. B. Ames for the support and guidance obtained throughout my graduate study. His cogent scientific thinking and articulate verbal and written communication skills are the qualities I hope to emulate during the course of my scientific career.

I sincerely wish to thank my thesis advisory committee members for the duration of my graduate study, Drs Doug Julin, Eric Baehrecke, Harold Smith and Bill Higgins for their critical evaluation of my work, valuable ideas and support. Special thanks are due, to Dr. Leslie Pick and Professor Sandra Greer for their generous understanding and willingness to replace Drs Eric Baehrecke and Bill Higgins respectively, on the committee, who had to withdraw for my defense due to scheduling conflicts.

I would like to thank past and present members of the Ames' lab- Masanori, without whose generous guidance and constant encouragement, during the initial phase of my PhD, this thesis would have been a distant DREAM; Nobuko, for her kind advice and support throughout my study; Alexandra for all the help during the final stages; Jennifer Wingard for the enjoyable company. I would also like to thank colleagues at CARB, especially members of third floor of CARB-IB, Fred Schwarz and lab members, for assistance with using ITC, Zvi Kelman, Harold Smith and their lab members especially JaeHo and Antonio, for their helpful discussions during the third floor lab meetings.

Special thanks to Eugene, Buvna and Celia Chen for their help with structural modeling and bio-informatics, and Vivek Gopalan for help with MS Word formatting when needed.

I take this opportunity to thank my parents for all their hard work, sacrifices and prayers that were directed towards my success as a human being and in my educational pursuit. I thank my immediate family- my brother Kittu, sister Latha and brother-in-law Narasimham and everyone in my extended family for being there and praying for my success. I thank my friends Subbu, Jinu, Lisa, Ajjai, Chandu, Nandha, Anil and Arun for their friendship, support and company, which helped me get through some tough times and made the rest enjoyable, during my current stay in the United States. I would like to express special and sincere thanks to my cousin Shanker whose support, being my roommate and close-confidant, was indispensable during the later stages of my graduate study.

Finally, I would like to acknowledge the super-natural force that drives me towards embarking on this journey and pursuing it with diligence and will power.

Table of contents

Figure Index

Table Index

Abbreviations

3-AT	-	3 aminotriazole
ADP	-	Adenosine di-phosphate
APS	-	Ammonium per sulfate
ATP	-	Adenosine tri-phosphate
cADPR	-	Cyclic adenosine di-phosphate ribose
cAMP	-	Cyclic adenosine mono-phosphate
CAT	-	Chloramphenicol acetyl transferase
CREB	-	Cyclic AMP response element binding protein
CREM	-	Cyclic AMP response element Modulator
CtBP	-	C-terminal binding protein
DEAE	-	Diethyl aminoethyl group
DNA	-	Deoxy ribonucleic acid
DRC	-	DREAM-recoverin chimeras
DRE	-	Downstream regulatory element
DREAM	-	Downstream regulatory element antogonistic modulator
EDTA	-	Ethylene di-amine tetra-acetate
ELISA	-	Enzyme linked immunosorbent assay
EMSA	-	Electrophoretic mobility shift assay
ER	-	Endoplasmic reticulum
GCAP	-	Guanylate cyclase activating protein
GR	-	Glucocorticoid receptor
HCl	-	Hydrochloric acid
IP3	-	Inositol 1,4,5 tris-phosphate
ITC	-	Isothermal titration calorimetry
KChIP	-	Potassium channel interacting protein
LTP	-	Longterm potentiation
NA	-	Nicotinic acid

NAADP	-	Nicotinic acid adenine di-nucleotide phosphate
NaCl	-	Sodium Chloride
NCS	-	Neuronal calcium sensor
NMR	-	Nuclear magnetic resonance
PAGE	-	Polyacrylamide gel electrophoresis
PDB	-	Protein data bank
PLC	-	Phospholipase C
RNA	-	Ribonucleic acid
SDS	-	Sodium dodecyl sulphate
SEC	-	Size exclusion chromatography
YPAD media	-	Yeast extract peptone adenine dextrose media

Chapter 1: Calcium Signaling and Regulation of Gene Expression

1.1 Introduction

Living cells need to communicate with the environment in order to adapt or respond to external stimuli. An external stimulus acts as a signal that elicits a specific response from the cell. Thus, the external signal is a first messenger that activates a cell's response and the primary component inside the cell that triggers the response is called a second messenger [1]. The process of communication between a cell and its external environment through stimulus derived intracellular messengers is called signal transduction. Intracellular messengers are often small molecules such as cAMP [2] , inositol 1, 4, 5, tris phosphate (IP3) [3] and metal ions such as Ca^{++} [4] and Mg^{++} [5]. The salient feature of a second messenger is that its resting levels in the cell are low and there are specific "on" mechanisms that generate the messenger in sufficient amount, in response to the stimulus-derived signal, and "off" mechanisms that help in clearing the messenger once it has carried out its function. Such "on" and "off" mechanisms help in generating the messenger to transmit the signal and clearing it once the signal processing is complete [4], (fig.1-1) and also help in maintaining a steady levels of messenger in the cell, also called homeostasis (Greek: homoios: same; stasis: stand [6]).

1.2 Calcium as a biological messenger

In 1883, Ringer first attributed a regulatory role for calcium inside the cell (Reviewed in [7]). In his classic perfusion experiments with isolated frog heart, he observed that adding calcium salts to distilled water keeps the heart beating longer than when in distilled water

alone. Ringer's experiments paved the way for a generation of researchers whose work provided compelling evidence that favors the idea that calcium can regulate cellular processes and is not merely a structural component being a constituent of bone [8]. L. V. Heilbrunn and K Bailey have independently shown that calcium affects the components of muscle contraction. Heilbrunn applied calcium to the cut end of a muscle and observed a contraction, while K. Bailey discovered that ATPase activity of myosin is promoted by calcium but not magnesium ([9], reviewed in [8]). Further evidence from the studies on muscle contraction, upon membrane depolarization, also referred as excitation-contraction coupling [10, 11] and the discovery of calcium transport system in the cell [12-14] confirmed the importance of calcium as a signal. The role of calcium in excitation-contraction coupling was first demonstrated when isolated muscle fibers soaked in calcium free medium do not show a mechanical response upon membrane depolarization as against medium containing calcium (discussed in [10]). Furthermore, Hasselbach and Makinose observed that isolated vesicles of sarcoplasmic reticulum store calcium transported from the surrounding medium in a magnesium and ATP dependent manner (discussed in [12]).

Extending the above mentioned studies, along with several others (reviewed in [15]), Howard Rasmussen proposed a second messenger function to calcium [15, 16]. Indeed, calcium is shown to serve as second messenger in processes such as egg fertilization [17, 18], neurotransmitter release [19] and cell death [20]. That calcium is a universal signaling messenger was confirmed, from reports that identify calcium in a signaling role in bacteria and plants as well. Resting calcium levels in bacteria are in the nanomolar range, but increase in cytosolic calcium occurs in response to signals such as starvation

[21, 22]. Bacteria also contain calcium binding proteins [23] and calcium transporters [24] that maintain calcium homeostasis (see section 1.3). Calcium regulates various processes such as cell maintenance, motility, cell division, gene expression and sporulation of bacteria [22, 23]. Several external stimuli such as light, stress and wind trigger an increase in cytosolic calcium in plant cells [25, 26]. Thus, calcium plays an important role not only as a nutritional requirement, by virtue of its involvement in bone growth in animals [27] and cell wall development in plants [28] but also as a signaling component [7, 28, 29]. Likewise, in animals, calcium was shown to regulate cellular pathways ranging from cell proliferation [30] to cell death [20, 31] and several other processes such as motility [32, 33] and secretion [34] in between. Thus, the small size of Ca^{++} ion, the presence of well organized transport systems that can transport Ca^{++} into and outside the cell (see section 1.3), and the ability to form coordination complexes with varying coordination numbers (six-eight), make calcium an ideal second messenger [7] .

1.3 Calcium homeostasis

Cytosolic calcium levels (and nuclear calcium) are determined by a dynamic balance between uptake and release processes that transport Ca^{++} into the cytosol (and cell nucleus) from the cell exterior and/or internal stores (e.g. endoplasmic reticulum and or related organelles, fig.1-1, 1-3) and vice-versa [4, 35]. In mammals, basal levels of cytosolic/nuclear Ca^{++} are in the nanomolar (10^{-9} M) range [36, 37] as is the case with lower organisms such as yeast [37], compared to milli molar (10^{-3} M) range in the cell exterior and internal stores [38]. The large concentration gradient of Ca^{++} between cytosol and cell exterior is maintained with the help of Ca^{++}-ATPase pumps that utilize

energy in the form of ATP to transport calcium from the cytosol into the ER lumen and/or cell exterior [39] (fig (1-1, 1-3). Various ion exchangers [40] and a mitochondrial calcium uniporter [41] also assist in transporting calcium out of the cytosol (fig.1-1, 1-3) [4, 42]. Nuclear calcium has been shown to be in equilibrium with cytosolic calcium due to its diffusion through nuclear pores [35, 43]. However, recent studies suggest there may be an independent signaling network that regulates nuclear calcium levels as well [44, 45].

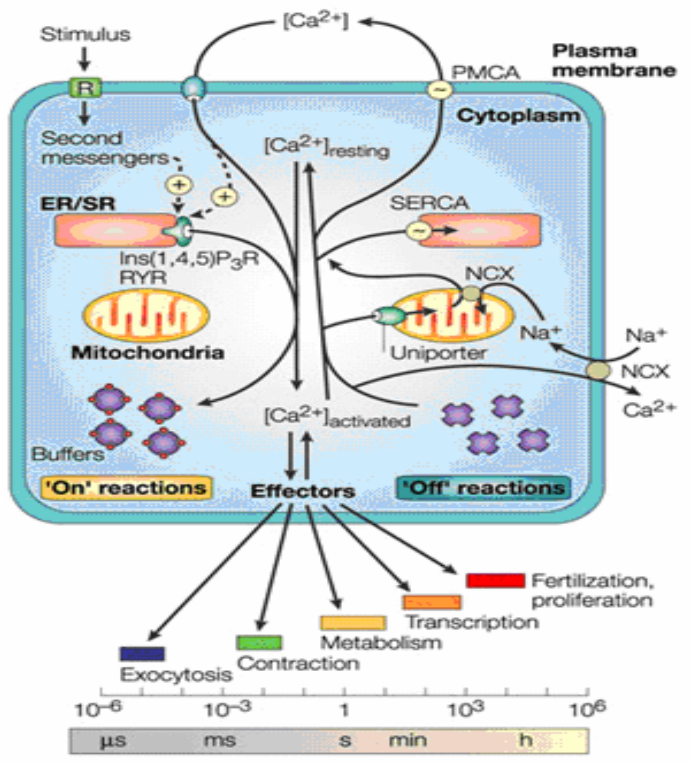

Figure-1-1: Mechanisms responsible for calcium homeostasis in the cell. Examples of processes controlled by calcium-dependent effectors are shown with their respective time scales of occurrence. ER/SR: Endoplasmic reticulum/Sarcoplasmic reticulum; PMCA: Plasma membrane Ca^{++} ATPase; R: receptor; SERCA: sarco/endoplasmic reticulum Ca^{++} ATPase; Ins(1,4,5)P_3R: Inositol 1,4,5 tris phosphate receptor; RYR: Ryanodine receptor; NCX: sodium calcium exchanger. (Figure reproduced from [4])

A transient rise in cytosolic/nuclear Ca^{++} concentration (termed Ca^{++} influx) occurs in excitable cells when ion channels (see [46] for various types of calcium channels) open during membrane depolarization [47] or receptor stimulation that generates second messengers causing the release of calcium from internal stores (fig. 1-1, 1-3). These messengers include inositol 1,4,5-trisphosphate (IP3) [48, 49], sphingosine 1-phosphate [50], cyclic ADP ribose (cADPR) [51], nicotinic acid adenine dinucleotide phosphate (NAADP) [52] and calcium itself through a mechanism called calcium induced calcium release (CICR) [53-55]. IP3 is generated by different isoforms of the enzyme Phospholipase C that are stimulated by different kinds of receptors such as G-protein-coupled receptors (PLCβ), tyrosine-kinase-coupled receptors (PLCγ) (fig.1-3), an increase in Ca^{++} concentration (PLCδ) or activation through Ras (PLCε) (reviewed in [4]). A newly identified isoform of PLC, PLCζ was reported to be injected into the egg by the sperm and is responsible for Ca^{++} oscillations during egg fertilization [56]. IP3 mobilizes calcium through IP3 receptor, an intracellular receptor that acts as a calcium channel on the ER membrane [57] (fig.1-3). Ghosh T. K. and co-workers (1990) have reported that sphingosine 1-phosphate, a cellular metabolite derived from ceramide, can also be a regulator of calcium homeostasis in mammaliam systems [50]. Later it was confirmed to be a regulator of calcium release in yeast and plants [58]. Sphingosine-1-phosphate is synthesized with the help of an enzyme sphingosine kinase that phosphorylates sphingosine derived from sphingolipids [58] and modulates calcium release from ER through a sphingolipid Ca^{++} release-mediating protein of endoplasmic reticulum (SCaMPER) [59] (fig.1-3).

Recently two new second messengers, cADPR (cyclic adenosine diphosphate ribose) and NAADP (nicotinic acid adenine dinucleotide phosphate), were reported to function in increasing calcium levels in the cytosol [60, 61] (fig. 1-2, 1-3). Synthesis of cADPR involves cyclization resulting in the formation of an N-glycoside linkage between the anomeric carbon of the terminal ribose unit and the N^6- amino group of adenine moiety and removal of the nicotinamide group. NAADP synthesis involves a base-exchange reaction where the nicotinamide group in the substrate, NAD (Nicotinamide adenine dinucleotide), is exchanged with nicotinic acid (NA) [62]. Both reactions, synthesis of cADPR and NAADP are catalyzed by the same enzyme ADP ribosyl cyclase. While cADPR modulates Ryanodine receptor on the ER membrane, NAADP mobilizes calcium from the lysosomal reserve granule stores [60] and, through NAADP receptor, from the ER (fig. 1-3).

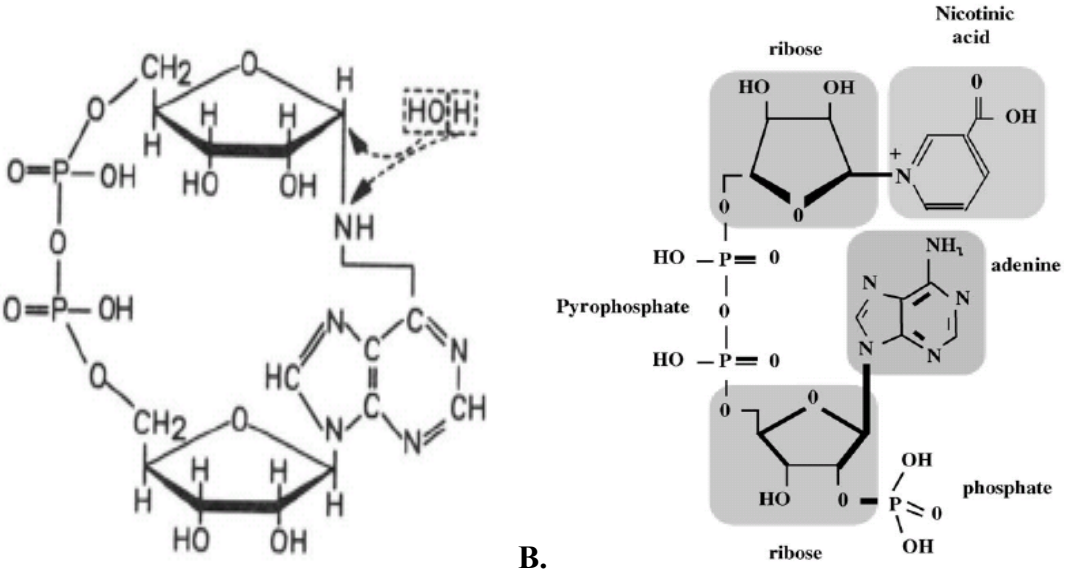

Figure 1-2: Structures of NADP derived messengers of calcium release. (A) cADPR (cyclic adenine diphosphate ribose) and (B) NAADP (Nicotinic acid adenine dinucleotide phosphate).

Cytosolic buffer proteins such as calbindin D-28, Calretinin and parvalbumin (table 1-1) sequester most of the calcium thus released resulting in a small fraction of free calcium binding to effectors (see section1.4) that activate various downstream processes operating over a wide range of timescales (fig.1-1), [4]. The increase in cytosolic free calcium, either slow and sustained or fast and short-lived, in turn translates into a specific cellular output at the level of gene expression [63, 64]. Thus, qualitatively different kinds of cytosolic calcium influx can occur due to the nature of the "on" mechanism operating or due to synergy of calcium signaling with other signaling pathways mediated by cAMP, MAP kinases, nitric oxide synthase (fig.1-3), [65].

The cytosolic/nuclear Ca^{++} concentration returns back to its resting level once receptor stimulation is turned off. "Off" mechanisms utilize Ca^{++}-ATPase pumps [39], exchangers [40] and a mitochondrial calcium uniporter [41] to clear calcium from the cytosol (fig.1-1, 1-3), [4, 42]. The Ca^{++} ATPases on plasma membrane (PMCA) and sarco/endoplasmic reticulum membrane (SERCA) utilize energy in the form of ATP and pump calcium to the cell exterior and into the stores respectively [39] (fig.1-1, 1-3). Sodium calcium exchanger on the plasma membrane utilizes the sodium gradient across the plasma membrane and exchanges three sodium ions to extrude one calcium ion [66] (figs.1-1, 1-3). The sodium thus transported into the cell is cleared using the Na^{+}-K^{+} ATP'ase on the plasma-membrane by utilizing energy in the form of ATP [67]. Mitochondria has a uniporter that uses the electro-chemical gradient resulting from the extrusion of protons and transports calcium into the matrix [42]. Thus, various components of calcium signaling form a "calcium signaling tool-kit" [4, 42], (fig.1-3)

that orchestrates the transmission of calcium signals and their subsequent removal from the cytosol.

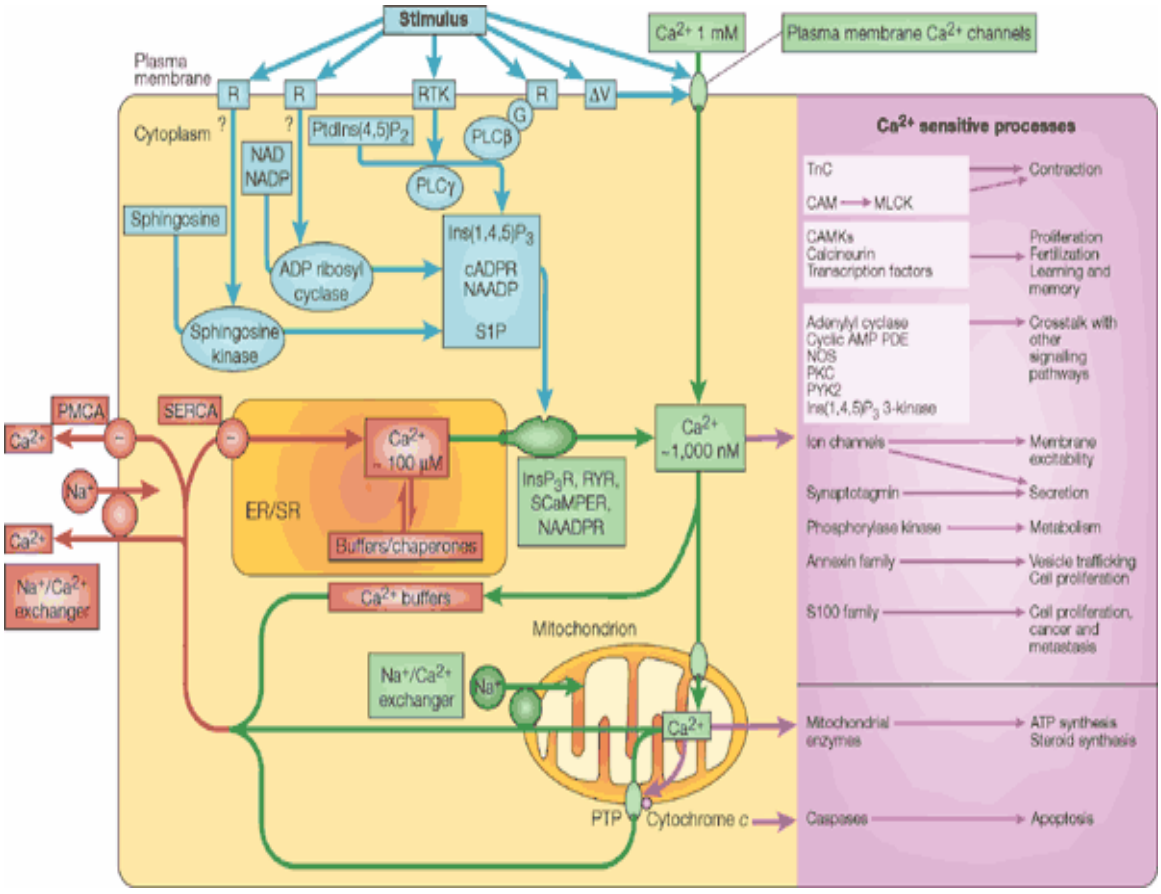

Figure 1-3: Schematic representation of calcium signaling toolkit. Cells have an extensive signaling toolkit that can be mixed and matched to create Ca^{++} signals of widely different properties. Ca^{++}-mobilizing signals (blue) are generated by stimuli acting through a variety of cell-surface receptors (R), including G-protein (G)-linked receptors and receptor tyrosine kinases (RTK). The signals generated include: inositol-1,4,5-trisphosphate ($Ins(1,4,5)P_3$), generated by the hydrolysis of phosphatidylinositol-4,5-bisphosphate ($PtdIns(4,5)P_2$) by a family of phospholipase C enzymes (PLCβ, PLCγ); cyclic ADP ribose (cADPR) and nicotinic acid dinucleotide phosphate (NAADP), both generated from nicotinamide-adenine dinucleotide (NAD) and its phosphorylated derivative NADP by ADP ribosyl cyclase; and sphingosine 1-phosphate (S1P), generated from sphingosine by a sphingosine kinase. ON mechanisms (green) include plasma membrane Ca^{++} channels, which respond to transmitters or to membrane depolarization (ΔV), and intracellular Ca^{++} channels — the $Ins(1,4,5)P_3$ receptor ($InsP_3R$), ryanodine receptor (RYR), NAADP receptor and sphingolipid Ca^{++} release-mediating protein of the ER (SCaMPER). The Ca^{++} released into the cytoplasm by these ON mechanisms activates different Ca^{++} sensors (purple), which augment a wide range of Ca^{++}-sensitive processes (purple), depending on cell type and context. OFF mechanisms (red) pump Ca^{++} out of the cytoplasm: the Na^+/Ca^{++} exchanger and the plasma membrane Ca^{++} ATPase (PMCA) pumps Ca^{++} out of the cell and the sarco-endoplasmic reticulum Ca^{++} ATPase (SERCA) pumps it back into the ER/SR. (TnC, troponin C; CAM, calmodulin; MLCK, myosin light chain kinase; CAMK, Ca^{++}/calmodulin-dependent protein kinase; cyclic AMP PDE, cyclic AMP phosphodiesterase; NOS, nitric oxide synthase; PKC, protein kinase C; PYK2, proline-rich kinase 2; PTP, permeability transition pore.) (Figure and legend reproduced from [42]).

1.4 Intracellular calcium binding proteins

The rise in cytosolic/nuclear calcium concentration during signal transduction triggers a variety of downstream signaling pathways mediated by various calcium-binding proteins (Table-1-1). Calcium binding to these proteins occurs at a local region of the protein and causes global conformational changes that promote its interaction with downstream targets. For, example, calcium binding to EF hands of calmodulin (CaM) promotes its interaction with diverse targets such as protein kinases (CaM kinases), ion channels (calcium-gated K^+ channels), and adenylate cyclase due to metal-induced changes in its conformation (reviewed in [68, 69]). Calcium bound troponinC activates tropomyosin, leading to the exposure of myosin binding sites in the actin filament thereby affecting muscle contraction [70]. Calcium binding to the regulatory subunit of the protein phosphatase, calcineurin promotes the dephosphorylation of a wide range of protein substrates important in neuronal signal transduction [71]. Thus, calcium-binding proteins act on a variety of signaling targets and their calcium-induced conformational changes are coupled to Ca^{++}-binding motifs that stabilize their structural interaction with downstream targets that control a wide variety of processes with different time scales of occurrence (shown in fig 1-1).

Protein	Protein Function
Annexin	Implicated in membrane trafficking, inhibition of PLA2
BoPCAR	G-protein coupled Ca+2 sensing receptor
Ca+2 activated K+ channel	Effector of membrane hyperpolarization
Ca+2 antiporters	Exchangers of Ca+2 for monovalent ions
Ca+2 ATP'ase	Pump of Ca+2 across membranes
Calcineurin B	Phosphatase
Calmodulin	Ubiquitous modulator of protein kinases and other enzymes
Calpain	Protease
Calreticulin	Ca+2 buffer/ modulator of nuclear hormone receptors
Calretinin, retinin, visinin, GCAPs	Activator of guanylyl cyclase
Gelsolin, Villin, α-actinin	Actin- cytoskeletal modulation
Inositolphospholipids-specific PLC	Generates InsP3 and diacylglycerol
InsP3 receptor, Ryanodine receptor	Effectors of intracellular calcium release
KChIPs	Modulators of voltage-gated K+ channels/ transcriptional regulation
Na+/Ca+2 exchanger	Effector of exchange of Ca+2 and Na+ across plasma membrane
Nidogen, nucleobindin, BM-40, COMP	Extracellular calcium binding proteins
Parvalbumin, Calbindin, Calsequestrin	Ca+2 buffer proteins
Phospholipase A2	Producer of Arachidonic acid
Protein Kinase C	Ubiquitous protein kinase
Recoverin	Phototransduction
Troponin C, Caldesmon	Modulators of muscle contraction
S100 proteins	Signal transduction,

Table-1-1: Examples of calcium binding proteins in mammalian cells (adapted from [36], with ref [72], [73], [74], [75]).

1.5 Calcium binding motifs

To date four kinds of calcium binding motifs have been characterized at the atomic level. They are – 1) Annexin domain [76, 77] 2) C2 domain [78-80] 3) C-lectin ([81, 82] and fig.1-5) EF-hand domain [83]. The chief difference between these individual structures is the way in which the calcium ion is coordinated by the negatively charged amino acid side chains of respective proteins (illustrated in figs 1-4, 5).

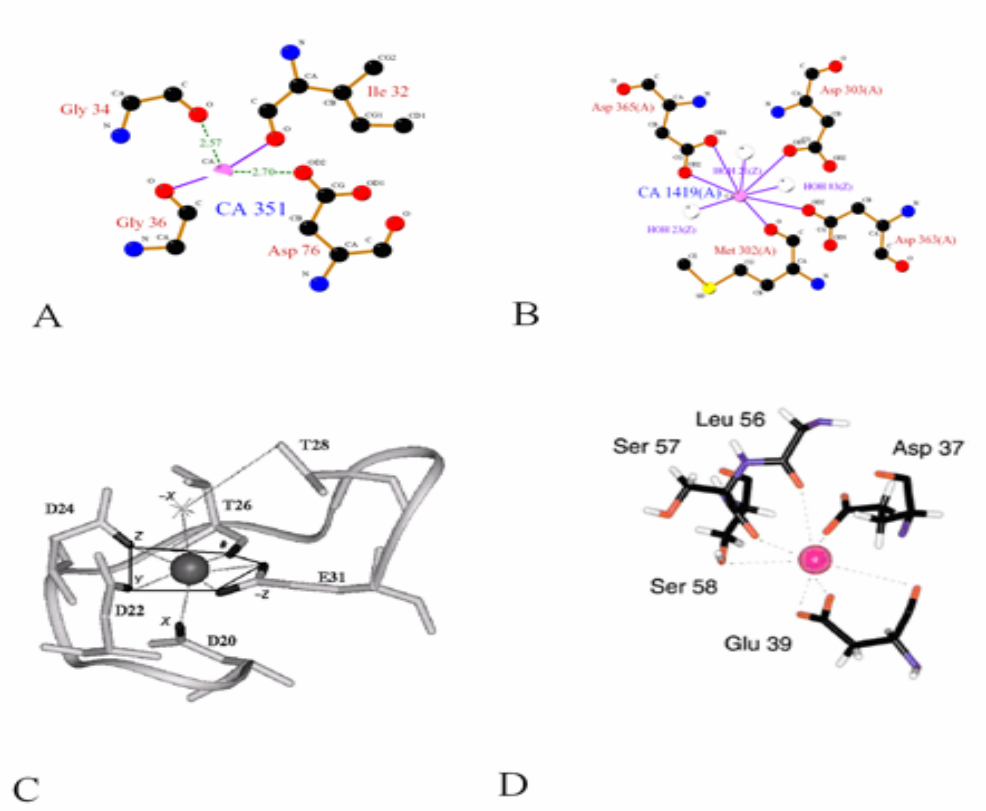

Figure 1-4: Diagrammatic illustration of calcium co-ordination motifs. (A) annexins and (B) C2 domains (C) EF hand and (D) gelsolin domain (A & B sourced from PDB website cooresponding to 1axn [84] and 1uov [85] respectively, C online CaBP data library [86], D adapted from [87]. Pink spheres in A, B and D, and black sphere in C denote calcium ion.).

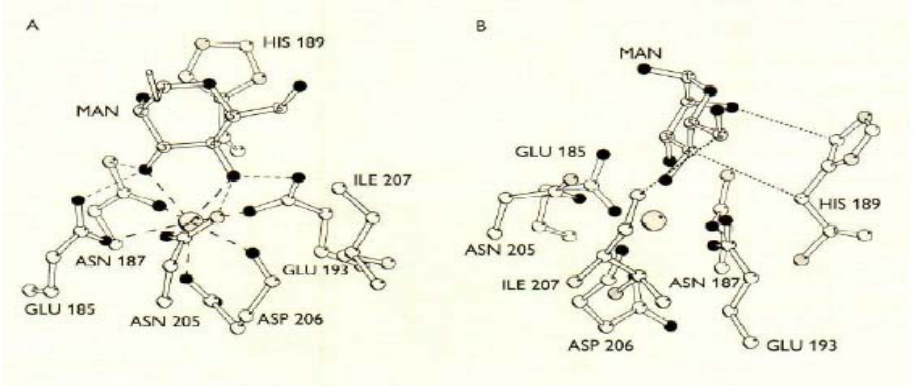

Figure 1-5: Binding of mannose at rat MBPsite 2**:** White, grey, and black spheres represent carbon, nitrogen, and oxygen atoms; the larger grey sphere represents the Ca-*. A. Co-ordination bonds are shown as long dashed lines, hydrogen bonds as short dashed lines. Side chain oxygen atoms of residues 185, 187, 193, and 205, and the main-chain carbonyl oxygen of residue 206, form the pentagonal, equatorial Ca-* ligands. B. This is a view approximately 90° to that of (A), showing van der Waals contacts (short dashed lines) between mannose and residues His 189 and ile 207. (figure and legend reproduced from [82]

The EF hand motif involves six residues in a 12-residue binding loop that coordinate the bound calcium with pentagonal bipyramidal geometry (fig.1-4C). By contrast, the other structural motifs contain 4-5 acidic residues that are far apart in linear sequence but are positioned close together in the tertiary structure to coordinate the bound calcium ion with a variable number of bound H_2O molecules. The selectivity of calcium over magnesium is because of the difference in solvation energy of these two ions in water [88, 89] (also see section 2.1). The disparity in the Ca^{++} coordination geometry, the number of bound water molecules and the functional diversity of the respective target proteins suggests a convergent evolution of these Ca^{++}-binding motifs.

A number of calcium binding proteins are targeted to cell membranes in response to calcium signaling. The bound Ca^{++} structurally bridges Annexin proteins and C2 domains to the membrane surface [90-92]. In both cases, Ca^{++} is coordinated on one side by residues of the protein and ligated along the opposite direction by a phosphoryl head group of the cell membrane. Calcium binding to C-lectins at the membrane surface dictates the specificity of carbohydrate recognition that helps in directing processes such as endocytosis and cell-cell interactions [82]. EF hand proteins especially those belonging to neuronal calcium sensing family, such as neurocalcin, recoverin and guanylate cyclase activating proteins (GCAPs) localize to membrane with the help of a myristoylated N-terminus [93-95]. Additional structural motifs such as parallel β-roll motif [96] and gelsolin [87] functionally bind calcium and membranes, in bacteria and mammals respectively. Several extracellular proteins with unknown three-dimensional structure, such as thrombospondins, fibrinogen, nidogen and integrins are localized to cell

membranes and have clusters of glutamate or aspartate rich regions that can bind calcium, albeit with weak affinity [72].

Most of the calcium binding proteins involved in cell signaling, especially EF hand proteins, exhibit high affinity binding to calcium followed by immediate conformational changes that allow them to recognize secondary effector molecules such as enzymes, ion channels and transcriptional factors (reviewed in [36] [29]). For example, calcium-induced interaction of calmodulin (CaM) with a variety of enzyme targets such as adenylate cyclase [97], phosphodiesterase [98, 99] and calcineurin [100] modulates their activity (reviewed in [101]), thereby affecting the downstream targets that regulate gene expression. The calcium-induced conformational changes in CaM lead to rearrangement of secondary-structure elements in the protein tertiary structure, thereby resulting in an open- form of protein due to exposure of hydrophobic sites that are otherwise buried in the apo-form also referred as closed-form (fig.1-6). The calcium-induced exposure of hydrophobic residues in the open state promote interaction with hydrophobic segments within target proteins and thus many EF-hand proteins such as calmodulin bind and activate target proteins only at high Ca^{++} levels.

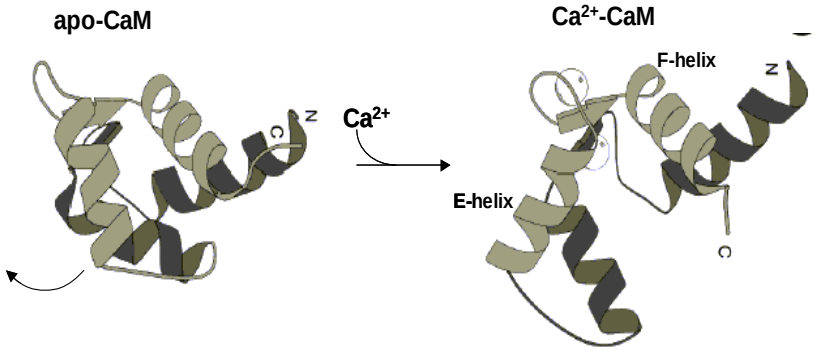

Figure 1-6: Calcium-induced structural changes in calmodulin. Figure courtesy: James Ames

These calcium-induced conformational changes are highly conserved in all EF-hand proteins and are best illustrated in the crystal structures of Troponin C [102], S100 proteins [103] and solution NMR and crystal structures of Calmodulin [104]. These calcium-induced conformational changes mediate cellular response to external stimuli by modulating different protein factors and ultimately affecting cellular processes such as motility, secretion, cell differentiation, apoptosis and gene expression.

1.6 Calcium and gene expression

Calcium regulation of gene expression involves three distinct pathways mediated by 1) calcium/Calmodulin dependent kinases (CaM kinases I-IV) [105], 2) calcium-dependent protein phosphatase 2A (calcineurin) [71] and 3) calcium-dependent protein kinase C (PKC) [106, 107] (Fig.1-6). These individual pathways promote gene expression via activation of specific transcription factor proteins. Increase in cytosolic calcium levels activates calmodulin that in turn activates CaM kinases that phosphorylate different transcription factor proteins such as CREB, SRF and MEF2 [105]. Direct activation of these transcription factors recruit histone acetyl transferases [108] [105], or form hetero-dimers with other transcription factors of the Jun family and regulate gene expression . Phosphorylation of MEF2 co-repressor protein, Cabin1 [109], by CaM kinase IV activates gene expression through de-repression. In addition, Calmodulin itself binds to basic helix-loop-helix (bHLH) transcription factors and directly inhibits gene expression [110]. Calcium-induced activation of calcineurin dephosphorylates the transcription factor protein, NFAT that in turn is targeted into the cell nucleus where it binds to various nuclear partners and activate gene expression [71]. A third pathway involves calcium

binding to the C2 domain of PKC that promotes phosphorylation of kappa B kinase that phosphorylates the inhibitory subunit of transcription factor NFκB leading to its nuclear translocation [106].

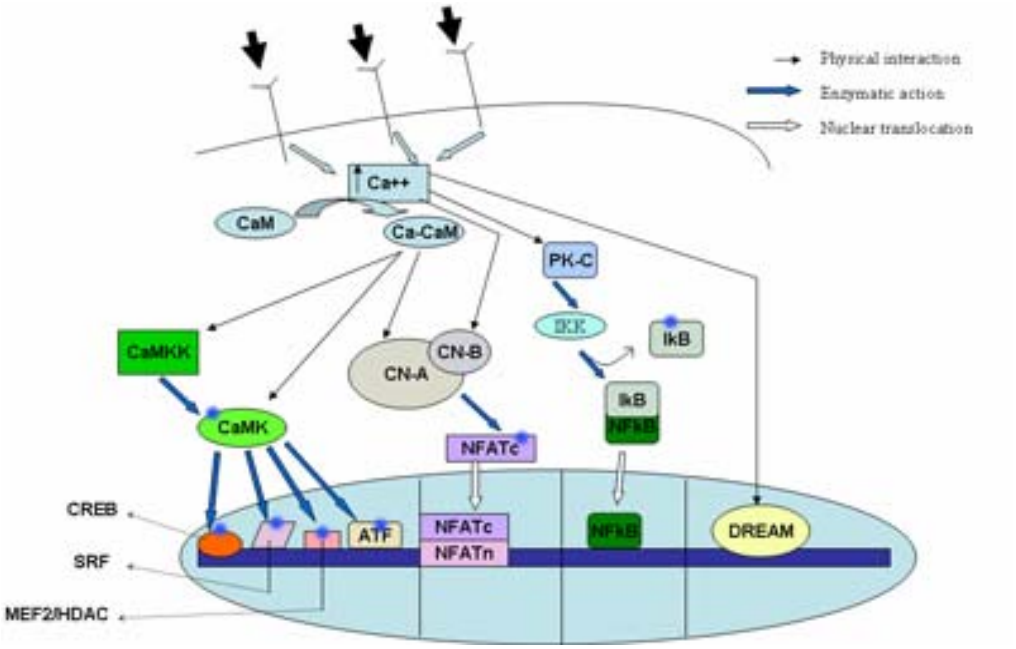

Figure 1-7: Schematic illustration of regulation of gene expression by calcium. See text for details. Bold arrows represent signal from the periphery. Blue dots represent phosphate. CaM: Calmodulin, CaMKK: Ca^{++}/Calmodulin dependent protein kinase kinase, CaMK: CaM kinase, CREB: cyclic AMP response element binding protein, SRF: serum response factor, MEF2: myocyte enhancer factor 2, ATF: activating transcription factor, CN-A: calcineurin subunit A, CN-B: calcineurin subunit B, NFATc: nuclear factor of activated T-cells cytosolic, NFATn: nuclear NFAT, PK-C: protein kinase-C, NFkB: nuclear factor kappa B, IkB: inhibitor of kappa B, IKK: IkB kinase, DREAM: Downstream Regulatory Element Antagonistic Modulator. Large black block arrows represent external stimulus.

Other signaling pathways mediated by cAMP and MAP kinase can also affect most of the known components involved in calcium signaling. For example, CREB/ ATF family transcription factors are also regulated via phosphorylation by protein kinase-A activated under elevated levels of cAMP [111]. Furthermore, ATF dependent transcriptional activation is also stimulated by activation of mitogen activated protein kinases (MAP kinases) which might also be regulated by a CaM kinase cascade [112].

An entirely new mechanism of Ca^{++}-regulated gene expression involves the Ca^{++}-binding protein, DREAM that modulates transcription by its direct binding to Ca^{++} and DNA targets [74, 113]. DREAM is a 29 kDa transcriptional repressor protein (its full name is **D**ownstream **R**egulatory **E**lement **A**ntagonist **M**odulator) identified in the brain to bind specific DNA sequences (downstream-regulatory-element, **DRE**) located downstream of the promoter of the prodynorphin and c-fos genes [114]. Under normal resting conditions (low intracellular Ca^{++}), the Ca^{++}-free form of DREAM binds tightly to the DRE and represses transcription (fig. 1-7). At high Ca^{++} levels resulting from agonist stimulation, Ca^{++} binding to DREAM leads to its dissociation from DNA targets, promoting activation of prodynorphin expression [113]. DREAM is the first reported calcium binding protein that directly binds to DNA and regulates transcription [74]. Subsequently however other EF hand proteins such as KChIP2 [115] and URE3BP [116] in *Entamoeba histolytica* were also reported to bind DNA and regulate transcription.

1.7 DREAM protein and gene expression

DREAM forced a rethinking of our conventional understanding of the link between Ca^{++} and gene expression. DREAM is a 29-kDa protein that belongs to the recoverin subfamily of EF- hand proteins that are expressed in the nervous system and function in a Ca^{++}-dependent manner. However, proteins such as frequenin are expressed in yeast (referred as Ncs1) [117] and DREAM itself is expressed in somatic tissues such as pancreas, thyroid gland and testes as well [113, 117]. Apo-DREAM (DREAM without bound calcium) was shown to bind DNA elements, called downstream regulatory elements (DRE), from the promoters of prodynorphin, c-fos [74], hrk [118] and

calcitonin [119] genes. The function of DREAM as a transcriptional repressor was interpreted based on the correlation between the DREAM-DNA interaction and increased prodynorphin expression in DREAM -/- mice [113]. In addition, the *in vivo* chloramphenicol acetyl transferase (CAT) reporter assays performed by co-transfecting plasmids that have DREs, fused upstream of the reporter along with DREAM expression vector into neuroblastoma cells showed a decrease in basal expression of reporter gene (CAT in this case) indicating a transcriptional repressor function of DREAM [74]. DREAM function as a repressor is also established, by correlating calcium induced loss of DREAM-DNA interaction with increased expression of hrk [118] and calcitonin [119] and thyroid specific transcription factor genes [120], as observed by increased levels of respective proteins on western blots or increased levels of mRNA using northern analysis. In addition, DREAM protein also regulates prodynorphin expression in pancreas [120, 121] and sodium/calcium exchanger NCX3 in hippocampus and cerebellum [122]. Biophysical analysis using size exclusion chromatography showed that Ca^{++} binding to DREAM causes changes in the protein oligomerization state [123] which might lead to its dissociation from DNA and hence derepression. Furthermore, DREAM was also shown to interact, in a two-hybrid system using N-terminus of DREAM as bait, with transcriptional co-repressor, C-terminal binding proteins (CtBP's) and repress transcription [124]. Interestingly, DREAM is also shown to act as transcriptional activation in conjunction with vitamin-D receptor [125] .

Sequence alignment of DREAM with other neuronal calcium sensing proteins (NCS proteins) across different species, shows that it bears ~45% similarity with respect to the EF-hand motifs (Fig.1-8). This level of sequence identity indicates that the main chain

three-dimensional structure of DREAM should be very similar to that of recoverin and the other NCS proteins. Indeed, the tertiary structure of the individual EF-hand motifs is highly conserved in all EF-hand proteins. EF- hands are helix-loop-helix motifs that have a conserved set of residues in the 12-residue loop, which help in the coordination of Ca^{++} ion [86]. However, depending on the composition of the amino acid residues in the loop, the selectivity and affinity towards metal ions can vary.

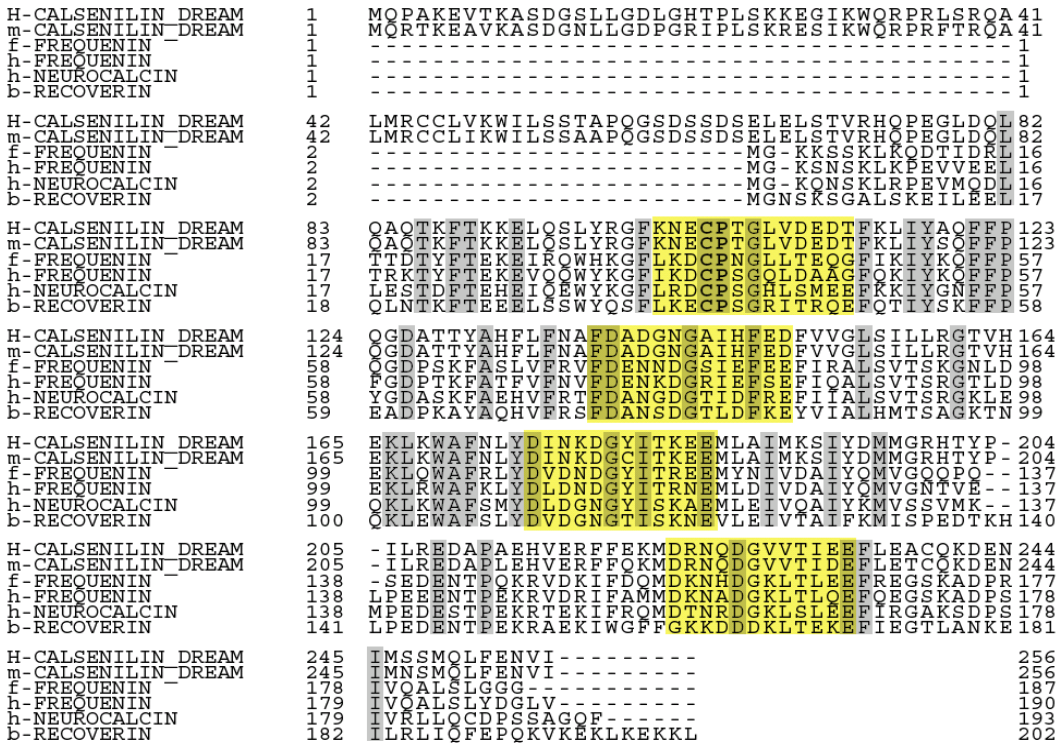

Figure 1-8: Amino acid sequence alignment of DREAM and the Recoverin family. Metal coordinating loops in EF hands are highlighted in yellow and highly conserved residues are shaded in grey. The proteins aligned are human calsenilin/DREAM, mouse calsenilin/DREAM, fly-frequenin, human homolog of frequenin, human neurocalcin and bovine recoverin.

Especially the residues in positions 1, 3, 5, 7, 9 and 12 are important in metal-ion coordination (fig.1-4C, fig. 2-3). DREAM has four EF- hands and the first EF hand is disabled for metal binding as a result of a disruption of the metal binding loop due to a

characteristic CPXG sequence (Cys 104 and Pro 105, in fig. 1-8) as seen in the crystal structures of other NCS proteins such as recoverin [126], neurocalcin [127] and KChIP1 [128]. In addition, the second EF-hand in DREAM has an aspartate in the 12^{th} position of the loop instead of a glutamate, as in the canonical EF-hand sequence. Studies on chicken myosin regulatory light chain show that this substitution, glutamate to aspartate at the 12^{th} position in the metal coordinating loop of EF hand, would increase selectivity of the EF-hand, making it a Mg^{++}/Ca^{++} site as opposed to Ca^{++} -specific site [129]. However, under physiological conditions (with ~millimolar free Mg^{++}) it is believed that this site is constitutively bound by Mg^{++} and confer structural stability [129].

Metal binding to EF-hand motifs causes significant conformational changes (fig.1-6) that regulate the function of each of the NCS proteins. The most striking illustration of a calcium-induced protein-conformational change was observed in recoverin, a Ca^{++} sensing protein involved in vision [75]. Calcium binding to recoverin leads to the extrusion of a buried myristoyl group that is attached to its N-terminus (called as a calcium-myristoyl switch), which helps in its membrane localization [75]. However, DREAM does not contain a myristoylation signal at its N-terminus. Instead, it is characterized by the presence of an additional stretch of residues in the N-terminal region (fig.1-8). The similarity in primary sequence of DREAM, notwithstanding the presence of an N-terminal tail, to recoverin suggests that the effects of metal binding in DREAM protein could be similar to that of Recoverin. Moreover, the C-terminus of DREAM (residues 65-256) comprising the four EF hands, is found to be sufficient for DNA binding in a Ca^{++} sensitive manner as removal of residues 1-65 does not affect metal and DNA binding properties of truncated protein [130] (fig. 1-9). Furthermore, DNA binding

to the N-terminal 1-70 residues (mut1-70) of DREAM polypeptide is calcium insensitive, sequence non-specific because DNA binding to mut1-70 persists even in the presence of calcium and is equally competed with excess of mutated and non-specific unlabeled DNA, in electrophoretic mobility shift assays (EMSA) (fig. 1-9 B, E).

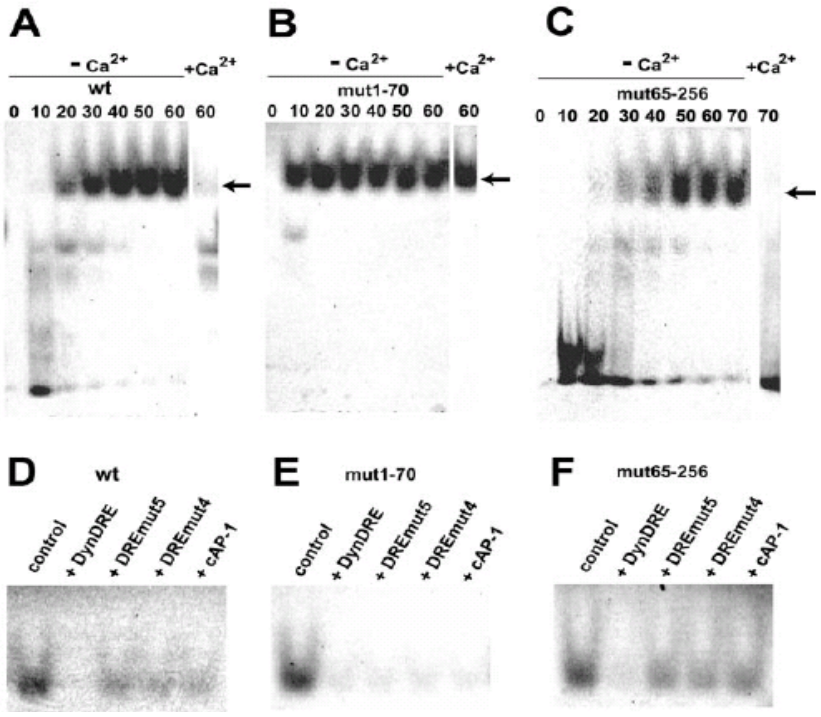

Dynorphin DRE:

5′-GAAGCCGGA**GT**CAAGGAGGCCCCTG-3

3′-TTCCGGCCT**CA**GTTCCTCCGGGGAC-5′

Figure 1-9: Fluorescent EMSA of DREAM-DRE interaction. *A,* EMSA titration of full-length mDREAM (0–60μM) into Cy5-labeled DRE (sequence shown-Dynorphin DRE) (5 nM) in the presence and absence of 10 mM Ca^{++}. The shifted band, corresponding to the ones seen in -Ca^{++} (*arrow*), was not detected in the presence of Ca^{++}; therefore, only the 60 _M lane is shown. *B,* EMSA titration of the N-terminal fragment (mut1–70) of mDREAM (0–60 μM) into Cy5-labeled DRE (5 nM) in the presence and absence of 10 mM Ca^{++}. The shifted band, corresponding to the ones seen in –Ca^{++} (*arrow*), was also detected in the presence of Ca^{++} (only the 60 μM lane is shown). *C,* EMSA titration of the C-terminal fragment (mut65–256) of mDREAM (0–70 μM) into Cy5-labeled DRE (5 nM) in the presence and absence of 10 mM Ca^{++}. The shifted band, corresponding to the ones seen in –Ca^{++} (*arrow*), was not detected in the presence of Ca^{++} (only the 70 μM lane is shown). For competition EMSA, (*D*) 40 μM wild type mDREAM, (*E*) 10 μM purified mut1–70, and (*F*) 80 μM purified mut65–256 were incubated with 5 nM Cy5-labeled DynDRE. (*D*) 75 nM (15-fold excess), (*E*) 325 nM (65-fold excess), and (*F*) 75 nM (15-fold excess) of unlabeled DynDRE, DREmut5, DREmut4, or cAP-1 were added to the same sample as the control lane, respectively. In DREmut4 G10 and T11(represented in bold) are mutated to A10 and A11 respectively. In DREmut5 G10 (represented in bold) in DRE is mutated to A10. (Figure and legend sourced from [130]).

Calcium binding to DREAM affects its interaction with protein targets as well. Ledo F. and colleagues (2002) [131] have shown that in the absence of Ca^{++}, DREAM physically interacts with CREB, disrupts CREB-CRE interaction and thus inhibits CRE (cAMP Response element) mediated transcription using co-immunoprecipitation experiments, EMSA and *in vivo* reporter assays respectively. Presence of calcium abolished DREAM-CREB interaction and led to increased reporter gene expression [131]. DREAM was also identified as a binding partner to presenilins and voltage-gated potassium channels in two hybrid screens that used C-terminal 103 amino acid residues of Presenilin2 (PS2) [132] and the N-terminal 180 residues of rat Kv4.3, Kv4.2 subunits [73] as baits respectively. However, the same protein, DREAM was variously named as Calsenilin and KChIP3 (Potassium channel interacting protein) respectively in these studies. Calsenilin/DREAM regulates the proteolytic processing of presenilins and may potentiate presenilin-induced apoptosis and is involved in Alzheimer's disease pathology [133-136]. Calsenilin/DREAM also reverses the presenilin-mediated enhancement of Ca^{++} signaling [137]and serves as a substrate for caspase-3 [137]. The KChIP3 protein (identical in sequence to Calsenilin/DREAM) binds tightly to Kv4.2 channels and activates channel kinetics only at high Ca^{++} levels [73]. Furthermore, it was shown in thyroid cells that a dominant negative mutant of DREAM, which is unable to bind calcium, affects cell cycle progression by delaying the expression of cyclin D3 through an uncharacterized mechanism [138]. Thus a single protein variously named Calsenilin/DREAM/KChIP3 performs different functions in different cellular compartments much akin to other multifunctional transcriptional activators such as β-catenin [139] and p53 [140]. Most of the localization studies found DREAM to be localized on membranes predominantly

[136] - supporting both Calsenilin and KChIP3 functions. But Zaidi et al. (2004) [141] have shown that Calsenilin/DREAM translocates into the nucleus in response to increase in cytosolic calcium levels. However, Ca^{++} binding to DREAM is not essential for nuclear localization, as mutant DREAM unable to bind calcium also localizes in the nucleus when cytosolic calcium levels increase [141]. This could mean that DREAM enters the nucleus in apo-form probably because the rise in Ca^{++} level is insufficient to promote calcium binding to DREAM but sufficient to activate another calcium dependent factor that might assist in DREAM's translocation. Details regarding the mechanism of DREAM translocation into the nucleus are still unclear.

The finding that DREAM binds Ca^{++} was initially surprising because DRE was originally identified in the screen for promoter elements involved in PK-A dependent regulation of prodynorphin gene [114]. However, DREAM does not contain PK-A phosphorylation sites. This apparent paradox was resolved when it was shown that DREAM interacts with PK-A phosphorylated α-CREM (cAMP responsive element modulator) and derepresses transcription [142]. In this study [142], it was shown that DREAM and α-CREM are involved in a two-site interaction that is mediated by a leucine charged domains and a leucine zipper in both the proteins. Transcription of prodynorphin in rat is controlled by five regulatory elements distributed along the 2kb stretch of the promoter region [114]. The distal region of promoter has three CRE's (cAMP responsive elements) and the proximal region has a non-canonical AP-1 site and DRE. DREAM is also shown to interact with CREB via the leucine charged domain and repress CRE-mediated transcription at low Ca^{++} levels [131]. This single site interaction involves a leucine charged domain and is disrupted at high Ca^{++} levels leading to derepression. It is well

known that mutual negative interference between different transcription factors through direct interaction also could lead to transrepression [143]. For example activity of CREB, NF-κB, and Oct1 transcription factors is attenuated by direct protein-protein interaction with glucocorticoid receptor (GR) [143, 144]. Thus DREAM presents a convergence point for PK-A and calcium mediated regulation of prodynorphin expression.

Cheng et al.(2002) and Lilliehook et al. (2003) independently generated transgenic mice that are devoid of DREAM (dream -/- mice) and observed no general behavioral or learning disabilities (using rotarod and Morris watermaze tests) in the knockout mice when compared to wild type littermates [113, 145]. This means that the knockout mice were indistinguishable from wild type mice except for the specific phenotypes observed in either study. Cheng et al. observed elevated levels of prodynorphin expression and higher levels of dynorphin peptides in dream -/- mice, when compared with wild type mice [113] (fig.1-10), that supports DREAM's transcriptional repressor function as reported in [74].

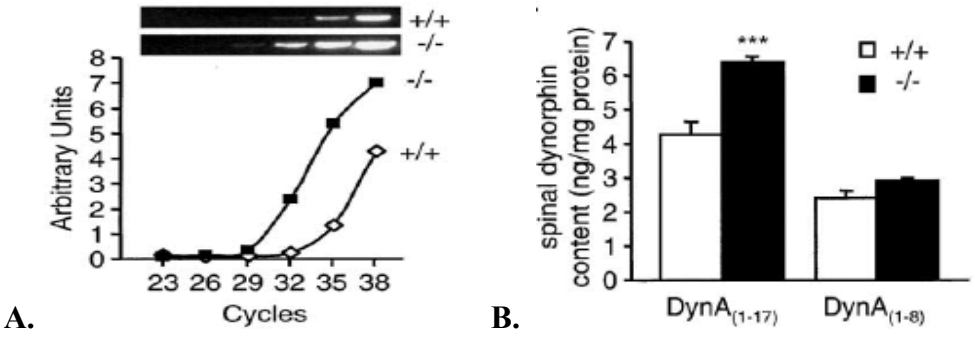

Figure 1-10: Comparison of prodynorphin expression and dynorphin peptide levels in wild type and dream -/- mice. (A) Basal expression of prodynorphin in wild type (+/+) and knockout (-/-) mice assessed by semiquantitative RT-PCR. The curves represent the relative abundance of prodynorphin PCR product in the two genotypes. (B) ELISA quantitation of spinal dynorphin $A_{(1–17)}$ and dynorphin $A_{(1–8)}$ levels in wild type (n = 5) and *dream* -/- (n = 5) mice 3 hr following intrathecal administration of the peptidase inhibitors, *p*-hydroxymercuribenzoate (8 nmol) and phosphoramidon (4 nmol). Triple asterisk indicates $p < 0.001$ versus wild type (two-tailed Student's t test). Figure and legend sourced from [113].

Moreover, dream -/- mice show a striking phenotype of ongoing analgesia, i.e. lack of pain upon application of noxious stimuli such as tail-flick test, intra peritoneal injection of $MgSO_4$ and acetic acid (fig.1-11) [113]. Lilliehook et al. observed similar results in the tail-flick test in their knockout study but, surprisingly, found that the threshold current required for exhibiting escape behavior (running and vocalizing) in the shock-sensitivity tests was much lower [145] (fig.1-12).

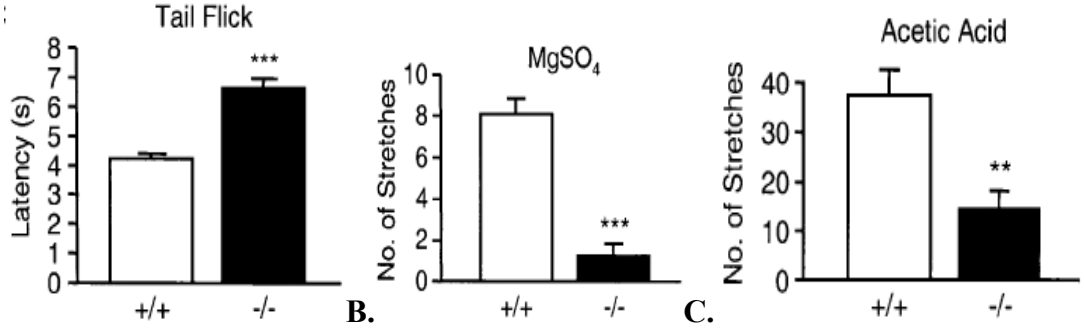

Figure 1-11: Tests for pain phenotype in dream -/- mice. (A) Tail-flick test in wild type and dream -/- mice. Values represent the latency (s) to tail flick from the heat source. Triple asterisk indicates $p < 0.001$ versus wild type (two-tailed Student's t test). (B and C) Visceral pain in response to (B) $MgSO_4$ (120 mg/kg) or (C) acetic acid (0.6%). Values represent the number of abdominal stretches (writhes). n = 8–12 for each group. (B) Triple asterisk indicates $p< 0.001$ versus wild type. (C) Double asterisk indicates $p < 0.01$ versus wild type. Figure and legend sourced from [113].

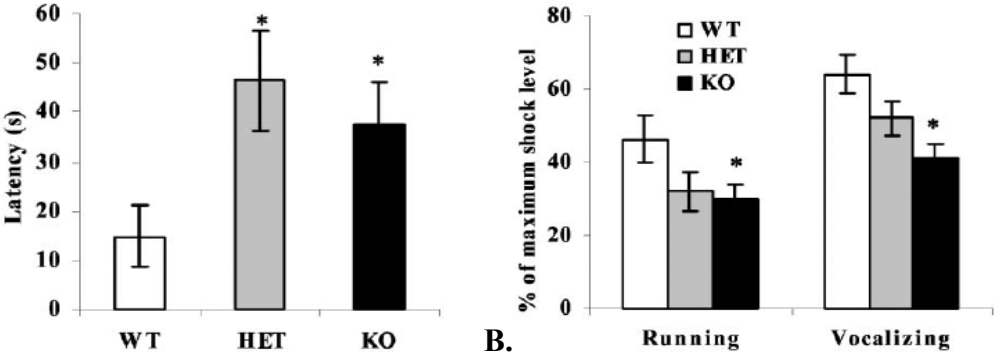

Figure 1-12: Behavioral assessment of calsenilin knockout mice. *A*, Tail-flick test. Values represent latency to withdraw tail. *B*, Shock sensitivity. Values represent percentage of maximum shock level (0.08 mA) required to elicit two stereotypical behavioral responses, running and vocalizing. All data are presented as mean +/- SEM, and *p* values were calculated using the Student's *t* test. Wild-type mice (WT), *n* = 8; heterozygous mice (HET), *n*=5; knock-out mice (KO), *n*=8. **p* 0.05. Figure and legend reproduced from [145]

However, while researchers in both the studies did not observe any difference in expression of presenilins between wild type and knockout mice (as observed by western blots), decreased levels of amyloid beta peptides in calsenilin knockout mice as compared to wild type (using ELISA quantification) were reported by Lilliehook et al. (2003). While Cheng et al. found reasonable expression of DREAM in the spinal cord (as observed by western blots), Calsenilin knock out is said to have no detectable DREAM expression in spinal cord (using β-gal marker). The authors of the Calsenilin knockout study attribute this difference to a possible expression of Calsenilin in very low quantities in spinal cord and low sensitivity of β-gal marker as test for protein expression levels.

In order to assess the effect of knocking out DREAM protein on its KChIP function each group followed a different approach. Cheng et al. measured heart-to-body mass ratio and assessed heart function using echocardiographic analysis to correlate the knockout phenotype with loss of KChIP3 function. Previous studies on transgenic mice overexpressing dominant negative Kv4.2 showed enlargement of heart by 10-16 weeks of age leading to cardiac failure and death [146]. Similarly, studies on KChIP2 -/- mice showed alterations in potassium current resulting in increased susceptibility to cardiac arrhythmias [147]. In terms of heart morphology, function and contractility dream -/- mice were indistinguishable from their wild type littermates [113]. However, it must be noted that the only KChIP natively expressed in heart is KChIP2 and DREAM is exactly identical to KChIP3 [73]. In this regard, the calsenilin knockout study attains significance, as Lilliehook et al. correlate long-term potentiation (LTP) with A-type potassium currents in brain slices of wild type and knockout mice. The authors observe that the knockout mice exhibit increased LTP and decreased A-type potassium currents as compared to the

wild type. Long-term potentiation is a phenomenon of long lasting synaptic enhancement upon repetitive activation of excitatory synapses [148]. Thus, the authors surmise that loss of transient outward A-type potassium currents, which are essential to oppose membrane depolarization and excitability [149] might be the reason for increased LTP in the knockout mice. Thus, the two independent knockout studies complement each other in terms of the characterization of the effect of knockout on various functions of DREAM protein. In summary, the two knockout studies of DREAM protein combined, provide evidence for DREAM's multi-functionality as calsenilin, DREAM and KChIP3. Further reports on additional characterization of these knockout mice are still awaited.

1.8 DREAM and pain

Since the DREAM knockout study (see section 1.7) specifically showed elevated prodynorphin levels concomitant with ongoing analgesia, this protein might be an interesting target for effective pain management. Dynorphin is an endogenous opiate that acts through κ opioid receptor. Increased biosynthesis of prodynorphin is observed under various conditions associated with neuropathic pain. Although opioid anti- nociceptive property during inflammation is believed to be mediated via μ- opioid receptor, μ- opioid receptor agonists such as morphine have been ineffective during neuropathic pain [150]. Moreover excessive administration of μ-agonists leads to addiction, tolerance and withdrawal [151]. Further dynorphin was shown to inhibit the release of substance-P in the spinal cord in a κ opioid receptor mediated manner [152]. Although the actual mechanisms of pain manifestation and its eradication are quite complex and still not completely understood, since DREAM is thought to influence the pain pathway by

regulating the expression of prodynorphin gene it would present an interesting possibility of being a therapeutic target.

1.9 Aim and scope of this study

My current study on DREAM protein aims to characterize its molecular structure and functional relationships. Specifically, since DREAM contains four EF hand calcium binding motifs it is essential to know the binding potential of these binding sites and their effect on the protein structure. Furthermore, there is limited knowledge about the region of DREAM protein involved in DNA recognition. Hence, this study aims to identify the DNA binding regions using a high throughput yeast one-hybrid screen and an in vitro approach using chimeric protein constructs that have individual and combination of EF hand motifs in DREAM swapped with those of recoverin. The rationale is that the main chain structures of recoverin and DREAM are likely to be similar due to their high sequence identity. Therefore, substituting individual EF-hand motifs from recoverin should not perturb the overall three-dimensional structure. However, since recoverin does not bind DNA and has different metal binding properties, substitution of DREAM EF hands with that of recoverin might abolish DNA binding without destroying the overall main chain fold and therefore identify the DNA binding surface on DREAM. Thus, understanding the metal binding properties and their effect on the protein structure as well as the structural determinants of DNA recognition in DREAM protein could provide insight into the rational design of analgesic drugs that selectively target DREAM.

Chapter 2: Calcium and Magnesium binding to DREAM

2.1 Introduction

DREAM protein was identified as a transcriptional repressor that can integrate Ca++ and cAMP signals [74, 142]. The novel aspect of DREAM protein is that it is the first reported calcium-sensor that binds DNA and regulates gene-expression [74]. Calcium binding to DREAM is shown to be a key determinant in its interaction with protein [131] and DNA [74] targets.

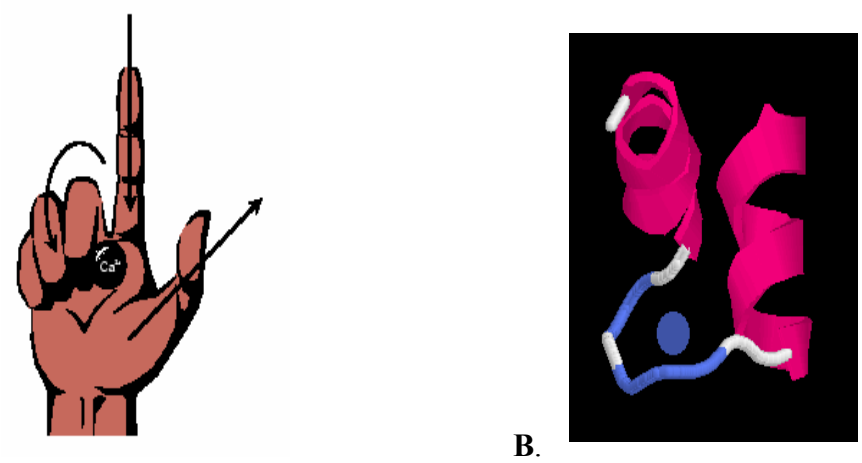

Figure 2-1: Illustration of an EF hand motif (for description see text). (A) Figurative description, and secondary structure representation (B). (A) was sourced from [153] and (B) was sourced from [154].

DREAM contains four EF hand (fig.2-1, 2) calcium-binding motifs similar to those in calmodulin [155] and troponinC [102]. The four EF hand motifs share > 45% identity with those of recoverin and other members of neuronal calcium sensor (NCS) family of

proteins part of the EF hand super-family. While all the members of the NCS family, share similar sequence identity in the 12-residue loop region, the inherent metal

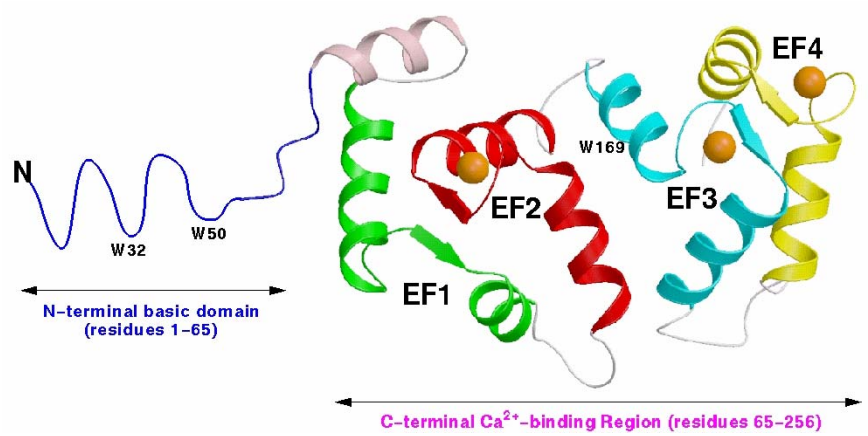

Figure 2-2: Ribbon diagram of the main chain structure of DREAM showing the four EF hands. The structure was modeled based on previous crystal structures of recoverin and neurocalcin. Figure courtesy: James Ames.

binding selectivity and affinity of each EF hand and the metal-binding induced effects on the protein oligomerization are markedly different. Metal binding was shown to influence the oligomerization status and target interaction of some of the NCS family proteins that would turn out to be a key determinant of their function. For example, KChIP1 [128] and neurocalcin [127] are shown to exist as dimers in Ca^{++} bound form whereas GCAP2 [156] exists as dimer in Ca^{++}-free state. DREAM, however was shown to bind DNA as a tetramer [74, 130] and upon Ca^{++} binding dissociates DNA and exists as a stable dimer [123] .

While EF hands of NCS proteins comprise of non-binding, Ca^{++}/Mg^{++}-binding and Ca^{++} selective binding sites, different NCS proteins exhibit different oligomerization properties upon metal binding. For instance, the sequence CPXG (figs.1-8, 2-3) in the first EF hand

of most of the NCS family proteins disables calcium binding as seen from the studies of Muralidhar et al. (2004) on peptides corresponding to the four EF hand motifs in Neuronal calcium sensor-1 protein (Ncs1) [157]. Presence of unfavorable residues in a key metal coordinating position (position 3 in the EF hand loop, figs.2-3, fig.1-4C) was cited as the reason for this disability. Drake et al. (1997) [158]specifically studied the contribution of coordinating side chain at loop position 3 [158, 159], using various mutants of *E. coli* galactose binding protein as model for the EF-loop and reason that presence of cysteine at loop position 3 leads to loss of Ca^{++} binding[158]. Lack of metal binding to the first EF hand, which contains the CPXG sequence in its loop, is also confirmed from the crystal structures of Recoverin [126], neurocalcin [127], frequenin [135] and KChIP1 [128].

Figure 2-3: Amino acid sequence in the four EF hands of DREAM. Residues circled in red denote the position mutated in the protein for this study and the respective mutations depicted across the circled residue. Figure courtesy: James Ames.

The second EF hand in DREAM (figs. 1-8, 2-3) has an aspartate instead of the usual glutamate residue in the 12^{th} position of the calcium-binding loop. The presence of an aspartate in the 12^{th} position increases the selectivity of the EF hand to bind magnesium as compared to calcium under physiological conditions [129]. This is because the shorter side chain of Asp favors the mono-dentate coordination of Mg^{++} as opposed to bidentate coordination of Ca^{++} [158, 160] (also fig.1-4C). The selectivity of an EF hand towards calcium or magnesium is determined by the composition of amino-acid residues in the 12-residue loop [158, 160-162]. Furthermore, considering the fact that the resting levels of magnesium in the cell are close to 10^{-3}M [163], the ability of an EF hand to bind magnesium as well [129] adds another level of regulating these proteins in terms of structural changes upon metal binding. While free Mg^{++} levels are shown to change in response to stimulation by neurotransmitters such as glutamate [5] the effect of changing $[Mg^{++}]$ on the function of NCS proteins is largely speculative. Many NCS proteins and other EF hand proteins, however, functionally bind magnesium and exhibit magnesium induced conformational changes [162, 164, 165] . Some proteins, for e.g. parvalbumin, show similar effects on protein conformation upon binding calcium or magnesium as observed by tryptophan fluorescence emission and ultra violet differential spectroscopy [166, 167]; while VILIP and NCS1 proteins show quite different effects as observed by tryptophan fluorescence emission [164].

Magnesium binding to NCS proteins helps in modulation of Ca^{++} sensitivity of EF hands and changes in protein-conformation that affect their interaction with downstream targets [168, 169]. Furthermore, increase in free Ca^{++} levels was shown to result in the displacement of Mg^{++} in GCAP1 [168]. However, direct binding measurements, aimed at

determining the metal binding stoichiometry of DREAM, show that DREAM binds, at saturation, three calcium ions in the absence of Mg^{++} ([130], fig.2-4) and two calcium ions in the presence of Mg^{++} (James Ames unpublished observation, fig.2-4). This means- out of the four EF hands, while the first hand is disabled for Ca^{++} binding due to unfavorable residues in the first EF hand (see above), one more EF hand is unable to bind Ca^{++} because of the presence of Mg^{++}. Thus, it is unlikely that Ca^{++} will displace Mg^{++} that is bound to EF-2 of DREAM, under normal physiological conditions (low Ca^{++} and high Mg^{++}) (fig.2-4), which is corroborated by the ITC experiments that involved titration of Ca^{++} into DREAM, in the presence of Mg^{++} (fig.2-7B).

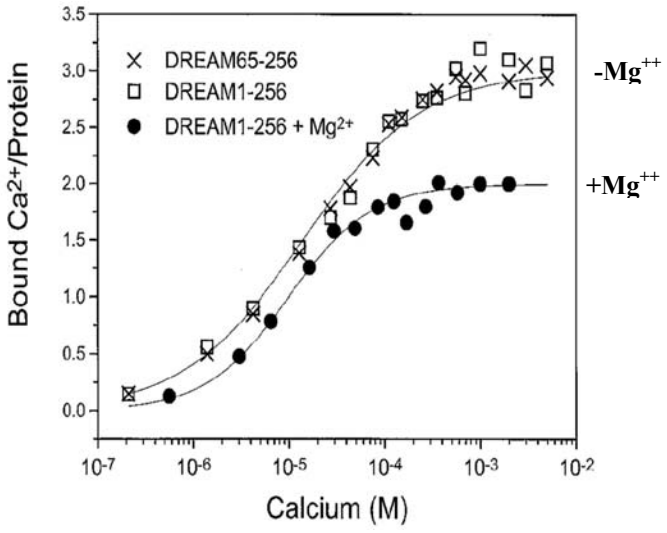

Figure 2-4: Equilibrium calcium binding measurement using titration of $^{45}Ca^{++}$ into DREAM protein. The number of ions bound/protein is plotted *versus* the free calcium concentration. The actual method is described in [130]. DREAM1-256: full-length DREAM protein, DREAM65-256: truncated DREAM protein devoid of N-terminal 1-64 residues (used in the present study), Hollow squares and crosses represent titration of $^{45}Ca^{++}$ into full-length and truncated DREAM protein respectively, in the absence of Mg^{++}. Dark circles represent titration of $^{45}Ca^{++}$ into full-length DREAM protein in the presence of 5 mM Mg^{++}. Figure courtesy James Ames.

Thus, motivated by prior metal-binding studies on NCS proteins (see above) and earlier studies on DREAM from the lab (fig.2-4), I set out to characterize in more detail the specific binding energetics of both Mg^{++} and Ca^{++} to each of the individual EF-hands of DREAM protein. For this purpose, DREAM mutant constructs that have the 12^{th} residue in the EF hand metal-binding loops of EF-2, EF-3 and EF-4 mutated (shown in fig-2-3) were obtained from Mitsu Ikura lab and soluble recombinant proteins were expressed in *Escherichia coli*. The expressed proteins were purified and used for performing isothermal titration calorimetry and gel filtration experiments. While I performed the ITC of magnesium binding to apo-form and calcium binding to magnesium-loaded form of DREAM, the rest of the work described in the metal-binding study was done in collaboration with Masanori Osawa, who performed the ITC and gel-filtration experiments while training me in protein purification methods.

2.2 Materials and Methods

2.2.1 Expression and Purification of Mouse DREAM-C and Its Mutants

A deletion mutant of mouse DREAM (residues 65–256, named DREAM-C) was shown previously to exhibit functional binding to DNA and Ca^{2+} [130]. The recombinant His-tagged DREAM-C protein was expressed in soluble form and was purified in milligram amounts as described previously [130]. cDNAs encoding wild-type DREAM-C and its mutants D150N, E186Q, and E234Q, inserted into pET15b (Novagen) expression vectors at NdeI and XhoI sites were obtained from M. Ikura's lab. These constructs were transformed into *Escherichia coli* BL21(DE3) (Stratagene) cells and were grown in 2 liters of LB medium with 100 μg/ml ampicillin at 37 °C. Recombinant DREAM-C

protein expression was induced by adding 0.5 mM isopropyl 1-thio-β-D-galactopyranoside to the cell culture once the cell culture reached an optical density of 0.5 at 600 nm, and the cells were then grown with shaking at 37 °C for 3 h or 16 °C overnight for the mutants. Cells were harvested by centrifugation and resuspended in buffer A (20 mM Tris·HCl, pH 8.0, 0.3 M NaCl, 1 mM β-mercaptoethanol, and 20% glycerol) supplemented with 1 mM phenylmethylsulfonyl fluoride, 0.2% Tween 20, 20 μg/ml DNase I, and 5 mM $MgCl_2$. Cells were then disrupted by sonication, and soluble protein fractions recovered by centrifugation were applied onto a nickel-loaded Hi-Trap chelating column on an AKTA purifier (Amersham Biosciences), previously equilibrated with buffer A. After washing with the buffer A (until $A_{280} < 0.01$), proteins were eluted with buffer A containing 0.3 M imidazole. The eluted solution was dialyzed against buffer B (10 mM Tris·HCl, pH 7.4, 1 mM EDTA, and 1 mM dithiothreitol) for 12 h. The dialyzed sample was applied onto a Hi-Trap DEAE-FF column (Amersham Biosciences) previously equilibrated in the buffer B, and eluted with NaCl gradient (0 to 0.3 M NaCl over 3 h) at a flow rate of 5 ml/min. Thus, the recombinant proteins were used for subsequent experiments without the cleavage of His-tag, because Ca^{++} or Mg^{++} binding to His-tag was shown to be negligible [170] and the presence of His-tag does not affect DREAM's interaction with DNA [130].

2.2.2 Size Exclusion Chromatography

Determination of the molecular weight of the purified DREAM-C in solution was carried out on a Superdex 200 HR 10/30 column (Amersham Biosciences) at 4 °C in the buffers containing 10 mM Tris-HCl (pH 7.6), 150 mM NaCl, 5 mM $MgCl_2$, 1 mM dithiothreitol, and 5 mM $CaCl_2$ for Ca^{2+}-DREAM-C, or 1 mM EGTA for Mg^{2+}-bound DREAM-C. 0.1 ml of

DREAM-C (protein concentration ranged from 10 to 460 μM) was loaded onto the column and eluted at a flow rate of 0.5 ml/min. Apparent molecular weights were calculated using a standard curve of V_e/V_o *versus* the log of the molecular masses of standard proteins: β-amylase (200 kDa), alcohol dehydrogenase (150 kDa), transferrin (81 kDa), carbonic anhydrase (29 kDa), and myoglobin (17 kDa). V_o is a void volume obtained using blue dextran (2000 kDa), and V_e is a volume of elution.

2.2.3 Preparation of Decalcified Protein Solutions

In order to obtain accurate measurement of calcium-binding energetics it is essential to have the protein in apo-form with no contamination of Ca^{++} in the buffers. Hence, all the buffers used for ITC were decalcified using Chelex 100 resin (Bio-rad). Decalcified ITC buffer (150 mM NaCl and 10 mM Tris-HCl, pH 7.6) was prepared by treatment with Chelex 100 resin (Bio-Rad). 1 mM dithiothreitol and 5 mM $MgCl_2$ were added after treatment with Chelex 100 and immediately before use. Containers and pipette tips were rinsed with 1 M HCl twice followed by a rinse with decalcified buffer. EDTA was removed from protein solution using Econo-Pac 10 DG gel filtration column (Bio-Rad Laboratories, Inc.) pre-equilibrated in 50 ml of the decalcified buffer. Before the ITC experiment, the sample cell and injection syringe of ITC machine (Microcal Inc.) were cleaned by the decalcified buffer extensively.

2.2.4 Mg^{++} and Ca^{++} Titration into DREAM-C by ITC

Binding of Mg^{++} and Ca^{++} to DREAM-C was measured by ITC [171], using a MicroCal VP-ITC MicroCalorimeter (MicroCal Inc.). The protein solution used in the titration was exchanged with decalcified buffer using Econo-Pac 10 desalting gel-filtration column as

described above. Stock solutions of $MgCl_2$ and $CaCl_2$ (0.5–2.0 mM), used as the titrant, were prepared using decalcified buffer as a diluent. A stock solution of $CaCl_2$ with 5 mM $MgCl_2$ was the titrant for Ca^{++} titration of Mg^{++}-bound DREAM-C. The experimental set up of an ITC instrument is shown in fig. 2-5.

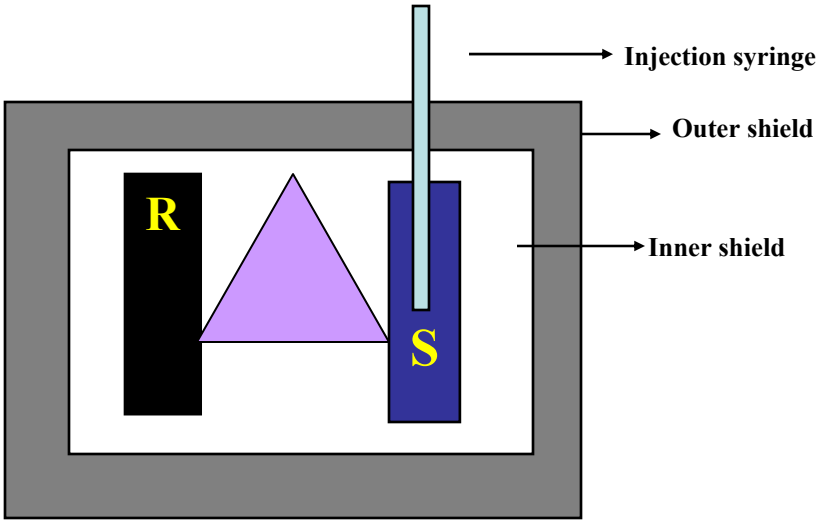

Figure 2-5: Design of a microcalorimeter. A sample (S) and a reference (R) cell are enclosed within an adiabatic shields and are connected with coils represented by the pink triangle so that they can exchange heat among themselves. The reference cell is maintained at constant temperature using a power circuit. During the experiment the reference cell contains the buffer used to solubilize the macromolecule where as the sample cell contains the solution containing the macromolecule. As the ligand is injected using the syringe the heat change is communicated to the reference cell through the coils (pink triangle) and a positive or negative feedback is generated if heat is absorbed or evolved respectively, which is reflected in the raw data.

A typical ITC experiment was performed at 25 °C on a protein solution (1.38 ml, 35–100 μM) by adding a total of 290 μl of concentrated $MgCl_2$ or $CaCl_2$ (0.50–2.0 mM) in 29 aliquots (10 μl each). The additions were 3 min apart to allow heat accompanying each increment to return to baseline prior to the next addition. For each addition, the molar heat (Q_t) was measured as a function of total ligand concentration (X_t),

$$Q_t = n^* M_t^* \Delta H^* V \{1+X_t/(n^* M_t) + 1/(n^* Ka^* M_t) - [(1+ X_t/(n^* M_t) + 1/(n^* Ka^* Mt)^2 - 4 X_t/(n^* M_t)]^{1/2}\}/2 \quad \text{.. Eq.1}$$

where n is the number of sites, M_t is the total protein monomer concentration, where ΔH is the molar heat of ligand binding, K_a is the metal-binding association constant ($1/K_d$), and V is the cell volume. The differential molar heat (dQ_t) measured in the ITC experiment was fitted by various binding models (sequential *versus* independent sites) using a nonlinear least squares minimization method [171, 172]. Thermodynamic parameters in the analysis are defined by,

$$\mathbf{\Delta G^o = \Delta H^o - T\Delta S^o} \qquad \text{... Eq.2}$$

Where **ΔGo**, **Δ Ho** and **ΔSo** are the free energy, enthalpy, and entropy change for single site binding and

$$\mathbf{\Delta G^o = - nRT \ln(K_a)} \qquad \text{... Eq.3}$$

where n is the number of moles, T is the absolute temperature, and R = 8.3151 J mol^{-1} K^{-1}.

2.3 Results and Discussion

2.3.1 Apo-DREAM-C binds two Ca^{++} with high affinity

ITC was used to analyze the binding energetics of metal binding to protein (fig-2-6). Calcium binding to metal-free DREAM-C (apo-DREAM-C), in the absence of magnesium, shows a multi-phasic isotherm that could be fitted by the binding of three or more Ca^{++} ions, consistent with previous binding studies [130, 173].

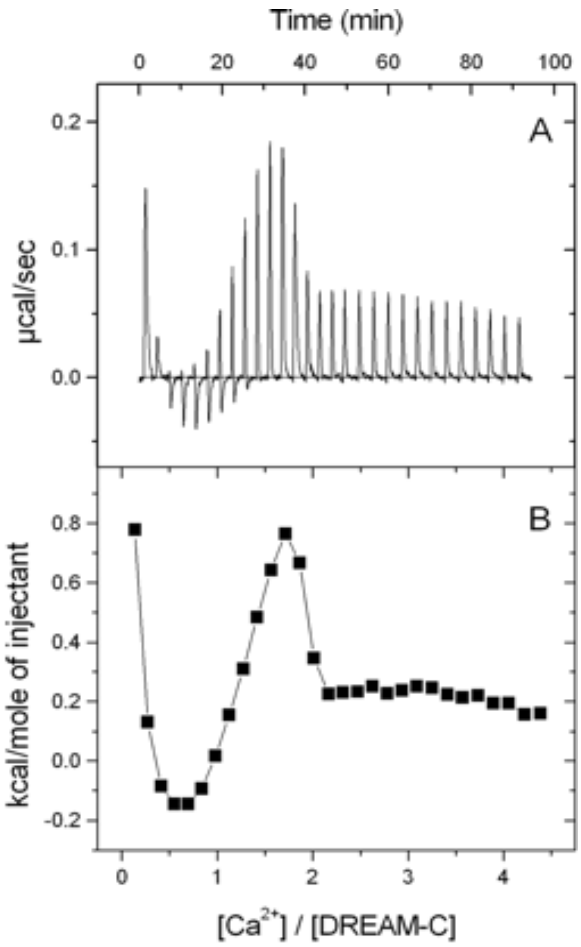

Figure 2-6: Isothermal titration microcalorimetric analysis of Ca^{++} binding to apoDREAM-C. Trace of the calorimetric titration of 29 x 10-µl aliquots of 1.3 mM $CaCl_2$ into the cell containing 46 µM apo-DREAM-C (*A*), and integrated binding isotherm (*B*). No correction was needed for the heat of dilution, because negligible heat was observed when adding aliquots of $CaCl_2$ (or $MgCl_2$) into a decalcified buffer blank. (figure and legend reproduced from [123])

A typical ITC experiment monitors heat released or absorbed with successive injections of the ligand molecule. Thus, the heat change (ΔH) is directly proportional to the amount of binding of ligand to the macromolecule (in this case Ca^{++} and DREAM respectively). As the binding reaches saturation no heat is released or absorbed and hence, the heat observed post-saturation is only heat of dilution of ligand molecule. Thus, the isotherm of Ca^{++}- apo-DREAM titration (fig.2-6), exhibits stoichiometric binding of two calcium ions (Kd = ~ 1- 10 uM) followed by one or more ions binding with much lower affinity. The multi-phasic isotherm may be explained, apart from the presence of multiple binding sites in DREAM, by the fact that metal binding to DREAM protein is accompanied by protein conformational changes. Specifically, previous studies from the lab have shown that apo-DREAM exists as a tetramer and calcium-bound DREAM as a dimer [130]. Thus, the isotherm is too complex for quantitative derivation of thermodynamic parameters of individual calcium binding sites. In order to dissect the metal binding properties of the individual EF hands, mutant DREAM-C constructs were prepared such that the acidic residues at the 12^{th} position of the calcium coordinating loop (fig 2-3) are replaced with a neutral residue (EF2: D150N, EF3:E186Q, EF4: E234Q). Replacing the negatively charged residues at the 12^{th} position in the calcium coordination loop with a neutral residue considerably lowers affinity towards calcium [159, 174].

An overlay of the Ca^{++}-binding isotherms for each of the EF-hand mutants in the absence and presence of magnesium is shown in fig-2-7A and B respectively. In the absence of magnesium, the isotherm of D150N (EF-2 mutated) exhibits stoichiometric binding of two Ca^{++} ions to the apo-protein but lacks the low affinity endothermic phase seen in wild

type, suggesting that EF-2 is the low affinity site, which shows non-stoichiometric binding in the wild-type isotherm. Thus, while EF-1 of

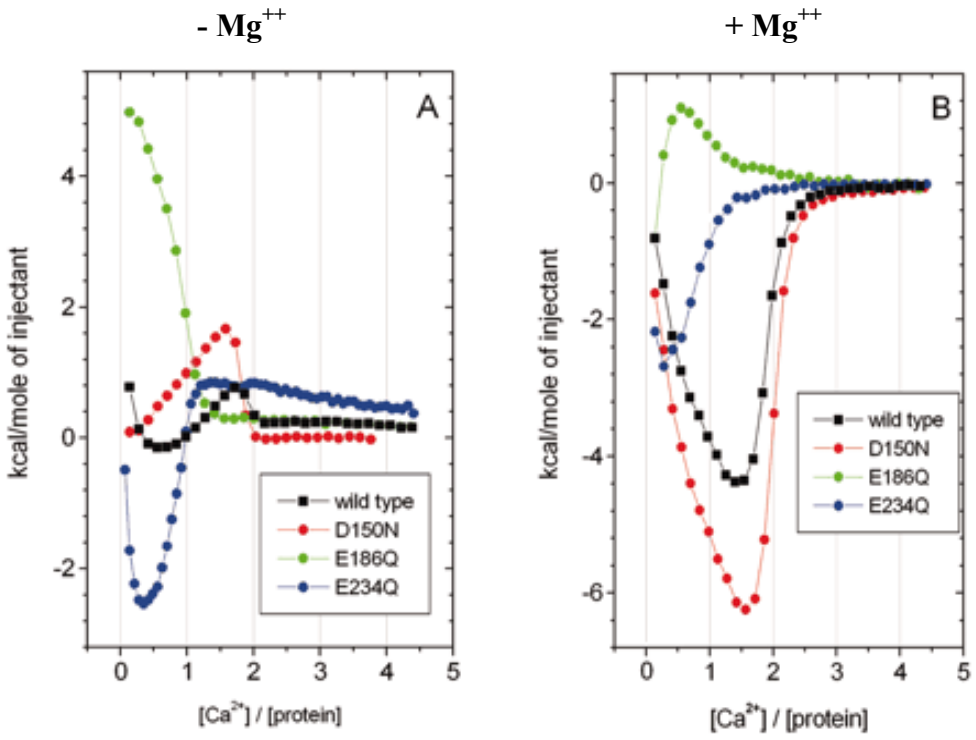

Figure 2-7: Comparison of Ca^{++} binding isotherms for DREAM-C and EF-hand mutants (D150N, E186Q, and E234Q). Ca^{++} binding isotherms of apoDREAM-C (without $MgCl_2$) and Mg^{++}-saturated protein (5 mM $MgCl_2$) are depicted in *A* and *B*, respectively. Wild-type DREAM-C, D150N, E186Q, and E234Q are shown in *black, red, green*, and *blue*, respectively. Figure and legend reproduced from [123].

DREAM protein is unable to bind Ca^{++} due to unfavorable substitutions in metal coordinating loop (fig.2-3, 2-4), EF-2 is concluded to be a low affinity Ca^{++} site for two reasons. They are- 1) DREAM binds two Ca^{++} ions, in equilibrium binding experiments, in the presence of physiological levels of Mg^{++} (fig.2-4), as disabling a bidentate coordination at loop position 12 in EF-2 primary sequence (Asp150 in DREAM as opposed to Glu in canonical EF hand sequence, fig.1-8) increases selectivity of this EF

hand to Mg^{++} rather than Ca^{++}. 2) Substitution of acidic Asp side chain at loop position 12 in EF-2 with Asn completely abolishes low affinity binding of Ca^{++} to apo-D150N mutant as compared with wild type in ITC experiments (fig.2-7A).

The Ca^{++}-binding isotherms of apo-E186Q (EF-3 mutated) and apo-E234Q (EF-4 mutated) exhibit two phases that correspond to a stoichiometric binding of a single Ca^{++} ion followed by low affinity binding to EF-2 (see above). The high affinity site of EF-3 mutant is strongly endothermic ($K_d \sim 1$ μM and ΔH = +5.2 kcal/mol) assigned to EF-4 binding Ca^{++}, while that of EF-4 mutant is exothermic ($K_d \sim 1$ μM and ΔH = -2.4 kcal/mol) assigned to EF-3 binding to Ca^{++}. Stoichiometric calcium binding to all the mutants and the resemblance of mutant isotherms with different phases in wild type isotherm indicates that binding to each site is independent of the others and that binding occurs in a sequential manner. The initial phase of wild type binding isotherm (0-1 equivalents) resembles that of E234Q and the later phase from 1-2 equivalents, resembles that of E186Q followed by non-stoichiometric binding in both the mutants similar to wild type. In addition, the binding isotherm of D150N from 0-2 equivalents closely resembles that of wild type, save for the initial endothermic phase which suggests a possible structural interaction between EF-2 and EF-3 that is abolished in D150N mutant. The lack of cooperative binding of calcium to the apo-DREAM-C indicates an unstructured protein devoid of long-range contacts that are required to stabilize the tertiary structure. The NMR studies described in Osawa et al. (2005)[123] indeed show poor chemical shift dispersion that is a hallmark of an unstructured protein (fig.2-9A). Thus, stoichiometric Ca^{++} binding to DREAM occurs in an orderly fashion first to EF-3 followed by EF-4.

Exothermic Ca^{++} binding to EF-3 and a 'U' shaped isotherm suggests a possibility of coupled equilibrium reactions that involve metal binding and concomitant protein conformational changes. In ITC experiments, the measured ΔH is a combination of ΔH of Ca^{++} binding that primarily involves dehydration of the ion and the ΔH of metal-induced conformational changes in DREAM protein. While dehydration of metal ion is an entropy driven process (increased randomness of solvent molecules after dehydration), protein conformational changes involve change in enthalpy (since a conformational change involves changes in hydrogen bonds, vanderwaal's interactions) [175]. Thus, since enthalpy changes of Ca^{++}, binding to EF-3 (E234Q in fig.2-7A) is exothermic ($\Delta H<0$); a protein conformational change upon metal binding is indicated. Likewise, endothermic ($\Delta H>0$) Ca^{++} binding to apo-E186Q (fig.2-7A) suggests that metal binding to EF-4 is entropy driven. Indeed, NMR studies on calcium bound DREAM show drastic conformational changes when compared with the apo-DREAM in the absence of metal ions and Ca^{++}-free DREAM, in the presence of Mg^{++} (see below fig.2-9A and B).

Thus, the wild-type DREAM-C has a low affinity (EF-2) and two high affinity calcium sites (EF-3 &4). Craig et al. (2002) showed that DREAM binds four calcium ions in their studies on DREAM protein using mass spectrometric methods suggesting that EF-1 might bind calcium as well [173]. However, the primary sequence of the first EF hand contains unfavorable substitutions (*e.g.* Cys-104, Pro-105, and Thr-113) that disable metal binding to EF-1 as shown in other NCS proteins [126, 128] (also see section 2.1). Consistent with these observations, our studies also do not observe calcium binding to EF-1 or the enthalpy of binding is zero. The apparent discrepancy in the mass spectrometry study may be due to enhanced affinity of DREAM towards calcium in the

gas phase species. Hence, under physiological conditions EF-1 does not bind Ca^{++} as indicated by previous equilibrium binding studies (fig.2-4) as well as ITC measurements in the present study (fig.2-7A)

2.3.2 Constitutive Mg^{++} binding at EF-2

The primary sequence of the EF-hand loop in EF-2 contains an Asp at the 12-position, instead of the well-conserved Glu, which increases its selectivity to magnesium [176]. When ITC experiments were performed by titrating Ca^{++} into the protein samples in the presence of physiological levels of Mg^{++} (fig.2-7B), the isotherms obtained differed remarkably from those in the absence of Mg^{++} (fig.2-7A). The isotherm of EF-2 mutant strongly resembles that of the wild type with a binding stoichiometry of two, as opposed to at least three Ca^{++} in the absence of Mg^{++}. The EF-3 and 4 mutants show one high affinity site each in the presence of magnesium, meaning that in the presence of magnesium DREAM-C can bind only two calcium ions with high affinity, to EF-3 and EF-4. Furthermore, the low affinity calcium binding observed in the wild type and EF-3 and 4 mutant isotherms, in the absence of magnesium is completely abolished in all mutants, in the presence of magnesium.

Taken together these observations imply that EF-2 constitutively binds Mg^{++} in the physiological conditions (with 5mM Mg^{++} and 0.1-100 μM Ca^{++}) and does not bind calcium in the presence of Mg^{++}. The shorter side chain of aspartate at the 12^{th} position in the metal coordinating loop favors magnesium binding rather than calcium binding as observed in other EF-hand proteins [129] (see section 2.1). However, it must be noted that the presence of Asp at loop position 5 will also lead to selective binding of Mg^{++} to

EF hand suggesting other residues in the EF hand loop also govern ion-selectivity [177]. Constitutive Mg^{++} binding to DREAM stabilizes the protein structure, as seen from NMR studies of James Ames and Masanori Osawa (fig.2-9) and might be important in its interaction with DNA targets.

The wild type calcium-binding isotherm obtained in the presence of Mg^{++} does not represent a linear combination of the mutant isotherms (Fig 2-7B). Thus, calcium binding to EF-3 and 4 does not represent two independent sites, suggesting some kind of cooperativity between the two sites because of Mg^{++} binding to DREAM. Magnesium binding confers stability to the protein structure, as seen in the NMR studies of Osawa et al [123], which might promote structural interaction between EF-3 and 4 as seen in the crystal structures of other EF hand proteins [126, 128, 135]. The recent crystal structure of KChIP1, a related NCS protein [128] shows calcium bound to only EF-3 and 4. The extensive contacts between the EF-3 and 4 may act as a switch that controls calcium-sensitive DNA binding of DREAM, as suggested previously [74, 130].

2.3.3 DREAM-C has a high affinity Mg^{++} site

The difference in the calcium-binding isotherms in the absence and presence of Mg^{++} at physiological levels motivated us to study the magnesium binding properties of DREAM protein. Hence, we tested magnesium binding to DREAM-C using ITC (fig-2-8). Not surprisingly, the isotherm when fitted by a two-site model showed an exothermic binding to a single Mg^{++} and an endothermic binding that represents two or more Mg^{++}. The exothermic phase from 0-1 equivalents of the isotherm represents binding of a single Mg^{++} followed by non-stoichiometric endothermic binding of Mg^{++} (*i.e.* 1 or more Mg^{++}

with K_d > protein concentration used for ITC). Analysis of the binding isotherm using a "two site" model (Microcal Origin software) revealed that DREAM-C has one Mg^{++} site with relatively high affinity (dissociation constant of 13 μM and ΔH = -0.79 kcal/mol), and two or more sites with much lower affinity (K_d in the millimolar range and ΔH = +3.97 kcal/mol).

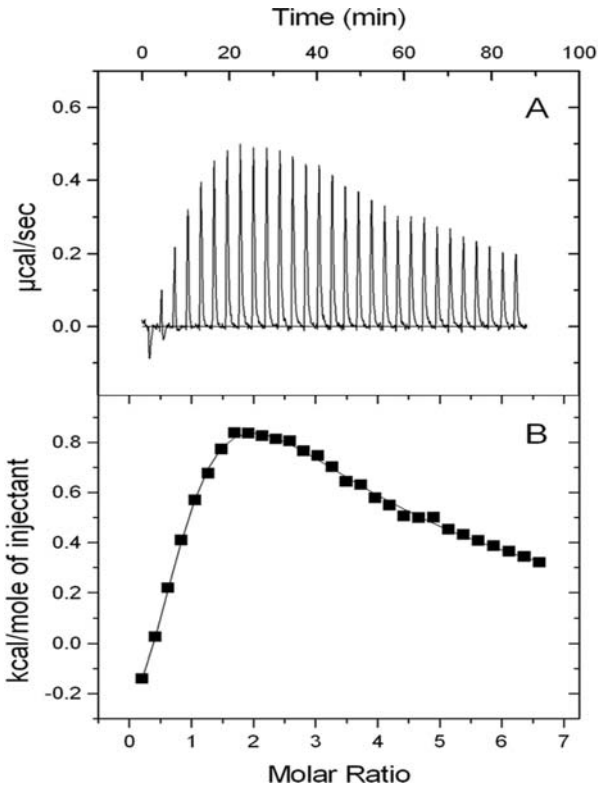

Figure 2-8: Isothermal titration microcalorimetric analysis of Mg^{++} binding to DREAM-C: Trace of the calorimetric titration of 29 x 10-μl aliquots of 2.0 mM $MgCl_2$ into the cell containing 69 μM apoDREAM-C (*A*) and integrated binding isotherm (*B*). The binding isotherm in *B* was fit using a two-site model where $n_1 = 0.91 \pm 0.01$, $K_1 = (7.5 \pm 0.7) \times 10^4$ [M^{-1}], $\Delta H_1 = -791 \pm 90$ [cal·mol^{-1}]; $n_2 = 2$ (fixed), $K_2 = (4.3 \pm 0.2) \times 10^3$ [M^{-1}], $\Delta H_2 = (3.97 \pm 0.06) \times 10^3$ [cal·mol^{-1}]. Figure and legend reproduced from [123].

2.3.3 Calcium- and magnesium-induced conformational changes

EF hand proteins well characterized so far for their Mg^{++} binding properties, calmodulin and parvalbumin, exhibit endothermic binding to Mg^{++} [175, 178]. Exothermic binding of Mg^{++} to DREAM suggests structural changes induced upon binding to magnesium.

Calcium-integrin binding protein (CIB), an EF hand protein family member, also exhibits significantly low ΔH that was explained by enthalpic cancellation between metal binding and concomitant structural changes in the protein [177]. To monitor protein conformational changes in a more direct manner, NMR studies on DREAM protein (performed by Masanori Osawa) show that both magnesium and calcium binding to DREAM lead to dramatic changes in the NMR spectra (Fig. 2-9). The NMR spectrum of apo protein exhibits broad resonances with very narrow chemical shift dispersion, indicating an unstructured molten-globule state. By contrast, the spectra of both Mg^{++}-bound and Ca^{++}-bound states exhibit sharper peaks with much greater chemical shift dispersion, consistent with the formation of stable tertiary structure. (turn overleaf for fig.2-9).

Size-exclusion chromatography studies and dynamic light scattering analysis both indicate that DREAM and all the EF-hand mutants are monomeric in solution in the presence of Mg^{++} (and absence of Ca^{++}), whereas Ca^{++}-bound DREAM forms a stable dimer (Fig. 2-10). A similar Ca^{++}-induced dimerization has been reported previously for other recoverin-like proteins such as neurocalcin [127] and KChIP1 [128]. The calcium-induced dimerization of DREAM is consistent with the recent crystal structure of Ca^{++}-bound KChIP1 that shows a stable dimer structure in the asymmetric unit [128].

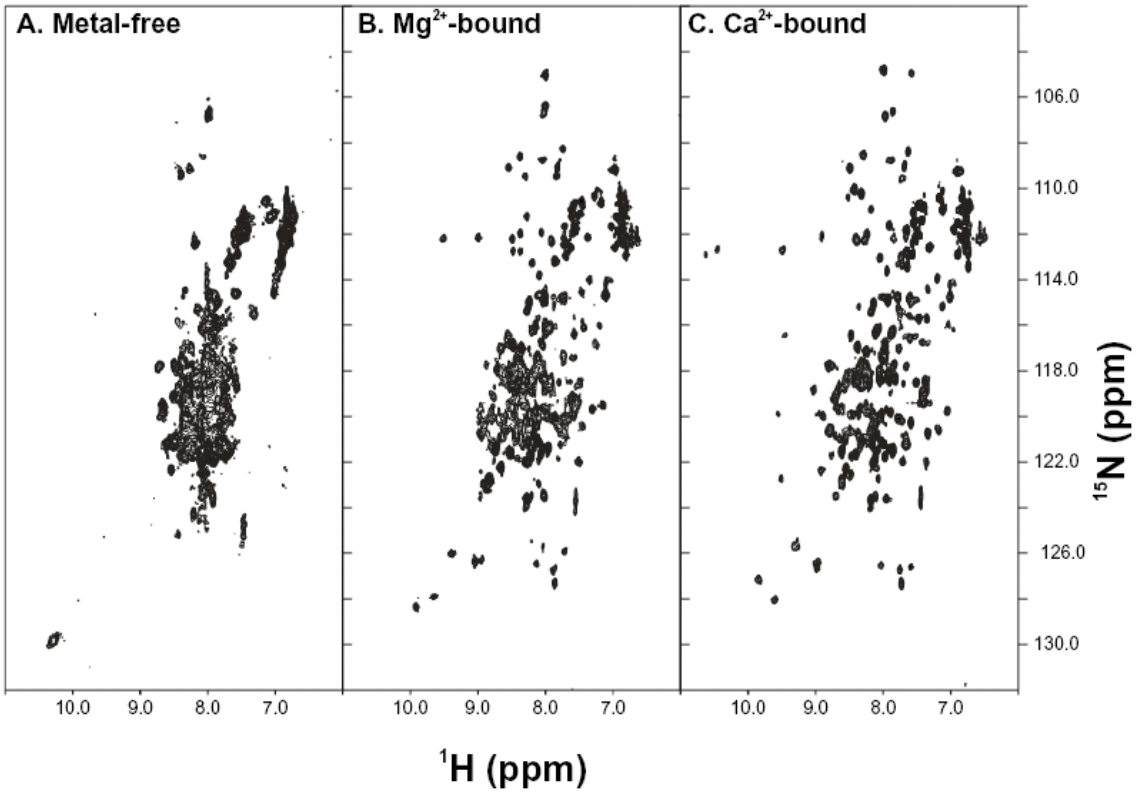

Figure 2-9: Two-dimensional 15N-1H HSQC NMR spectra of DREAM. NMR spectra of apo-DREAM-C (A), Mg++-bound DREAM-C (B), and Ca++-bound (C) DREAM-C. Each protein sample was uniformly labeled with nitrogen 15, and spectra were recorded at 600-MHz 1H frequency. Figure and legend reproduced from [123].

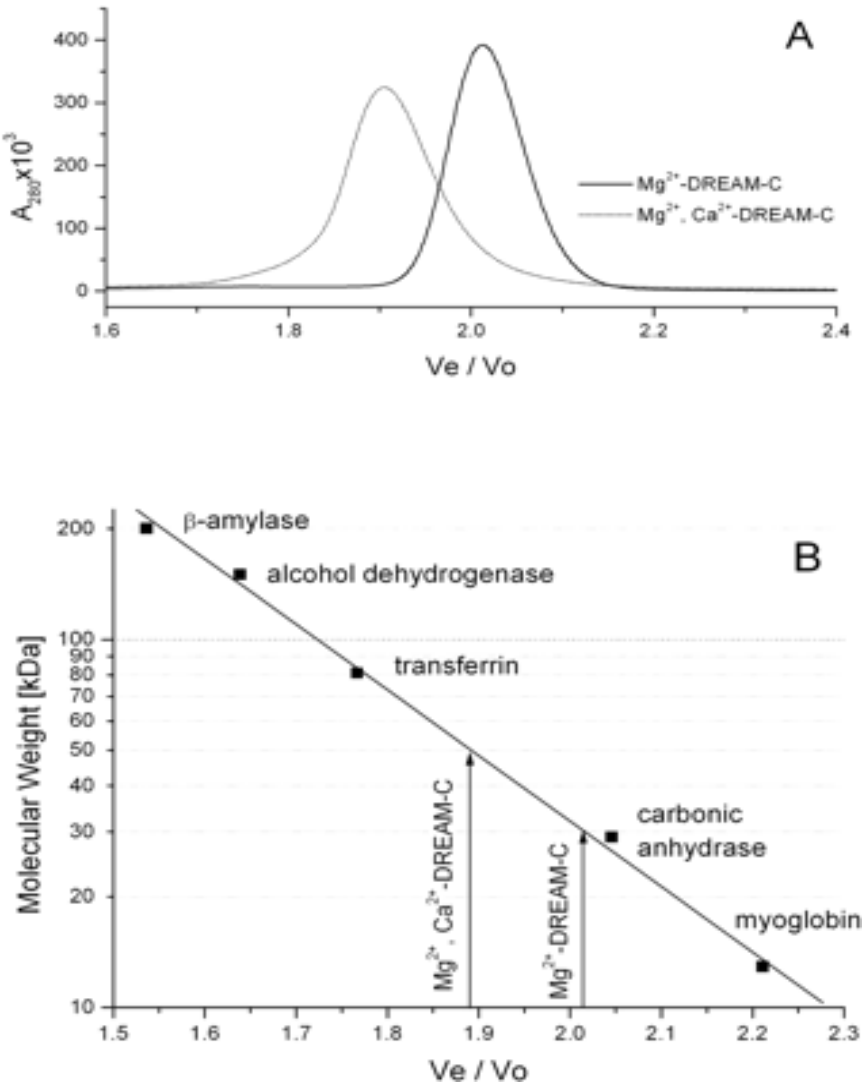

Figure 2-10: Molecular weight estimation of DREAM-C by size exclusion chromatography (SEC). *A*, size exclusion chromatograms of Mg^{++}-(*solid line*) and Mg^{++}/Ca^{++}-DREAM-C (*dotted line*). 100 µl of 200 µM protein solution were applied onto Superdex 200 HR (10/30) column (Amersham Biosciences) pre-equilibrated with the buffers containing 10 mM Hepes·NaOH (pH 7.6), 150 mM NaCl, 5 mM $MgCl_2$, 1 mM dithiothreitol, and 1 mM EGTA or 5 mM $CaCl_2$ for Mg^{++}-DREAM-C and Ca^{++}-DREAM-C, respectively. *B*, the standard curve for the molecular mass determination was created using β-amylase (200 kDa), alcohol dehydrogenase (150 kDa), transferrin (81 kDa), carbonic anhydrase (29 kDa), and myoglobin (17 kDa). Void volume of the column (*Vo*) was obtained as 7.81 ml using blue dextran (2000 kDa), and *Ve* is a volume of elution of each sample. *Arrows* indicate *Ve/Vo* values for Mg^{++}- or Ca^{++}-bound DREAM-C (50 µM). The molecular mass based on amino acid sequence of DREAM-C is 25 kDa. Estimated mass of Mg^{++}-DREAM-C : 30 kda (slightly higher apparent mass may be due to shape effects of the protein); Mg^{++}-Ca^{++}-DREAM-C: 50 kda. Metal binding to His-tag was previously shown to be negligible [170]; proteins were expressed in bacteria exactly as mentioned in the methods section above. Figure and parts of legend sourced from [123].

2.3.4 DNA Binding by EF-hand mutants

Electrophoretic mobility shift assay on the single EF-hand mutant proteins (Fig.2-11), by Kit Tong and Alexandra Dace, shows that all the mutants bind to DNA under the conditions previously described for wild type DREAM [74, 130]. The EMSA bands for each of the mutants disappear upon the addition of saturating Ca^{++}, suggesting the Ca^{++}-bound forms of mutants (similar to wild type) do not bind to DNA. These results suggest that binding of calcium to either EF-3 or EF-4 is sufficient to abolish DNA binding [123].

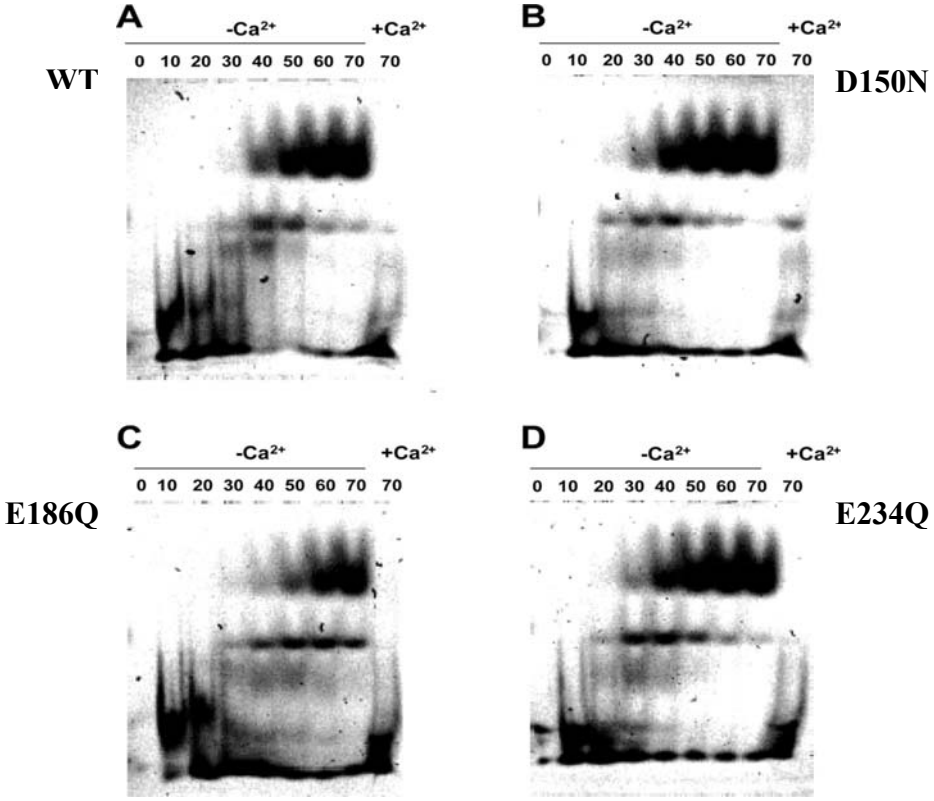

Figure 2-11. Fluorescence Electrophoretic mobility shift assay of DREAM-C/DRE interaction. 5 nM Cy5 labeled DRE oligonucleotide in 10 mM HEPES, pH 7.9, 2 mM dithiothreitol, and 8 mM Mg^{++} was incubated with 0–70 μM wild-type (*A*), D150N (*B*), E186Q (*C*), and E234Q (*D*) DREAM-C proteins expressed in bacteria exactly as mentioned in the methods section above, in the presence and absence of 10 mM Ca^{++}. Figure and legend sourced from [123]

2.3.5 Mechanism of Ca^{++}-sensitive DNA binding

The metal binding studies described above combined with previous studies on DREAM function can be summarized in the form of a model as shown in Fig.2-12. Magnesium bound DREAM in solution is a monomer, which binds to DNA as a tetramer at resting calcium levels and represses transcription [74, 130]. A rise in nuclear calcium concentration causes Ca^{++}-induced conformational changes in DREAM that promote dissociation of the tetramer into Ca^{++}-bound dimers that then dissociate from DNA and lead to derepression of transcription. The next chapters in this thesis attempt to identify the DNA binding residues/ motifs on DREAM protein to further test and refine this mechanism.

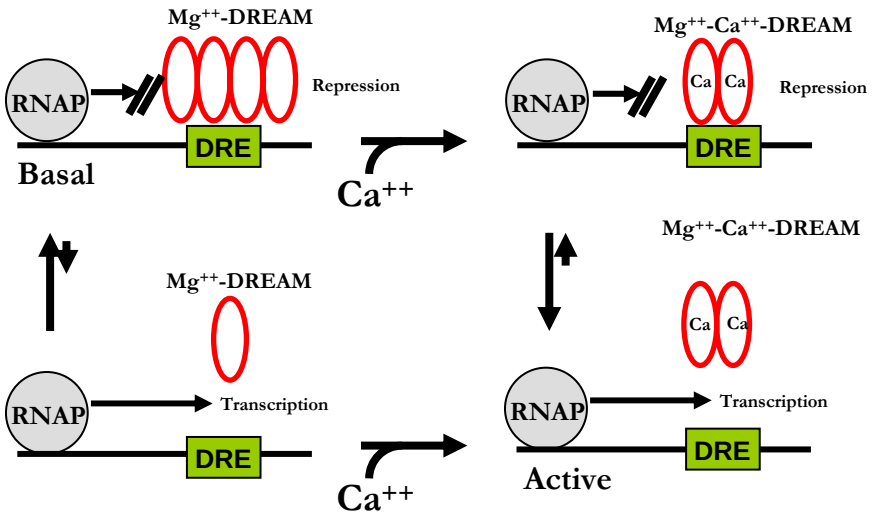

Figure 2-12: Schematic representation of calcium-sensitive DNA binding to DREAM. Figure courtesy: James Ames.

Chapter 3: Yeast one-hybrid study to map DNA binding residues in DREAM protein

3.1 Introduction

DREAM protein acts as a transcriptional repressor by physically interacting with a stretch of DNA, referred to as the Downstream Regulatory Element (DRE), that is present downstream of the transcription start site in the prodynorphin gene ([74], fig.3-1). DREAM provides a converging point between calcium and cAMP-mediated regulation of prodynorphin gene expression [74, 114]. Calcium binding to DREAM leads to its dissociation from DNA and hence derepression. DREAM affects gene expression through its interactions with α-CREM [142] and CREB [131] proteins that are modulated by cAMP-induced activation of protein kinase-A. While phosphorylation of α-CREM by protein kinase A (PK-A) is not essential for DREAM- α-CREM interaction, phosphorylated α-CREM interacts more strongly with DREAM and dissociates it from its DNA targets leading to derepression [142]. DREAM binds to CREB and impairs its ability to recruit CBP, in the absence of calcium, thus inhibiting CRE-dependent (cAMP response element) transcription [131]. More recently, DREAM is also reported to interact with C-terminal binding proteins [124] and repress transcription. Interestingly, DREAM also acts as transcriptional activator when it interacts with vitamin-D receptor [125]. Thus elucidating the mode of DNA recognition of DREAM protein would certainly help in understanding its effect on gene expression in relation to its DNA and multiple protein targets inside the nucleus.

Zaidi et al. (2004) showed that DREAM could translocate into nucleus under elevated calcium levels [141]. However, calcium binding to DREAM is not a prerequisite for its nuclear translocation as a mutant disabled for calcium binding also translocated to the nucleus [141]. In a study carried out to identify the key bases involved in binding to protein the sequence "GTCA" was reported to be important in specific DNA recognition by DREAM protein. Furthermore the nucleotide 'G' is the single most important determinant of the specificity [179]. Gel retardation experiments with mutated DRE wherein the 'G' is replaced with an 'A' show impaired DNA recognition by DREAM protein ([179], [130], Fig.3-1).

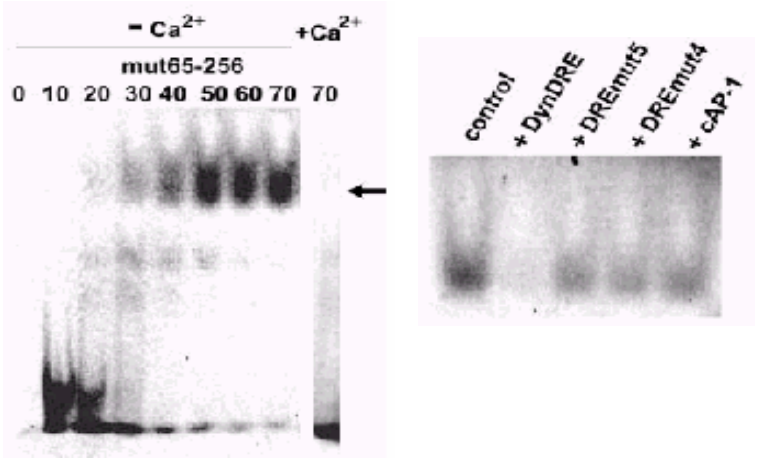

Dynorphin DRE:
5'-GAAGCCGGA GT CAAGGAGGCCCCTG-3
3'-TTCCGGCCT CA GTTCCTCCGGGGAC-5'
G→ A= DREmut5, GT→ AA= DREmut4

Figure 3-1 Electrophoretic mobility shift assay (EMSA) of DREAM devoid of the N-terminus in the presence and absence of calcium (left panel). The right panel shows the EMSA reactions where the labeled probe is competed with cold DRE, mutated DRE's (shown in the bottom panel, underlined residues mutated as described) and non-specific c-AP-1 DNA (Figure adapted from [130])

DREAM is believed to bind DNA as a tetramer, based on evidence from light-scattering studies performed on DREAM protein in solution with dynorphin and c-fos DRE elements[130]. These studies showed that the hydrodynamic radius of predominant species corresponds to a DREAM tetramer bound to DRE in a 1:1 stoichiometry. Other examples of proteins binding to DNA as tetramer include Arc repressor of phage P22 [180], p53 [181] and diphtheria toxin repressor [182]. The p53- DNA interaction comprises of two individual p53 dimers interacting with respective half-sites on DNA [181]. However, in the case of diphtheria toxin repressor two sets of homodimers contact DNA from both the sides and interact with two major grooves each on a 24 base DNA sequence [182]. Previous DNA binding studies on DREAM showed calcium sensitive binding to DNA [74, 130] at an approximate K_d = 30μM [130]. Lack of high-resolution structure of DREAM protein complexed with DNA impedes knowledge of its DNA recognition motif. Since the primary sequence of DREAM protein does not contain any known consensus DNA binding region, I proposed to identify the residues in DREAM protein responsible for DNA recognition using yeast-one hybrid method, a variant of yeast two hybrid [183]. Other methods to study protein-DNA interactions include gel-retardation assays, chromatin immunoprecipitation and DNA foot-printing using enzymes (DNAaseI, Exonuclease III) or chemical agents (hydroxyl radicals) [184-186]. More recently, mass spectroscopy was also described to be a robust way to characterize protein-DNA interaction [187-189]. However, the one–hybrid method is an efficient in vivo method and a high-throughput way of screening multiple single-site mutants of DREAM protein that are defective in DNA binding, hence identifying the specific

residues responsible for DNA recognition. The schematic illustration of the method is shown in the fig 3-2.

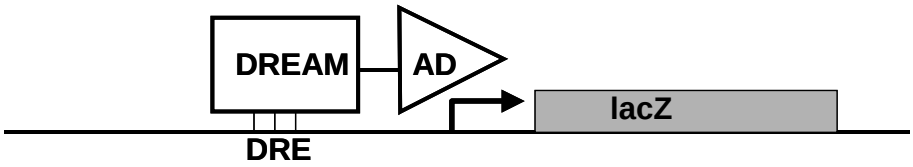

Figure 3-2: Matchmaker One-hybrid system for detecting DREAM-DRE interaction. Figure courtesy: James Ames.

3.2 Yeast one-hybrid

An interesting variant of the two-hybrid system [183], the yeast one-hybrid involves the fusion of a transcriptional activation domain to a putative DNA binding protein plus the target DNA binding element inserted upstream of a reporter gene. A positive protein-DNA interaction would result in activation of reporter gene transcription. The one-hybrid method can be used to identify unknown proteins that might bind to a known DNA element, unknown promoter elements to which a known protein with DNA binding activity could interact, and the residues in the protein that are responsible for protein-DNA interaction [190-192]. One-hybrid screens have been used to identify proteins that bind a TGFβ control DNA element [193], and to identify DNA binding residues in bovine papilloma virus E1 protein [194].

In order to embark upon screening single site mutants of DREAM protein, it must be established that DREAM-DNA interaction would prove to be a viable model to screen using the one-hybrid method. Hence I set out to perform the control experiment to test for

DREAM-DNA interaction using wild type DREAM protein fused with Gal4 or B42 activation domains and the DRE elements (either three tandem repeats or a single DRE site) inserted upstream of either the β-galactosidase gene or HIS3 reporter gene. If DREAM protein fused to the GAL4 activation domain interacts with the DRE element fused upstream of a reporter gene, the activation domain would drive the expression of the reporter gene, which can be observed when yeast strains containing the protein fusion and the reporter constructs are grown on selective media.

3.3 Materials and Methods

3.3.1 Yeast strains used in this study

YM4271 (Genotype: MATa, ura3-52, his3-200, ade2-101, ade5, lys2-801, leu2-3, 112,trp1-901, tyr1-501, gal4D, gal8D, ade5::hisG) Transformation Markers: trp1, leu2, ura3, his3) EGY48 (Genotype: MATa, his3, trp1, ura3, $LexA_{op(x6)}$-LEU2, Transformation Markers: his3, trp1, ura3).

3.3.2 Plasmid constructs used in this study

The vectors used in the one hybrid study, pJG4-5 (invitrogen), pLacZi (Clontech) and plasmids with protein fusion in pJG4-5 and reporter constructs for positive control were kindly provided by Dr. Harold Smith. Plasmid maps are shown in the fig 3-3. Plasmid constructs used in this study are shown in Fig. 3-3. DREAM ORF sequence amplified by PCR using oligos (forward primer: 5′-AAA AGA ATT CAT GCA GAG GAC CAA GGA AG-3′, reverse primer: 5′-AAA AGT CGA CCT CGA GTT ACT AGA TGA CGT TCT C-3′) and pet15b-DREAM (obtained from M. Ikura) as template. After

digestion with EcoRI and SalI, the PCR products were fused in frame with the B42 activation domain in the pJG4-5

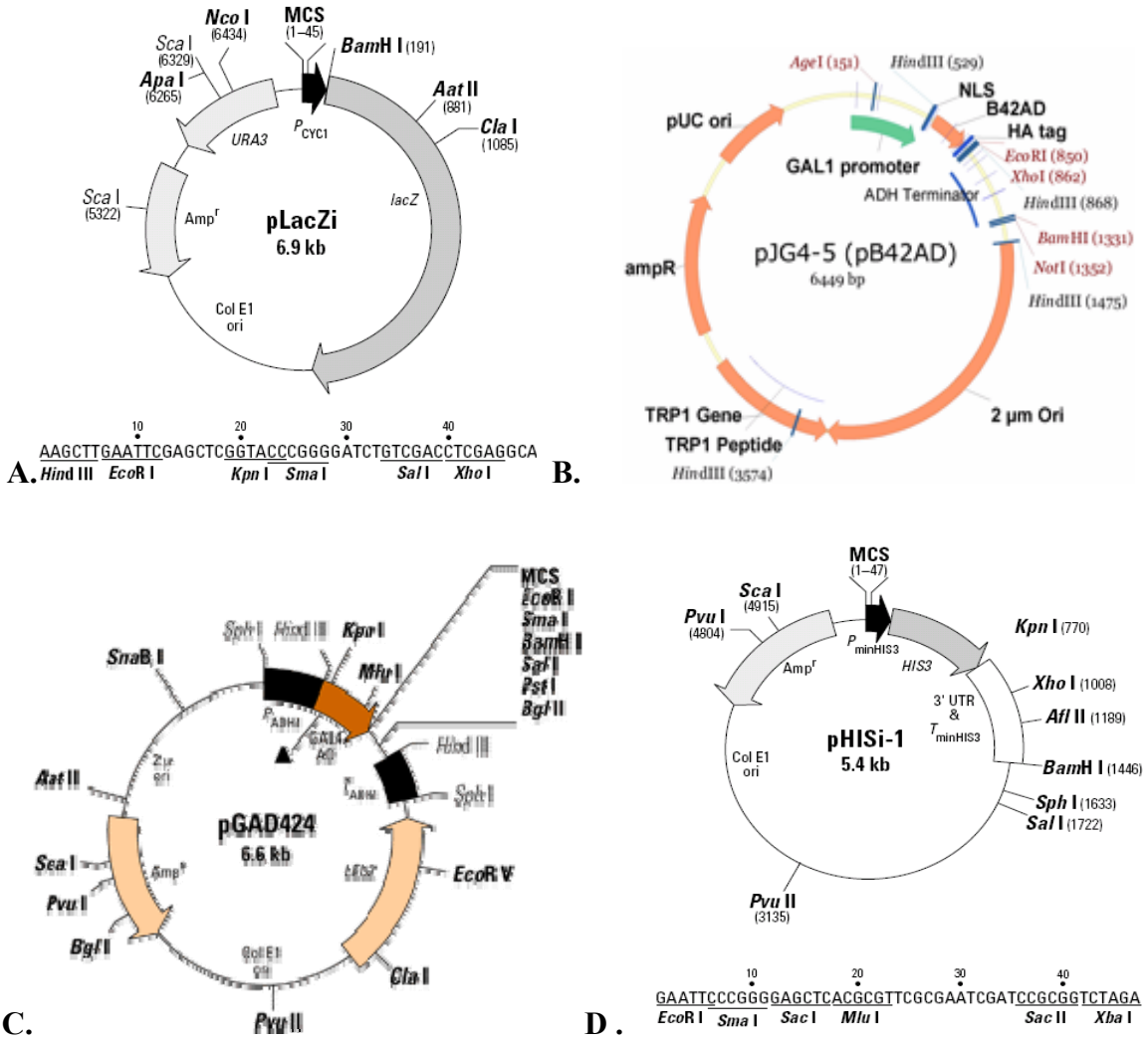

Figure 3-3: Plasmid maps of vectors used in the one-hybrid study (A,C,D:[195]; B:[196]),

vector at EcoRI and XhoI sites and Gal4 activation domain in pGAD-424 at EcoRI and SalI sites. DRE oligos (Lac-DRE) with three tandem repeats of DRE site (sense: 5′-AAT TCA TCG ATG CCG GAG TCA AGG CCG GAG TCA AGG CCG GAG TCA AGG-3′ Antisense: 5′-TCG ACC TTG ACT CCG GCC TTG ACT CCG GCC TTG

ACT CCG GCA TCG ATG-3′) and single DRE site (sense: 5′-AAT TCA TCG ATG CCG GAG TCA AGG-3′antisense: 5′-TCG ACC TTG ACT CCG GCA TCG ATG-3′) were first annealed were annealed by heating to 95 ^{o} C and slowly cooling to room temperature. The annealed oligos were cloned into pLacZi at EcoRI and SalI sites. His-DRE oligos (sense: 5′-AAT TCG TCG ACG CCG GAG TC A AGG CCG GAG TCA AGG CCG G AG TCA AGT-3′ and antisense: 5′-CTA GAC TTG ACT CCG GCC TTG ACT CCG GCC TTG ACT CCG GCG TCG ACG-3′) were annealed similar to the Lac-DRE oligos. The annealed oligos were cloned into pHisi-1 vector digested with EcoRI and XbaI enzymes. All bacterial transformants were selected on Luria-bertani media supplemented with 100 μg of ampicillin.

3.3.3 Yeast transformation

Transformation of yeast strains was performed as described by the manufacturer recommended protocol ([197], small-scale yeast transformation). Colonies from freshly streaked YPAD (see section 3.3.4) plates were inoculated in 10 ml cultures and grown overnight at 30^{o} C (~OD_{600} > 1.5). Cultures were then diluted into 50ml or 100 ml of fresh media until the OD_{600} = 0.2-0.3 and grown for additional 2-3 hours at 30^{o} C, until OD_{600} = 0.4-0.6. The cells were then harvested by spinning the cultures at 1000 x g for 5 min at room temperature followed by washes with sterile distilled water and 1x TE buffer (0.01 M Tris-HCl, 1 mM EDTA, pH 7.5 sterile). The final cell pellet is resuspended in 0.5 ml of sterile and freshly prepared 1x Lithium acetate (0.1 M Lithium acetate (LiOAc), sterile). 0.1 ml of the cell suspension was used for a single yeast transformation reaction. 0.1 ml of the yeast cell suspension was added to 0.1 μg (1 μg in the case of reporter

plasmid as it involves genomic integration) of plasmid DNA and 100 µg of sonicated salmon sperm DNA (used as carrier DNA). After mixing thoroughly using a pipette, 0.6 ml of PEG/TE/LiOAc solution (40% polyethylene glycol (PEG), 0.01 M Tris-HCl, 1 mM EDTA, pH 7.5, and 0.1M lithium acetate) was added to the mixture and mixed using the vortexer. This reaction mixture was then incubated by shaking at 230 rpm on a shaker at 30^{o} C for 30 minutes. After addition of 70µl of DMSO, the transformation reaction was subjected to heat shock at 42 ^{o} C for 15 min. The cells were then placed on ice for 2 min and spun at 14,000 rpm for 5 seconds. The supernatant was decanted and the cells resuspended in 0.5 ml 1x TE. 100 µl of the suspension was then plated on selective media to screen for transformants and incubated at 30^{o} C for 2-4 days.

Yeast transformations were carried out sequentially, first with the reporter plasmid (corresponding to pLacZi or pHisi-1 vectors) followed by the protein expression plasmid (corresponding to pGAD-424 or pJG4-5 vectors). The reporter plasmids were linearized by restriction digestion (NcoI digestion of pLacZi and XhoI digestion of pHisi-1 reporter vectors) before using for transformation. Yeast strains transformed with pLacZi reporter vectors were selected in synthetic dropout media devoid of uracil, and transformants containing pGAD424 and pJG4-5 plasmids were selected in media devoid of leucine and tryptophan respectively. Double transformants were selected using media devoid of uracil and tryptophan. The double transformants thus obtained were patched onto the selective media to observe the reporter gene expression.

3.3.4 Yeast media preparation

Synthetic dropout media were prepared to select transformants containing the respective plasmid constructs harboring the selective marker as described in the Clontech yeast protocols handbook [197]. YPAD contains 20 g/L Difco peptone, 10 g/L Yeast extract, 20 g/L glucose and 20 g/L Agar (for plates only) supplemented with 20mg/L of adenine. Synthetic dropout media were prepared with a base of 5 g/L of ammonium sulfate, 1.7 g/L of yeast nitrogen base (without amino acids and ammonium sulfate), 2% glucose, 2% Agar (for plates only) combined with a 0.6 g/L of SD/ DropOut powder commercially obtained from clontech (–His/–Leu/–Trp/–Ura DO Supplement Cat # 630425). Except for the selective marker required for transformed plasmids (pLacZi: uracil, pHisi-1: histidine, pGAD424: leucine, pJG4-5: tryptophan) the other missing components were added to the media in tiny amounts in approximation. Where mentioned, when His reporter strains are screened, the selective media also contained 15mM, 30mM, 45mM, or 60 mM 3-amino triazole which inhibits leaky expression of the *His3*-reporter gene. X-Gal indicator plates contained 2.8 mM KH_2PO_4, 4.2 mM $K_2HPO_4.3H_2O$ and 2% galactose plus 1% raffinose instead of glucose. pJG4-5 has a galactose-inducible promoter that only expresses the fusion protein in the presence of galactose as a carbon source and is inhibited by glucose. For screening healthy strains from stocks contaminated with 'petite' mutants [198] the stocks were streaked onto media with ethanol and glycerol as carbon source (YPEG media 20 g/L Difco peptone, 10 g/L yeast extract, 3% v/v glycerol 2% v/v ethanol and 20 g/L Agar supplemented with a speck of adenine).

3.3.5 Colony lift filter assay

Double transformants containing the *lacZ* reporter vectors and protein expression vectors were patched onto a fresh double dropout plate. These plates were then incubated at 30^{o} C for 2-4 days. A sterile Whatman #5 filter paper was pre-soaked in 5 ml of Z buffer/ X-gal solution [16.1 g/L Na_2HPO_4. $7H_2O$, 5.5 g/L NaH_2PO_4. H_2O, 0.75 g/L KCl, 0.246 g/L $MgSO_4$. 7H2O, pH 7.0, + 1.67 ml of 20mg/ ml stock solution of X-gal (5-bromo-4-chloro-3-indolyl-β-D-galactopyranoside) dissolved in N,N-dimethylformamide (DMF)] in a clean petri plate. Colonies were lifted using a clean and dry filter paper, the orientation marked and the filter immediately immersed in liquid nitrogen colony side up for 10 sec. The filter was then thawed and placed on the presoaked filter in Z-buffer/X-gal solution colony side up, incubated at 30^{o} C, and observed every 5 min to check for blue coloration.

3.3.6 Test for protein-DNA interaction in the yeast

DNA binding was screened using blue-white colony screening on double dropout media containing X-gal, galactose, and raffinose as carbon source (SD/-ura/-trp/X-gal: SD media + 10 ml of 10X KPO_4 stock buffer (3.8 g KH_2PO_4, 9.58 g K_2HPO_4.3H2O in 100 ml distilled H_2O) + 10 ml of 10X galactose/raffinose solution (20 g galactose, 10 g Raffinose in 100 ml distilled H_2O), as pJG4-5 vector has an inducible promoter that activates protein expression in the presence of galactose as carbon source.

3.4 Results

3.4.1 DRE reporter yeast strains exhibit high background expression under different reporter systems

Three tandem repeats of DRE element, $(5'\text{-GCC GGA GTC AAG G -}3')_3$, were inserted upstream of β-galactosidase in pLacZi plasmid (see section 3.3). When this reporter plasmid was co-transformed into yeast (YM4271 strain) along with pGAD-DREAM plasmid that contains DREAM protein fused to Gal4 activation domain, a successful interaction between DREAM and DRE would lead to activation of the reporter gene by the Gal4 activation domain. Thus, the assay helps monitor the reporter gene expression by using X-gal as substrate for β-galactosidase (LacZ) reporter gene expression. β-galactosidase is an enzyme that is a product of LacZ gene in the lac operon, which can hydrolyse the colorless X-gal (5-bromo-4-chloro-3-indolyl-β-D-galactoside) substrate to give a blue coloration to the colony [1].

Initial experiments were carried out, with reporter plasmids containing three tandem copies of the DRE element, to increase the probability of DREAM-DRE interaction. A yeast reporter strain transformed with the reporter vector devoid of DRE was used as a negative control. The yeast strain that contains p53Blue and pGAD53m plasmids, harboring a p53-specific DNA element in pLacZi vector and p53 protein in pGAD424 vector respectively, was used as positive control. The colony lift filter assay was performed to detect expression of the lacZ reported gene (Fig.3-5). The positive control reporter strain exhibited blue coloration after ~30 min from the incubation start time (spot 8 in fig. 3-4). After ~ 70 min, all the three strains harboring the DRE in their reporter plasmids exhibited blue coloration (spots 1, 2, 3 in fig.3-4). In contrast, none of the

strains containing the empty reporter vector, pLacZi (spots 4, 5, 6 in fig.3-4), exhibited blue color even after two hours of incubation at 30^{o} C. Thus, the Downstream Regulatory Element (DRE) is activating lacZ reporter gene expression spuriously and hence cannot be used to assay DREAM binding activity.

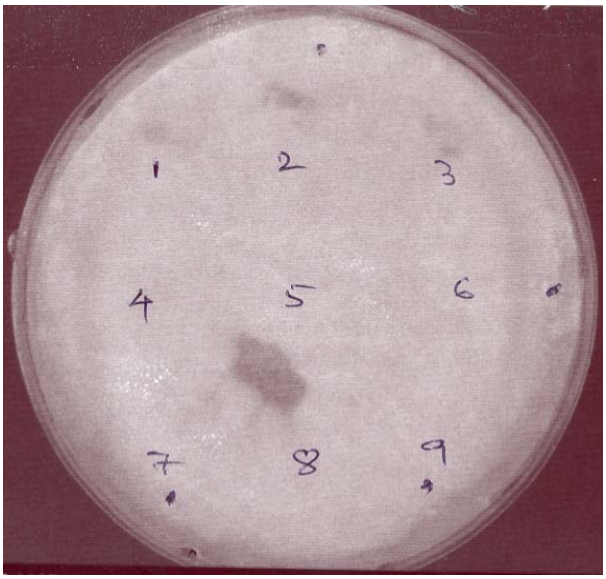

Figure 3-4: Colony lift filter assay of yeast double transformed reporter strains (host: YM4271). 1,2,3 show the pLac-DRE reporter strains transformed with pGAD-424, pGAD-DREAM and pGAD-53m protein plasmids respectively. 4,5,6 show pLacZi reporter strains and 7,8,9 show p53Blue reporter strains transformed with each of the three protein plasmids respectively. The picture was taken between ~70-75 min after the start of incubation at 30^{o}C, the dark spots indicate blue coloration of the yeast patches and positive reporter activity.

To overcome this problem, a His3 reporter gene was tested because background expression can be controlled by 3-amino triazole (3-AT). 3-AT is a histidine analogue that inhibits histidine biosynthesis by inhibiting the HIS3-encoded enzyme imidazole glycerol phosphate dehydratase, which is required in yeast for the synthesis of the amino acid histidine [199] [200]. In order to identify the concentration of 3-AT that sufficiently inhibits background growth on histidine-deficient media, each of the His3 reporter yeast

strains were grown in the presence of 15 mM, 30 mM, 45 mM, or 60 mM 3-AT on SD/-His medium. However, contrary to the expectation that 3-AT would inhibit background HIS3 expression leading to growth arrest, the reporter strains containing the DRE element showed robust growth even at 60mM 3-AT (Table 3-1). While the reporter strain with pHisi-1 alone ceased to grow at 60 mM 3-AT, the strains harboring the DRE element did not show growth arrest even at 60 mM 3-AT. The strains with p53-specific DNA element showed reduced growth at 60mM 3-AT.

3- AT concentration	**pHisi-1**	**pHis-DRE**	**p53His**
15 mM 3-AT	++++	++++	++++
30mM 3-AT	+++	++++	++++
45 mM 3-AT	+	++++	++
60mM 3-AT	-	++++	+

Table.3-1: Qualitative results in terms of cell viability in the presence of 3-AT, of the yeast reporter strains harboring His reporter plasmids (host: YM4271).

These results were attributed either due to overactive reporter due to the presence of three tandem copies of DRE element or leaky reporter gene expression from the results in the case of empty reporter vector. Hence, all the reporter plasmids were reconstructed with a single copy of DRE upstream of the reporter gene and used to test the protein-DNA interaction. At this stage, it became very difficult to work with the yeast strains as repeated transformations to obtain double transformants produced no colonies on the double dropout plates. This problem was possibly due to a mutation in the host strain that leads to a mitochondrial defect and slows down the growth rate dramatically. These

mutants are referred as “petites” [198]. Repeated attempts to rescue the strains by selecting for healthy strains on minimal media using glycerol and ethanol as carbon sources were unfruitful and eventually, the yeast strains we had even ceased to grow on rich media (YPAD). Hence, a different yeast strain, EGY48, was used in subsequent experiments.

3.4.2 DREAM cannot bind DNA in the one-hybrid:

In order to check the suitability of the yeast-one hybrid to test DREAM-DNA interaction, experiments were carried out using a different strain of yeast, EGY48. The experimental design was similar to previous set of experiments described in section 3.4.1. When the reporter yeast strain containing the DRE element (either single copy or three tandem repeats) inserted upstream of the lacZ reporter gene, was transformed with vector containing DREAM protein, and grown on selective media containing X-gal and galactose (to induce protein expression), there was no reporter gene expression, as observed by the lack of blue coloration (fig.3-5). The positive control containing the reporter and protein plasmids obtained from Harold Smith lab, showed blue coloration as expected (fig. 3-5). The absence of reasonable reporter gene expression in case of DREAM-DRE containing double transformant yeast strains points to a lack of or impaired interaction between DREAM and DRE. Effectively, this means that under the conditions of this assay system DREAM protein could not recognize the DRE element.

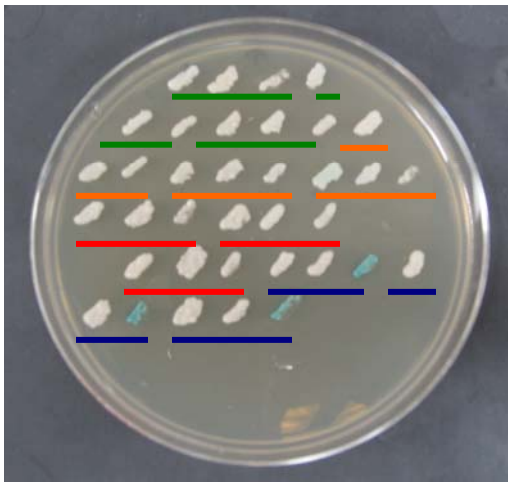

PV / RV	pJG4-5 E/O	pJG-DREAM E/O	pJG-HESp E/O
pLacZi	-/-	-/-	-/-
pLac-3DRE	-/-	+/-	-/-
pLac-1DRE	-/-	+/-	-/-
pLac-HESr	-/-	-/-	+/+

Figure 3-5: DREAM does not bind DNA in one hybrid. Right panel shows the experimental design where the columns correspond to the protein vector (PV) and rows correspond to reporter vectors (RV). Each successive three patches on the plate represent the three protein plasmids transformed into the designated reporter vector in triplicates (denoted by underlined colors; green: pLacZi; orange: pLacZi with three tandem copies of DRE fused upstream of reporter (lacZ); red: pLacZi with single copy of DRE fused upstream of reporter; blue: pLacZi with positive control reporter (HESr) fused upstream of reporter). Results are denotedby + for blue coloration indicative of reporter gene expression, - for no reporter expression. E/O indicates expected/observed results.

3.5 Discussion

Two different yeast strains, YM4271 and EGY48, used to test DREAM-DRE interaction showed different results in the yeast one-hybrid experiments. The difference in results can be explained due to differences in each of the yeast strains and the different methods used to probe DREAM-DRE interaction (colony-lift assay vs. blue-white colony screening respectively).While the experiments using YM4271 yeast strain resulted in spurious activation of reporter gene expression, experiments with EGY48 resulted in no activation of reporter gene expression. The spurious activation in strain YM4271 precludes any further analysis. However, there are a number of possible reasons for the apparent lack of DREAM-DNA interaction when using yeast strain EGY48. They are 1)

high resting calcium levels in yeast that might hamper its DNA recognition; 2) sequestration/inhibition by endogenous yeast factor; 3) insufficient DREAM protein expression; 4) possible degradation of DREAM protein; 5) disruption of DNA binding site due to fusion with B42 activation domain; and 6) mis-localization of DREAM protein, all of which can be tested experimentally.

While resting nuclear calcium levels in *Sacharomyces cerevesiae* are yet unknown, resting cytosolic calcium levels were shown to be in the 10^{-9} M range [37] at which concentrations wild-type DREAM is unable to bind calcium [123]. A one-hybrid experiment with a dominant-negative DREAM mutant that has its calcium binding sites impaired would address the problem with abnormal calcium levels in yeast. In the event the absence of reporter gene expression was due to high calcium in yeast, the dominant negative mutant, which is incapable of binding calcium, would prevent calcium-induced inhibition of DREAM-DRE interaction thereby leading to reporter gene expression.

DREAM is known to interact with various proteins that regulate transcription in eukaryotes ([124, 125, 131, 142]). Thus, it is quite possible that an endogenous yeast factor is sequestering DREAM protein from binding DNA by means of a physical interaction. A pull down experiment with lysates of yeast strains containing the expression plasmid harbouring DREAM ORF, using anti-DREAM antibody would address this problem. Pull-down of a yeast protein along with DREAM would imply sequestration of DREAM protein by an endogenous factor resulting in lack of reporter gene expression. Absence of a yeast protein in the pull-down experiment might indicate an additional possibility wherein the endogenous yeast protein directly interacts with the

DRE element, thus precluding DREAM binding to DRE and repressing the expression of the reporter gene. Similar experiments with the yeast strains used for hybrid with YM4271 as host strain would address if an endogenous factor were activating reporter gene expression either in conjunction with or independent of DREAM protein. The presence of blue color in all the reporter strains that contain the DRE element in the experiments involving YM4271 (fig.3-4) suggests a possible involvement of yeast endogenous factor that might be activating the reporter gene expression.

The one-hybrid experiment involves expression of DREAM protein in yeast. Failure to detect a DREAM-DRE interaction might imply low protein levels resulting due to insufficient protein expression or due to protein degradation. Expression of recombinant proteins in yeast may lead to activation of stress pathways, prime among which is the unfolded protein response [201] that may result in ER-associated degradation (ERAD) of recombinant protein. If DREAM fusion protein in yeast were expressed in an unfolded state, the protein might be degraded and hence unavailable for binding to the DRE. A western blot using anti- DREAM antibody, on the yeast protein extracts prepared from the reporter strains with DREAM plasmid grown in the presence of galactose and raffinose as carbon source would test the level of expression of DREAM in the yeast cells. Furthermore, the occurrence of degradation may be inferred if the anti-DREAM antibody recognizes low molecular weight polypeptides, representing DREAM degradation products, on the western blot.

Another distinct possibility that can explain the failure to detect DREAM-DRE interaction would be impaired nuclear translocation of DREAM in the yeast. DREAM

protein requires elevated levels of calcium in order to translocate into the nucleus, although not in a quantity where it can bind calcium itself [136]. Moreover, DREAM does not contain a nuclear localization signal and so might have to depend on other factors, as yet unknown, to translocate into the nucleus. It is plausible that such factors responsible for its nuclear localization in mammals are absent in yeast cell. Further, the protein folding resulting due to DREAM-B42AD fusion may result in masking of the nuclear localization signal in B42AD as well. Immunofluorescence experiments using anti-DREAM antibody would directly monitor the localization of DREAM protein in the yeast cell.

One drawback of the yeast-hybrid system stems from the possible misfolding of the protein because of fusion to the activation domain [202]. Thus, improper folding of DREAM protein when fused with B42 activation domain could have precluded its interaction with DRE in yeast. Misfolded proteins are generally prone to forming insoluble aggregates. Separation of soluble and insoluble fractions of the yeast lysates that contain DREAM expression plasmid coupled with a western blot on each of the fractions using anti-DREAM antibody would identify if the protein forms insoluble aggregates.

In summary, the yeast one–hybrid experiment carried out to test DREAM-DRE interaction could not detect binding as visualized by the absence of reporter gene expression. With multiple reasons possible for to explain this failure, experiments directed to probe each of these options deviate from the initial objective of mapping DNA binding residues in DREAM protein. Hence, an in vitro approach to probe the protein-

DNA interaction using chimeric protein constructs was adopted as an alternative method to identify the DNA binding motif in DREAM protein.

Chapter 4: Probing the DNA binding Site Structure of DREAM Using DREAM-Recoverin Chimeras

4.1 Introduction:

Protein-DNA interactions play a pivotal role in the regulation of life processes such as DNA replication, gene expression and chromosome maintainence. In response to external or internal stimuli, such as growth factors and metabolic stress respectively, there occurs a remarkable alteration in the protein-DNA "interactome" (the complete set of protein-DNA interactions in vogue at a given instant in space and time in the cell), thereby leading to changes in gene expression. A number of proteins (e.g. transcription factors and repressor proteins) contain specialized structural motifs such as helix-loop-helix [203], helix-turn-helix [204], leucine zipper and zinc finger [205] motifs in their tertiary structure that help in the recognition of DNA and regulate gene expression. These motifs recognize DNA via both direct and indirect interactions between the polar side-chains of amino-acid residues and the nitrogenous bases in DNA. Sequence-specific interactions are formed mainly by intermolecular hydrogen bonding and/or salt bridge interactions in the major groove [206]. Non-specific interactions with the phosphate backbone also contribute to the binding energy by inducing bending [207] or kinking [208] in the overall structure.

DREAM protein binds to a sequence of DNA referred as the Downstream Regulatory Element (DRE) ([74, 130] and fig. 3-1) and represses transcription of various genes such as prodynorphin [74], hrk [118] and calcitonin [119]. DREAM was shown to interact

with DNA using in vivo reporter assays that measured chloramphenicolacetyl transferase (CAT) [74, 179] reporter activity in neuronal cell lines [74, 179]. Ledo et al. (2000) characterized this interaction using mutated DRE probes and showed that the sequence 'GTCA' in DRE is the core element required for DREAM-DRE interaction. By generating single base mutations in this consensus sequence they report that the nucleotide 'G' is the single most important determinant that governs the protein-DNA recognition. Furthermore, DNA elements with an inverted GTCA core- ACTG, can also interact with DREAM [179] as is the case with c-fos DRE [74].

Much is known about the effects of DREAM-DNA interaction on gene expression [74, 119, 125]; however, the exact region of the protein structure that recognizes DNA is still unknown. Since an attempt to structurally characterize DREAM-DRE interaction using the yeast one-hybrid system failed to yield positive results (Chapter 3), I decided to probe the structure of the DNA binding site using chimeric protein constructs with specific regions of DREAM swapped with corresponding regions of recoverin. Recoverin is an EF hand calcium sensor protein in retinal rod cells [209] that has ~45% sequence identity to DREAM. Therefore, the main chain structures of DREAM and recoverin are expected to be very similar such that the swapping of individual EF-hands between recoverin and DREAM should cause a minimal perturbation to the overall structure. Although the main chain structures of recoverin and DREAM are very similar, their surface charge properties are clearly different. The surface of recoverin contains many negatively charged side chain groups of Asp and Glu, whereas the surface of DREAM is overall positive. The net negative surface of recoverin may explain recoverin's inability to bind negatively (-) charged DNA in the presence or absence of calcium (see section 4.3.5). In

addition, the calcium binding properties of recoverin vary from that of DREAM protein. EF hands 3 and 4 of DREAM are high affinity calcium binding sites and EF-2 is a magnesium binding site (see section 2.1), whereas EF-2 and EF-3 of recoverin bind calcium [210] and recoverin does not contain a specific magnesium-binding site (see section 2.1 for description). DREAM protein exhibits a calcium-induced dimerization, whereas recoverin does not (see section 4.3.3). Thus, generating DREAM-recoverin chimeras would not only alter the charge of the putative DNA binding site but also alter the metal binding and oligomerization properties of the protein as well.

In this study, I prepared a variety of chimeric constructs described below (Fig. 4-1) by systematically substituting each individual EF-hand of recoverin into DREAM. I report here my studies on these chimeric constructs designed to probe the structure of the DNA binding site and elucidate the calcium-dependent protein oligomerization properties. Previous in vitro studies on DREAM-C (C-terminal residues of DREAM, 65-256 comprising the four EF hands) showed that the N-terminal tail (residues 1-64) is not essential for functional DNA binding [130]. Hence, all the DREAM-Recoverin chimeras used in this study are generated devoid of the N-terminal tail region.

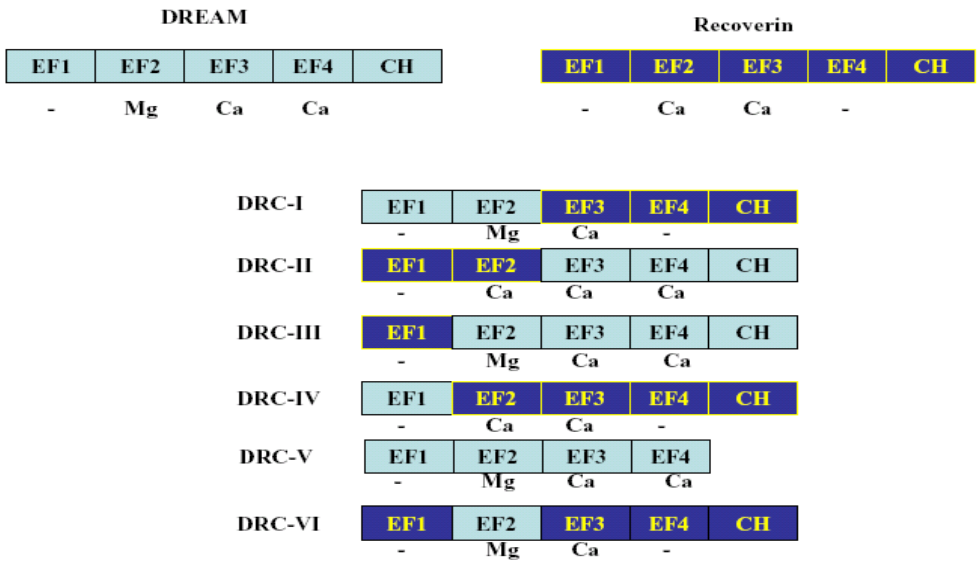

Figure 4-1: Schematic representation describing the generation of DREAM-Recoverin chimeras (DRC's). Affinity of EF hands to calcium or magnesium is indicated below each chimera. Black rectangles indicate the name of each protein, light turquoise rectangles indicate EF hands from DREAM and blue rectangles indicate EF hands from recoverin. (CH: C-terminal Helix).

4.2 Materials and Methods

4.2.1 Construction of DRC plasmids

Full- length cDNA constructs coding for DRC proteins were generated using two successive rounds of PCR amplification termed as SOEing (Splicing by Overlap Extension) as described previously [211]. DREAM cDNA cloned into pet15b was described previously [130] and recoverin cDNA cloned into pet11a was obtained from Nobuko Katagiri (CARB). Chimeric DRC fragments were cloned into pet15b at NdeI and XhoI sites. DREAM or Recoverin cDNA fragments were amplified using PCR using Pfu turbo DNA polymerase (Stratagene or recombinant enzyme prepared in Zvi Kelman lab) and oligos described in Table 4-1. Standard PCR conditions used are 1) 95 ^{o}C for 2', 2) 95 ^{o}C for 1', 3) 62 ^{o}C for 1', 4) 72 ^{o}C for 1' 5) linked to step 2) for 29 cycles. Following the final cycle an additional 10' of extension was done at 72 ^{o}C to ensure complete

extension of 3' termini. PCR products were purified either by Geneclean-II (Qbiogene) or by Wizard PCR purification kit (Promega) and quantified by ultra violet-spectrophotometry. An absorption spectrum from 240-340 nm was obtained and after correction for baseline, an OD260 of 1.00 was equated to 50 μg/ml of double stranded DNA. Equimolar amounts of DREAM and Recoverin PCR fragments (0.2pmol) were used as templates for a second round of PCR with forward and reverse primers of N-terminal and C-terminal halves respectively, thus generating full-length DRC DNA fragments. Pet15b vector DNA was sequentially digested with NdeI (New England biolabs) overnight followed by XhoI (NEB or Takara) digestion for 3-5 hours at 37 ^{o}C using compatible digestion buffers for each enzyme from NEB. The 5' phosphates were cleaved by incubating the double digested vector with Shrimp alkaline phosphatase (Amersham lifesciences) to prevent self-ligation of the vector during ligation. The purified DRC full-length PCR fragments were digested with NdeI and XhoI simultaneously for overnight at 37 ^{o}C using compatible digestion buffer from NEB (NEB-4). The digested pet15b vector and PCR products were then mixed in 1:5 (30 fmol: 150 fmol) ratio in a total volume of 5-7.5 μl and ligated at 16 ^{o}C for 1 hour after adding equal volume of solution I (2x ligation mix) from DNA ligation kit ver 2.1 from Takara Bio Inc. 10 μl of the ligation reaction was transformed into sub-cloning efficiency DH5α competent cells (GIBCO-BRL) and plated on LB media supplemented with 100 μg/ml of ampicillin and grown overnight at 37 ^{o}C. Positive clones were screened after minipreps using Wizard plus miniprep kit (Promega), by diagnostic double digest using NdeI and XhoI enzymes and confirmed by DNA sequencing. DRC's I-VI were assayed in the present study.

4.2.2 Expression and purification of wild type and DRC proteins

Positive clones for each of the protein constructs were transformed into BL-21 (DE3) singles (Novagen) and stock cultures were prepared from fresh colonies grown in 3 ml LB with 100 µg/ml ampicillin for 6-8 hours at 37 ^{o}C and divided into 1.25 ml aliquots. Each aliquot of stock culture was inoculated into 50ml of LB media with 100 µg/ml ampicillin and grown at 37 ^{o}C for 2.5- 3 hours. This pre-culture was then diluted to OD600= 0.01-0.05 into 1 liter of LB or M9 media (12.66 g $Na_2HPO4.7H_20$, 3.0 g KH_2PO4, 0.5 g NaCl, 1.0 g NH_4Cl, 0.2 g $MgSO_4$, 20 µl $CaCl_2$ per liter + 3g glucose in 50 ml H_2O (autoclaved separately)). The cultures were then grown for additional 2.5-3 hours or until OD600 = 0.5-0.8 and induced with 0.5mM of IPTG (Isopropyl beta-D galactopyranoside). Protein expression was allowed to proceed by growing the cultures at 37 ^{o}C for 3.5 hours or at 16 ^{o}C overnight. The cells were then harvested by centrifuging the cultures at 7000 rpm using JLA-8.1 rotor in Beckman Avanti J-20 XP centrifuge. The cell pellet was resuspended in 40 ml of Ni-NTA binding buffer (20mM Tris pH 8.0 (Sigma), 0.3M NaCl, 5mM Imidazole (Sigma), 10 % Glycerol (Fisher or Sigma), 2mM beta-mercapto ethanol (Sigma)) and flash frozen in liquid nitrogen or immediately proceeded with sonication. Frozen biomass was thawed and sonicated using Branson Sonifier (VWR) for 5 x 2' at 50% duty cycle and output 6. The lysate was then cleared of the membranes and other insoluble cell debris by ultra-centrifugation at 45,000 rpm for 1 hour in Ti-50.2 rotor in Beckman ultra-centrifuge. The centrifuged lysate was immediately applied onto HisTrap FF column (Amersham biosciences) pre-equilibrated with 100 ml dH_2O and 50-100 ml Ni-NTA binding buffer at 4 ^{o}C. $MgCl_2$ and Tween 20 [123, 130], were avoided in this study (unless otherwise mentioned) as they were

observed to result in protein aggregation and precipitation during subsequent steps (James Ames personal communication, present study). Protein sample bound to the column was washed extensively with 150-200 ml or Wash buffer (Binding buffer + 0.2% Tween 20) and then with ~500 ml of binding buffer. The proteins were then eluted using elution buffer (Binding buffer + 0.3 M imidazole) at a flow rate of ~2.8 ml/min. The eluted protein sample was then dialysed overnight at 4 ^{o}C in 2 liters of Buffer A (20 mM Tris-HCl pH 7.4, 1mM EDTA, 10% glycerol, 2mM DTT). The dialysate was filtered and applied onto a Hi-Trap DEAE column (Amersham biosciences) pre-equilibrated with Buffer A at room temperature or 4 ^{o}C. After the OD 280 of the flow-through is < 0.001 the bound protein is eluted in gradient with 0-100 % Buffer B (Buffer A + 0.6 M KCl) over 150 ml at a flow rate of 5ml/min. The DEAE eluted protein fractions were processed individually for electrophoretic mobility shift assay (EMSA) or pooled together where mentioned. Ni-NTA eluates were pooled and dialysed against 20 mM Tris-HCl pH 7.4, 1mM EDTA, 10% glycerol, 100mM Nacl, 2mM DTT, overnight at 4 ^{o}C before they were used directly for EMSA. The highest concentrated protein fraction was either concentrated to ~150 μM using Amicon 15 ml centrifugal concentrators or directly used for gel-filtration experiments. Where mentioned batch purification of protein samples was done by applying the sonicated cell lysate of 500 ml cell culture resuspended into 20 ml binding buffer made into 2 x 10 ml aliquots, onto Ni-NTA superflow resin (Qiagen) pre-equilibrated with Ni-NTA binding buffer (see above) by iterative incubations of 10' and spinning for 6' at 4 ^{o}C. 3 ml of resin was first spun at 4,000 xg at 4 ^{o}C and washed with water and binding buffer with 3 iterations of incubation and spinning. Washing and elution were done using same buffers described above. Three washes with 10 ml wash

buffer containing 0.2 % tween 20, followed by 5 washes with binding buffer. After spinning the final wash solution, the supernatant was decanted and protein sample was eluted using 2 ml elution buffer.

4.2.3 Western blotting analysis on DREAM

DREAM protein fractions eluted from DEAE column were assayed by western blot using anti-DREAM antibody (rabbit polyclonal anti-DREAM, SC-9142, Santacruz biotech). As a positive control recombinant DREAM, as a 51 kda GST fusion protein (sc4520-WB) was purchased from Santacruz biotech. One microliter of protein sample each from DEAE fractions #10, #11, #12 and #13 with protein concentrations 12, 20, 47, 68 μM respectively and two microliters of 100 μg/ml control protein sample (GST-fusion protein) were loaded onto 12% SDS PAGE-gel run in duplicates for 1 hour using NuPage gel system (Invitrogen) at 110 V. At the end of the run, one of the gel was stained using GelCode Blue (Biorad) and the other was used for performing western transfer. Western transfer was performed using Trans- Blot Semi-Dry apparatus from Biorad for half hour onto nitocellulose membrane preincubated with transfer buffer (25mM Tris, 192mM glycine, 20% methanol) for 30 min. The transfered membrane was then incubated with primary antibody (rabbit polyclonal anti-DREAM) diluted 1/800 in blocking buffer (75mM phosphate buffer pH 7.2, 68mM NaCl supplemented with 0.1% tween 20 and 5% skim milk powder) for 1 hour at room temperature. The membrane was then washed with PBS-T (75mM phosphate buffer pH 7.2, 68mM NaCl supplemented with 0.1% tween 20) thrice for 10 min duration each time followed by incubation with secondary antibody (goat anti-rabbit IgG conjugated with Horse radish peroxidase) for 30 min at room temperature. Detection was performed using Super Signal West Dura kit (Pierce

biotech inc.) following manufacturer's recommendations. The blots were then exposed for 2 min to Biomax light chemiluminiscent screens (KODAK) and processed using KODAK film processor.

Protein	Template	Oligonucleotide primers
DRC- I	pet15bDREAM	1) 5′ AAAAAA**CATATG**AGTGAACTGGAGTTATCCACGGTG3′
		2) 5′ ATAGAGGGAGAAGGCCCACTGGAGCTTCTCATGGACCG3′
	pet11aRecoverin	3) 5′ CTTCGAGGGACGGTCCATGAGAAGCTGGAGTGGGCCTTC3′
		4) 5′ AAA***CTCGAG***TCAGAGTTTCTTTTCCTTCAGTTTCTCCTTC3′
DRC-II	pet15bDREAM	5) 5′ AGCGCGGGCAAGACCAACCAGAAGCTCAAGTGGGCCTTC3′
		6) 5′ AAA***CTCGAG***TTACTAGATGACGTTCTCAAACAGCTG3′
	pet11aRecoverin	7) 5′ AAAAAA**CATATG**GGGAACAGCAAGAGTGGGGC3′
		8) 5′ ATAGAGATTGAAGGCCCACTTGAGCTTCTGGTTGGTCTTG3′
DRC-III	pet15bDREAM	9) 5′ TTCCAGACCATCATGAGGAAGTTCTTCCCCCAGGGAGATG3′
		10) Used 6) as reverse primer
	pet11aRecoverin	11) Used 7) as forward primer
		12) 5′ ATAGGTGGTGGCATCTCCCTGGGGGAAGAACTTGGAGTA3′
DRC-IV	pet15bDREAM	13) Used 1) as forward primer
		14) 5′ ATAGGCCTTGGGGTCGGCCTCAGGGAAGAACTGGGAATAAATG3′
	pet11aRecoverin	15) 5′ TTCAAACTCATTTATTCCCAGTTCTTCCCCAGTGGCCGG3′
		16) Used 4) as reverse primer
DRC-V	pet15bDREAM	17) Used 1) as forward primer
		18) 5′ AAA***CTCGAG***CTTCTGACAAGTCTCCAGAAATTCATCAATGG3′
DRC-VI	pet15DRC-III	19) Used 7) as forward primer
		20) 5′ AGGGAGAAGGCCCACTGGAGCTTCTCATGGACCGTCCCTC3′
	pet15DRC-I	21) 5′ GGTCCATGAGAAGCTGGAGTGGGCCTTCTCCCTCTATG3′
		22) Used 4) as reverse primer

Table:4-1: Oligonucleotide primers used for generating DREAM-Recoverin chimeras (DRC's). First primer in each case is the forward primer. NdeI sites (CATATG) in the forward primers are highlighted in bold and underlined, XhoI sites (CTCGAG) bold, italicized and underlined.

4.2.4 NMR spectroscopy

Samples for NMR analysis were prepared by dissolving ^{15}N-labeled DREAM-C or each of the DRC- chimeras or Recoverin (0.2–0.5 mM) in 0.3 ml of a 95% H_2O/5% [^{2}H]H_2O

solution containing 10 mM [$^2H_{11}$]Tris (pH 7.4), 5 mM [$^2H_{10}$]dithiothreitol, 50 mM KCl, and either 5 mM EDTA (apo), 5 mM $MgCl_2$ (Mg^{++}-bound), or 5 mM $CaCl_2$ plus 5 mM $MgCl_2$ (Mg^{++}/Ca^{++}-bound). All NMR experiments were performed at 32 °C on a Bruker Avance 600-MHz spectrometer equipped with a four-channel interface and triple-resonance probe with triple-axis pulsed field gradients. The ^{15}N-^1H HSQC spectra were recorded on samples of ^{15}N-labeled proteins (in 95% H_2O, 5% ^2H_2O). The number of complex points and acquisition times were: 256, 180 ms (^{15}N (F_1)), and 512, 64 ms (^1H (F_2).

4.2.5 Size exclusion chromatography

Determination of the molecular weight of the purified DREAM-C and the DRC's in solution was carried out on a Superdex 200 HR 10/30 column (Amersham Biosciences) at room temperature, in the buffers containing 10 mM Tris-HCl (pH 7.6), 150 mM NaCl, 5 mM $MgCl_2$, 1 mM dithiothreitol, with 1 mM EGTA for Ca^{++}- free samples and with 5 mM $CaCl_2$, for Ca^{++}- bound samples. 0.1 ml of protein samples (protein concentration 150 μM except in the case of DRC-II , in which case the protein sample was difficult to concentrate and hence was used at ~40 μM, see fig.4-6B) was loaded onto the column and allowed to run at a flow rate of 0.5 ml/min. Low protein concentration used may, however, prevent dimer formation if the dimerization affinity is low . Apparent molecular weights were calculated using a standard curve of V_e/V_o *versus* the log of the molecular masses of standard proteins: β-amylase (200 kDa), Bovine serum albumin (67 kDa), myoglobin (17 kDa), and cytochrome c (12 kDa). V_o is a void volume obtained using blue dextran (2000 kDa), and V_e is a volume of elution. The value of V_e/V_o is inversely related to the molecular weight of the migrating species. Thus, for DREAM-C SEC, previous studies in the lab showed that calcium-free DREAM-C exists as monomer irrespective of

protein concentration DEAE fractions were directly applied onto the column. However, calcium-bound DREAM-C was found to exist as a monomer at concentrations less than or equal to 50 µM. At concentrations greater than 50 µM DREAM-C exists as a dimer, as seen from decreasing V_e/V_o values (Masanori Osawa unpublished observation, fig.4-2).

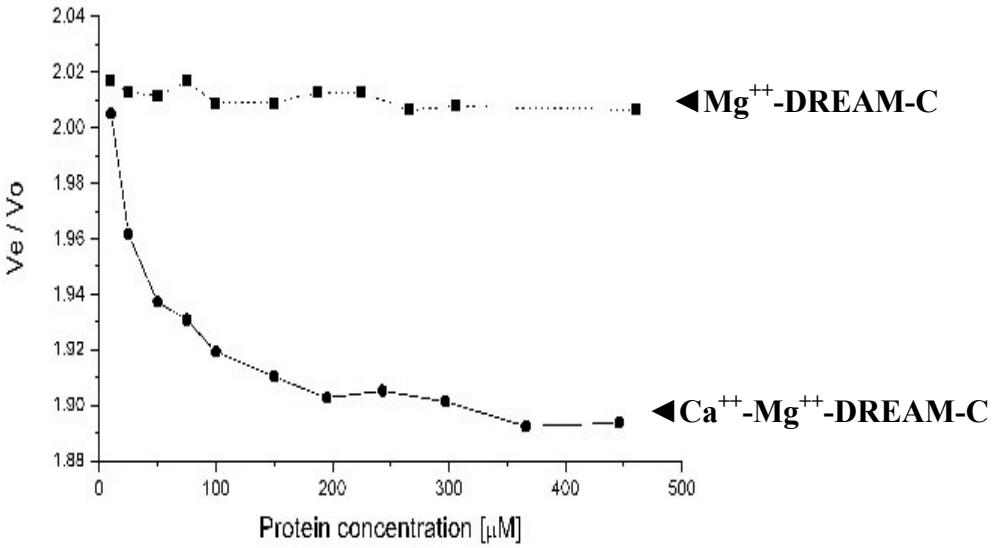

Figure 4-2: Oligomerization of DREAM as a function of protein concentration on SEC. V_e/V_o (see section 4.2) for DREAM-C in the presence and absence of Ca^{++} plotted against increasing protein concentration on X-axis shows Mg^{++}-DREAM-C being monomer irrespective of protein concentration, but Ca^{++}-Mg^{++}-DREAM-C forming dimer starting from ~50 µM. Figure courtesy: Masanori Osawa.

Increased dimerization with increase in protein concentration might indicate a low affinity dimerization of DREAM protein. Hence, protein samples were concentrated to ~150 µM in the calcium bound form using Amicon centrifugal concentrators before application onto gel-filtration column. Precipitates resulting from the concentration of samples were removed by centrifugation at 14,000 rpm on bench top centrifuge. Protein concentrations were estimated using extinction coefficients obtained by using ProtParam tool on Expasy molecular biology server (http://us.expasy.org/). The values (in units of M^{-1}, cm^{-1} at 280 nm) are DREAM-C & DRC-V: 14565; DRC-I: 16960; DRC-II: 21555;

DRC-III:20065; DRC-IV: 19940; DRC-VI:22460.All the samples were centrifuged at >10,000 xg for 10 min at 4 ^{o}C before applying onto gel-filtration column.

4.2.6 Electrophoretic mobility shift assay

Synthetic oligonucleotide (10pmol) (Integrated DNA technologies, IA) representing the sense strand of DRE (5'-GAAGCCGGAGTCAAGGAGGCCCCTG-3') of human prodynorphin [74, 123, 130] or of c-fos (5'-CTGCAGCGAGCAACTGAGAATCCA AGAC-3') was 5'-end labeled using γ-P^{32}- Adenosine triphosphate (GE healthcare) with T4 polynucleotide kinase (Takara Bio) as per manufacturer's recommendations. The labeled sense strand was then annealed with 4-5 fold excess of respective unlabeled anti-sense strand (dyn-DRE-AS = 5'-CAGGGGCCTCCTTGACTCCGGCTTC-3', c-fos-DRE-AS= 5'-GTCTTGGATTCTCAGTTGCTCGCTGCAG-3') in annealing buffer (30mM HEPES-NaOH pH 7.5, 60mM NaCl) by heating to 99 °C for 3' and then incubating at 65 °C for 20' followed by slow cooling at room temperature 3-5 hours or overnight. Unincorporated radionucleotides were then removed using Microspin G-25 columns (GE healthcare) and specific activity was measured using liquid scintillation counter (Perkin-Elmer).

Protein samples eluted from the DEAE column were used, directly, for binding reactions. 100 fmol of labeled double stranded DRE was added to EMSA reaction mixture comprising 12-75 μM protein sample, 10 mM HEPES, pH 7.9, 8 mM $MgCl_2$, 0.1 mM EDTA, 2 mM dithiothreitol, 0.05 unit/ml (1 A260 unit = 50 μg) of poly(dI-dC) (Amersham Biosciences), and with or without 10 mM $CaCl_2$. The reactions were incubated at 4 °C for 1 hour. Protein-DNA complexes were resolved in 5% non-

denaturing polyacrylamide/0.25 x TBE/1% glycerol gels at 200 V for 2 hours min in 0.25 x TBE and 0.5 mM $MgCl_2$ running buffer. Gels were then dried and exposed to phosphor screens (GE health care) or X-OMAT X-ray films (KODAK) and developed on STORM system or KODAK film processor. EMSA bands were quantified using ImageQuantTL (GE health care) by dividing the counts from the band shift with the sum of counts in the shifted band and the duplex probe at the bottom of the gel.

Previously reported incubation of 5 hours at room temperature [130] resulted in complete degradation of the probe with exo- and endonucleases. Hence, where mentioned binding reactions were incubated at 4°C overnight. Competition with cold specific and non-specific probes was done by co-incubating unlabeled double stranded oligonucleotides as mentioned with the EMSA reactions. Unlabeled double stranded DNA elements used in competition experiments were c-fos-DRE (see sequence above), DREmut5 (5′-GAAGCCGGA**A**TC AAGGAGGCCCCTG-3') and c-AP1-sense strand (5'-AAGCTTGCATGACTCAGACAG-3'). In experiments testing salt dependence on band shift, appropriate amounts of salt was added to bring the initial DEAE fractions on par with later DEAE fractions. Salt concentrations of DEAE fractions were approximated based on the position of protein elution on the salt gradient.

Supershift experiments were performed, by co-incubating 15 µg each of anti-his antibody (Genscript), anti-DREAM antibody (FL-214, Santacruz) and anti-HNF4 antibody (Santacruz) with the DNA binding reactions.

4.3 Results and Discussion

4.3.1 DREAM-Recoverin chimeras retain stable tertiary structure

Two-dimensional NMR spectroscopy was performed on each of the DREAM-Recoverin chimeras in the presence of calcium and magnesium to ascertain the stability of protein structure. Previous studies on wild-type DREAM-C using ^{1}H-^{15}N HSQC NMR showed that addition of calcium and magnesium dramatically improves stability of DREAM protein under NMR conditions. All the DREAM-Recoverin chimeras (DRC's) showed well-dispersed spectra similar to wild type with uniform intensities (fig.4-3), indicating the presence of stably folded tertiary structure in each case. Each of the peaks in the spectra represents a single amide proton in a unique chemical environment, providing an overall fingerprint of the protein conformation. The observed spectra of each of the chimeras reveal that the chemical shifts of both substituted and unsubstituted residues are largely unperturbed in the chimeric proteins, particularly for the downfield shifted and non-overlapping resonances. For example, the downfield shifted peak of DRC-I (highlighted red in Fig. 4-3) assigned to an amide resonance of EF-3 (Gly 180) has a chemical shift very similar to that of the corresponding residue of EF-3 in recoverin (Gly 115). Similarly, for DRC-II the downfield shifted peak assigned to EF-2 has a chemical shift similar to that of the corresponding residue of EF-2 in recoverin (Gly 79). The preserved chemical shifts for the recoverin-substituted residues and well-dispersed NMR spectra imply that the structure of each substituted EF-hand must remain structurally intact in all the chimeras, making them suitable for functional assays using EMSA to test for their individual DNA binding properties.

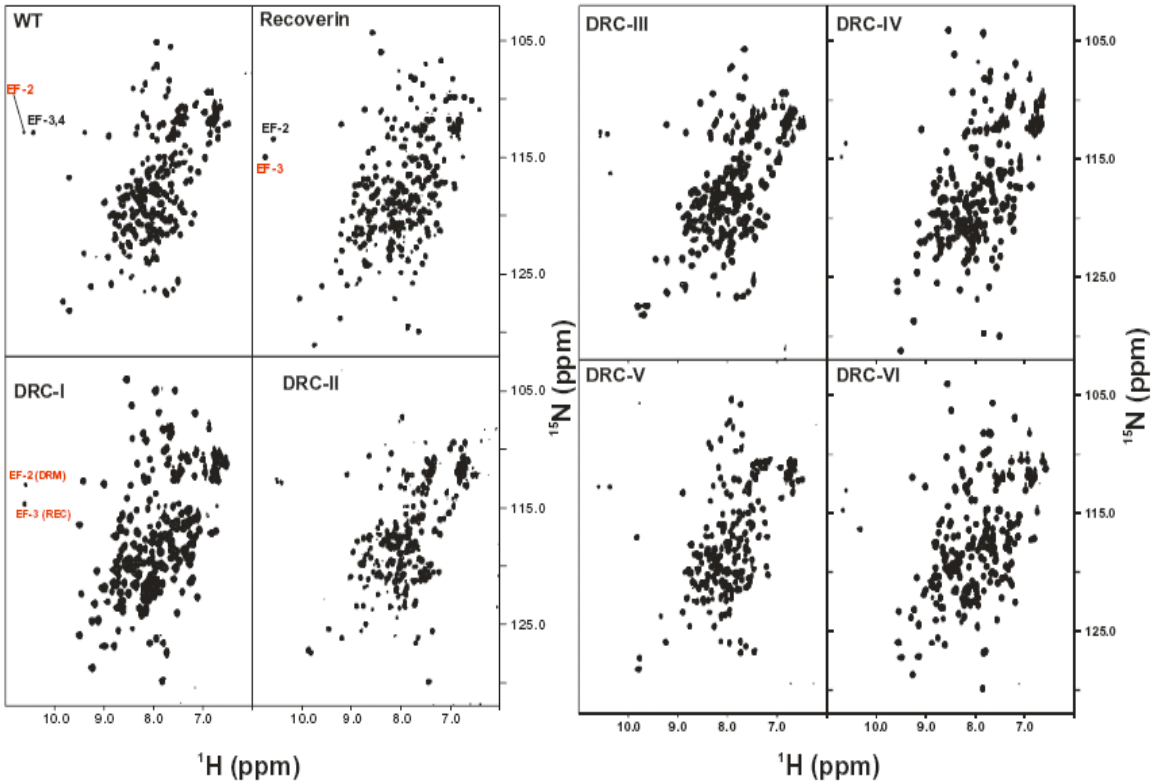

Figure 4-3: Two-dimensional ^{15}N-^{1}H HSQC NMR spectra of calcium bound protein samples of wild type-DREAM-C (WT), Recoverin, DRC-I, DRC-II, DRC-III, DRC-IV, DRC-V, DRC-VI. Each protein sample was uniformly labeled with nitrogen 15, and spectra were recorded at 600-MHz 1H frequency. DRM: wild type DREAM-C; Rec: wild type recoverin. Figure courtesy: James Ames.

4.3.2 Oligomerization properties of DREAM-recoverin chimeras vs. Ca^{++}

The oligomerization state of DRC proteins were assessed using size exclusion chromatography (SEC) (Figs 4-4 to 4-7). Molecular weights were estimated using the standard curve plotted using beta amylase, bovine serum albumin, myoglobin and cytochrome c standards (Fig.4-4C). For suitable comparison, wild type DREAM-C and recoverin protein samples were run on SEC as well. Consistent with previous studies (see 2.2.2), DREAM-C eluted as a monomer in Mg^{++}-bound, calcium-free state and as dimer (consistent with previous observations of Masanori Osawa, fig.4-2) in calcium-bound state (Fig. 4-4). Although the estimated molecular mass of calcium-bound DREAM-C based on the V_e/V_o values was 38 kda, it was interpreted to be a dimer. Previous studies in the lab, using dynamic light scattering showed that at 87 μM protein concentration

calcium-bound DREAM-C showed a hydrodynamic radius of 3.13 nm that corresponds to 45.7 kda [130]. Thus, the reason for lower apparent mass of Ca^{++}-DREAM-C may be due to a dynamic exchange between monomeric and dimeric DREAM-C while passing through the size column. Recoverin on the other hand eluted as a monomer in both calcium-free and calcium-bound states (Fig.4-5). Estimated molecular weights of DRC's along with a summary of SEC results are shown in Table 4-2. The difference in peak heights of SEC elutions of DRC proteins is due to concentration of the protein samples to ~150 μM in the calcium bound state but not in the calcium free state (for details see section 4.2.5).

Briefly, all chimeras (except DRC-II, DRC-IV and DRC-V) are monomeric in the Mg^{++}-bound state similar to wild type. Mg^{++}-bound forms of DRC-II and DRC-IV are dimeric and DRC-V forms large protein aggregates. In the Ca^{++}-bound state, all chimeras (except DRC-IV and DRC-V) are predominantly monomeric, in contrast to Ca^{++}-induced dimerization of wild type. The calcium-bound DRC-II exhibits a low molecular weight species (fig.4-6B) that can only be explained by calcium-induced changes in the protein that may lead to the apparent slow mobility on the size column relative to calcium-free form. Specifically, binding of calcium to DRC-II might result in conformational changes in DRC-II protein that promote its interaction with the column resulting in the apparent slower mobility. The apparent aggregation of DRC-V in both Mg^{++}-bound and Ca^{++}-bound states may be related to removal of the C-terminal helix, perhaps leading to exposure of hydrophobic residues in EF-3 and EF-4 that otherwise would be sequestered by the C-terminal helix as seen in the structure of KChIP1. However, considering the effect of protein concentration on DREAM oligomerization in the presence of calcium,

similar experiments on each of the chimeras in the absence and presence of calcium would provide an estimate of the dimerization affinity of each of the chimeras.

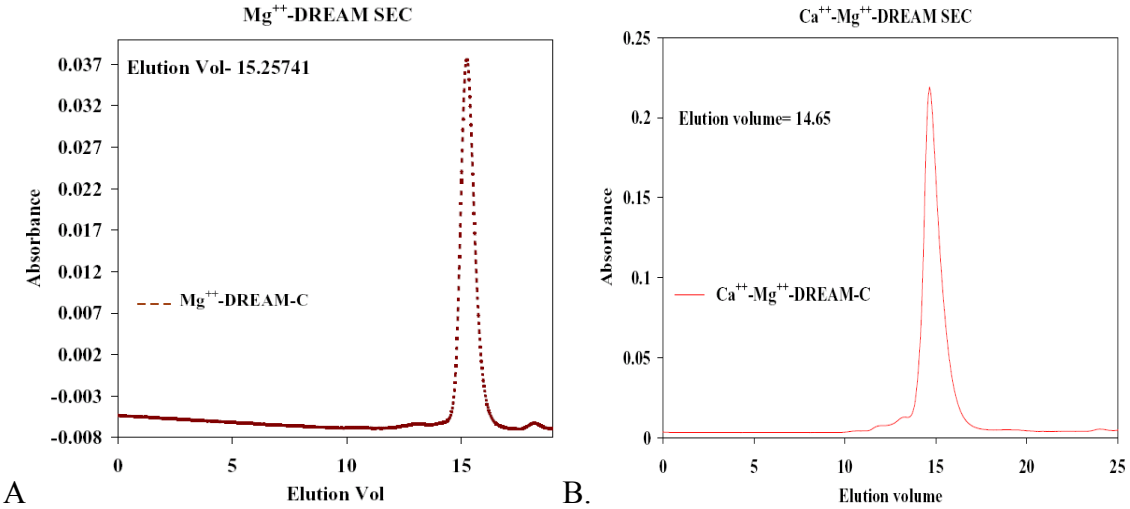

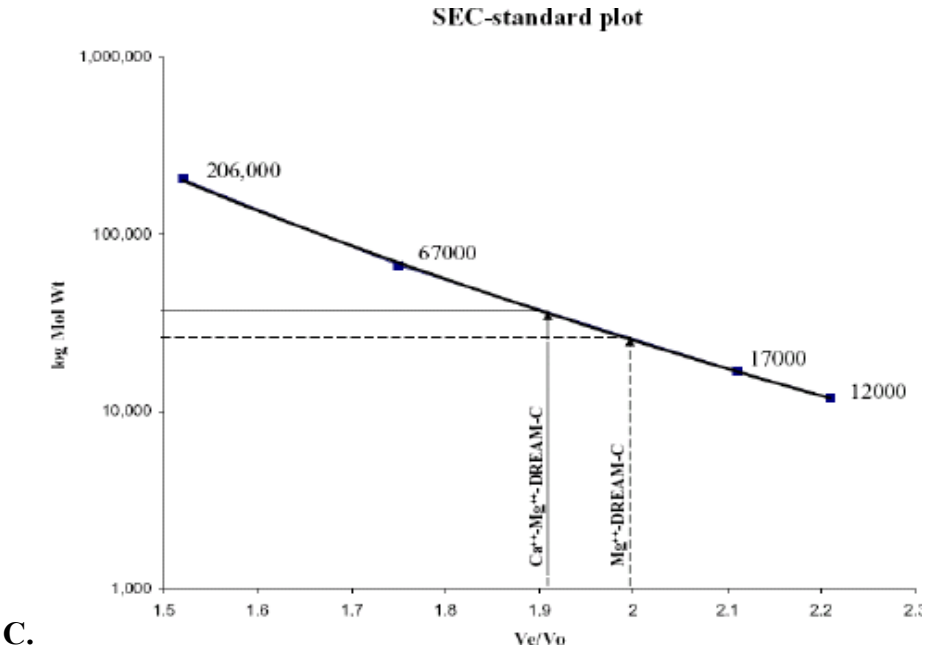

Figure 4-4: Size exclusion chromatograms of DREAM-C in calcium-free (A) and calcium-bound (B) forms. Protein concentrations were 80 µM in (A) and 150 µM in (B). (C) Standard curve for molecular mass determination created using beta amylase (206 kda), BSA (66 kda), Myoglobin (17 kda) and cytochrome c (12 kda) with molecular masses of standards indicated at each data point on standard curve. Void volume V_o was obtained as 7.60526 using blue dextran (2000 kda). V_e is the elution volume of each sample. Estimated mass of Mg^{++}-DREAM-C was 26.8kda; estimated mass of Ca^{++}-Mg^{++}-DREAM-C was 38 kda (less than apparent dimer molecular weight of Ca^{++}-Mg^{++}-DREAM-c is consistent with previous studies (fig.4-2- Ca^{++}-Mg^{++}-DREAM-C curve at 150 µM concentration).

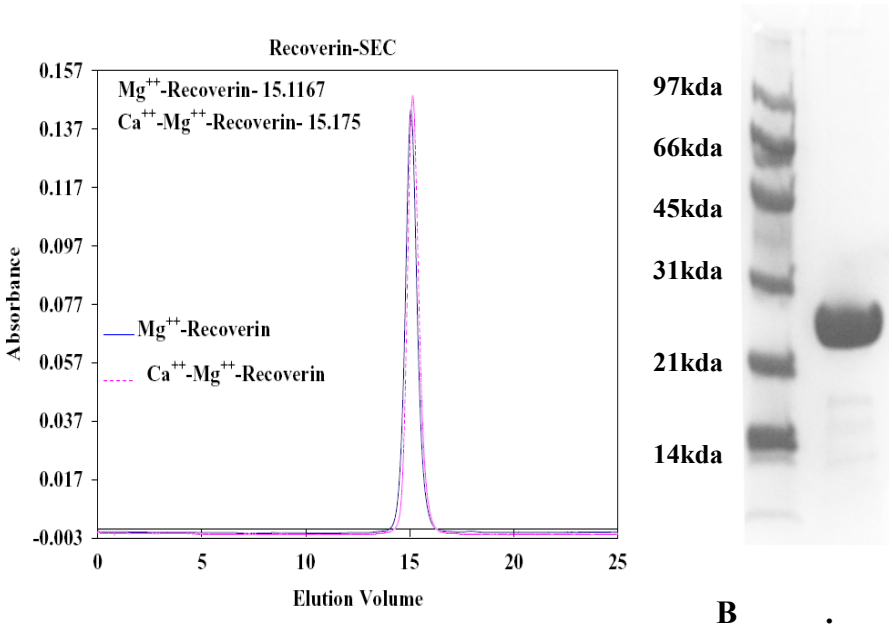

Figure 4-5: Overlaid size exclusion chromatograms of calcium-free (blue) and calcium-bound Recoverin (protein concentration ~120 μM) (A). SDS PAGE of recombinant Recoverin (unmyristoylated) used for running SEC, Molecular weight markers from top represent 97, kda, 66, kda, 45 kda, 31 kda, 21 kda, and 14 kda. Recoverin migrates at ~25 kda. Estimated molecular mass of recoverin in SEC was 26.8kda.

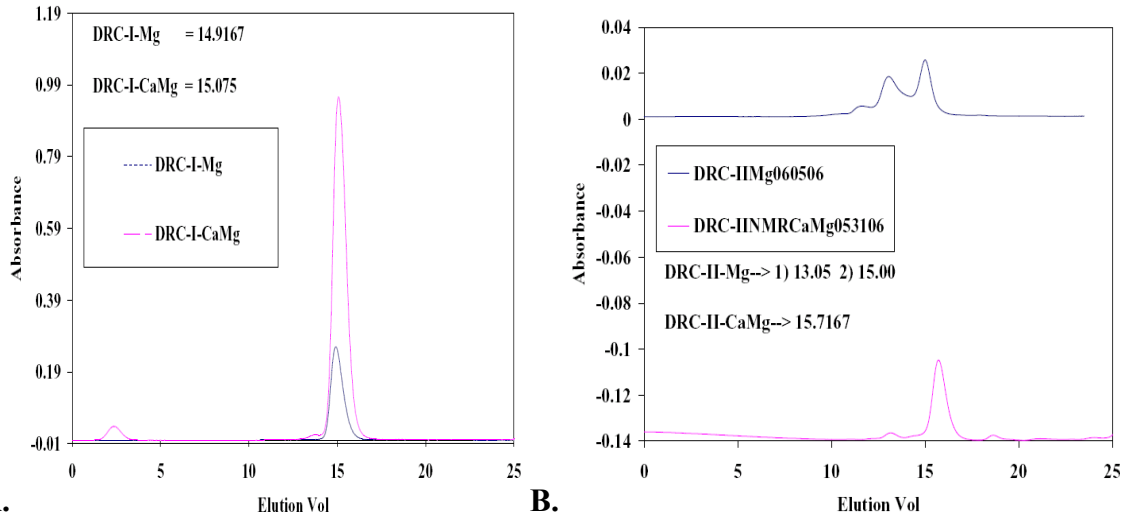

Figure 4-6: Overlaid size exclusion chromatograms of calcium-free and calcium-bound DRC-I (A), DRC-II (B). Blue traces represent calcium-free state, pink and red traces represent calcium-bound state. Estimated molecular masses are summarized in Table 4-2.

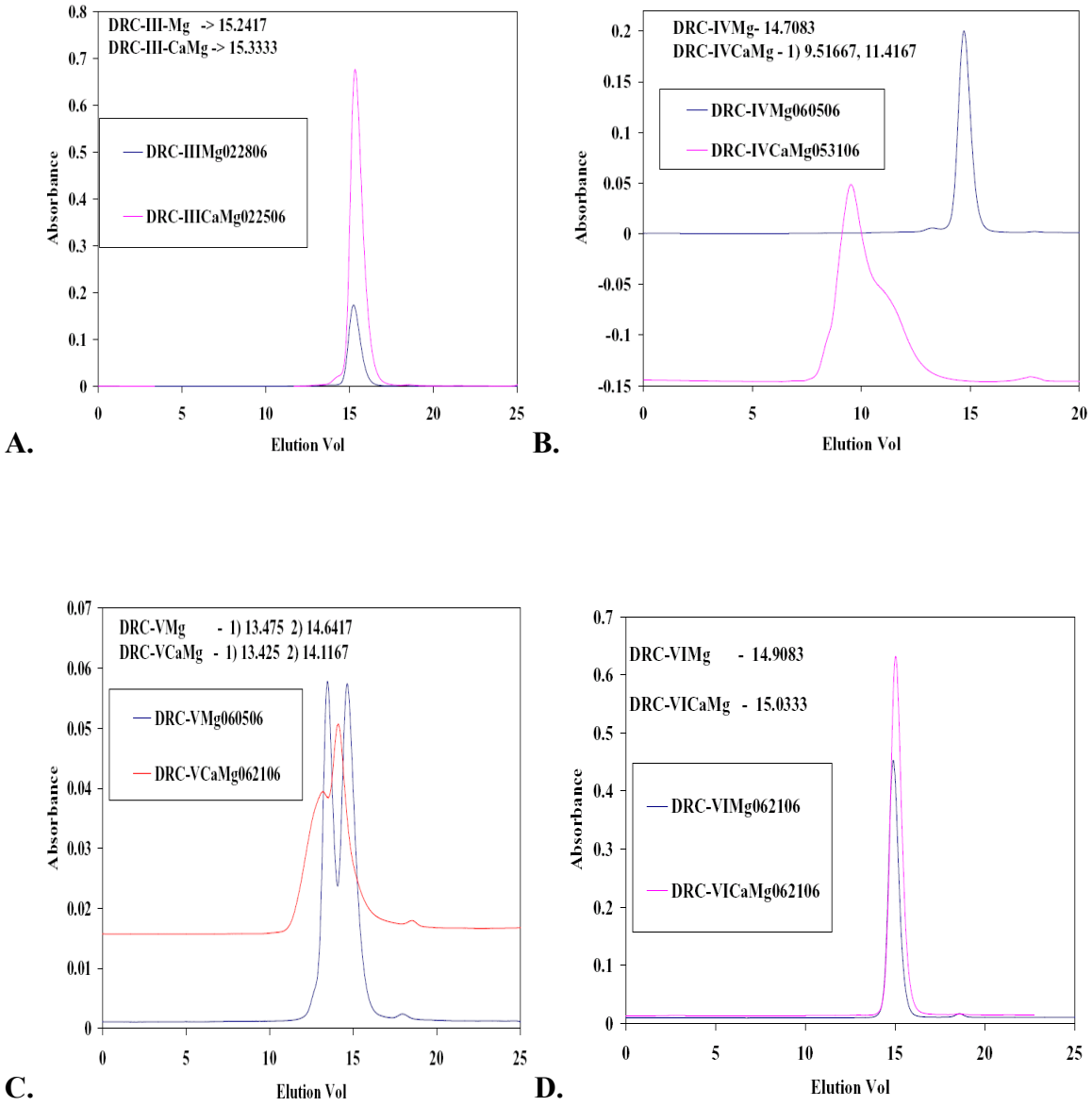

Figure 4-7 : Overlaid size exclusion chromatograms of calcium-free and calcium-bound DRC-III (A), DRC-IV (B), DRC-V (C), and DRC-VI (D). Blue traces represent calcium-free state, pink and red traces represent calcium-bound state. Estimated molecular masses are summarized in Table 4-2.

Std	Mol.Wt	LogMolWt	Elution Vol	Ve/Vo	Est.MolWt.	comments
BetaAmylase	206,000	5.31	11.6	1.52	211kda	
BSA	67000	4.83	13.35	1.75	73.5kda	
Myoglobin	17000	4.23	16.13	2.11	17.9kda	
CytochromeC	12000	4.1	16.87	2.21	12.6kda	
MgDREAM	25000	4.4	15.3	2	26.8kda	monomer
CaMgDREAM©	25000	4.4	14.65	1.91	38kda	dimer
Recoverin-Mg	23000	4.36	15.12	2	26.8kda	~monomer
Recoverin-CaMg	23000	4.36	15.175	2	26.8kda	~monomer
		4.4				
DRC-I-Mg	25000	4.4	15	1.96	31.3kda	~monomer
DRC-I-CaMg	25000	4.4	15.1	1.97	30.1kda	~monomer
DRC-II-Mgpk1	26000	4.42	13.05	1.71	87.5kda	tri-tetramer
DRC-II-Mgpk2	26000	4.42	15	1.96	31.3kda	~monomer
DRC-II-CaMg	26000	4.42	15.7	2.1	18.3kda	monomer
DRC-III-Mg	26000	4.42	15.24	2	26.8kda	monomer
DRC-III-CaMg	26000	4.42	15.3	2	26.8kda	monomer
DRC-IV-Mg	25000	4.4	14.71	1.92	36.5kda	dimer
DRC-IV-CaMgpk1	25000	4.4	9.52	1.24	983kda	aggregate
DRC-IV-CaMgtrail	25000	4.4	11.42	1.5	233kda	aggregate
DRC-V-Mgpk1	23000	4.36	13.5	1.77	67.4kda	trimer
DRC-V-Mgpk2	23000	4.36	14.64	1.91	38kda	dimer
DRC-V-CaMgtrail	23000	4.36	13.43	1.76	70.4kda	trimer
DRC-V-CaMgpk	23000	4.36	14.12	1.85	48.3kda	dimer
DRC-VI-Mg	26000	4.42	14.91	1.95	32.5kda	~monomer
DRC-VI-CaMg	26000	4.42	15	1.96	31.2kda	~monomer

Table 4-2: Summary of SEC results. All descriptions follow the time of elution pattern (from left to right on X-axis). Columns from left to right labeled as 1) standards, Molecular weight in kilo daltons, $\log_{10}$ molecular weight, elution volume, Ve/Vo (Vo measured by blue dextran= 7.65), Estimated Molecular weight from V_e/V_o using standard plot (Fig 4-4), comments. © indicates concentrated DREAM-C sample to 150 μM.

4.3.3 Magnesium inhibits dimerization of DREAM in the absence of calcium

In the absence of calcium, wild type (fig. 4-4), DRC-I (fig.4-6A), DRC-III (fig. 4-7A), and DRC-VI (fig. 4-7D) proteins, all exist in a monomeric state, whereas DRC-II (fig.4-6B) and DRC–IV (fig.4-7B) are not monomeric. The monomeric chimeras each contain the high affinity magnesium-binding site from the EF-2 of DREAM protein. Conversely, replacing EF-2 of DREAM with that of recoverin in DRC-II (Fig.4-6B) and DRC-IV (Fig.4-7B) results in dimeric or higher order oligomers, suggesting that magnesium binding to EF-2 stabilizes the monomeric form of the protein, which was also observed in

the case of wild-type DREAM protein (see section 2.1 and [123]). In the case of DRC-V (Fig. 4-7C), since the C-terminal helix is missing, the protein may have many of its hydrophobic residues exposed that may promote the observed oligomeric states in the presence or absence of calcium.

4.3.4 Head-to-tail Dimerization of DREAM

All the chimeras (except DRC-IV and V) are monomeric in the calcium-bound state (Fig 4-7), in contrast to the dimeric calcium-bound wild type (Fig.2-10). The results from the SEC of DRC-I and DRC-II suggest that Ca^{++}-induced dimerization can be abolished by perturbing any pair of EF hands from the N-terminus or the C-terminus of the DREAM protein, which implies that the dimer interface may not be localized to a particular EF-hand, but instead may span all four EF-hands. The SEC data of DRC-IV show that the presence of a single EF hand (EF-1) from DREAM protein results in calcium-induced oligomerization. However, lack of a complete data set from chimeras with individual EF-hands of DREAM in isolation, and the possibility of the calcium-induced olimerization effect stemming from the inherent instability of the chimeric protein preclude such a definite conclusion. Crystal structure of KChIP1 [128], a closely related protein to DREAM, shows a head to tail dimer formation in the presence of calcium. Thus, it is plausible to speculate that DREAM may also form a head-to-tail dimer that involves intermolecular contacts between EF-1 and EF-4 plus EF-2 and EF-3. However, the SEC results of DRC proteins do not rule out a head-to-head dimer formation. A model for Calcium-bound DREAM dimer based on KChIP1 structure is presented in fig 4-8 A.

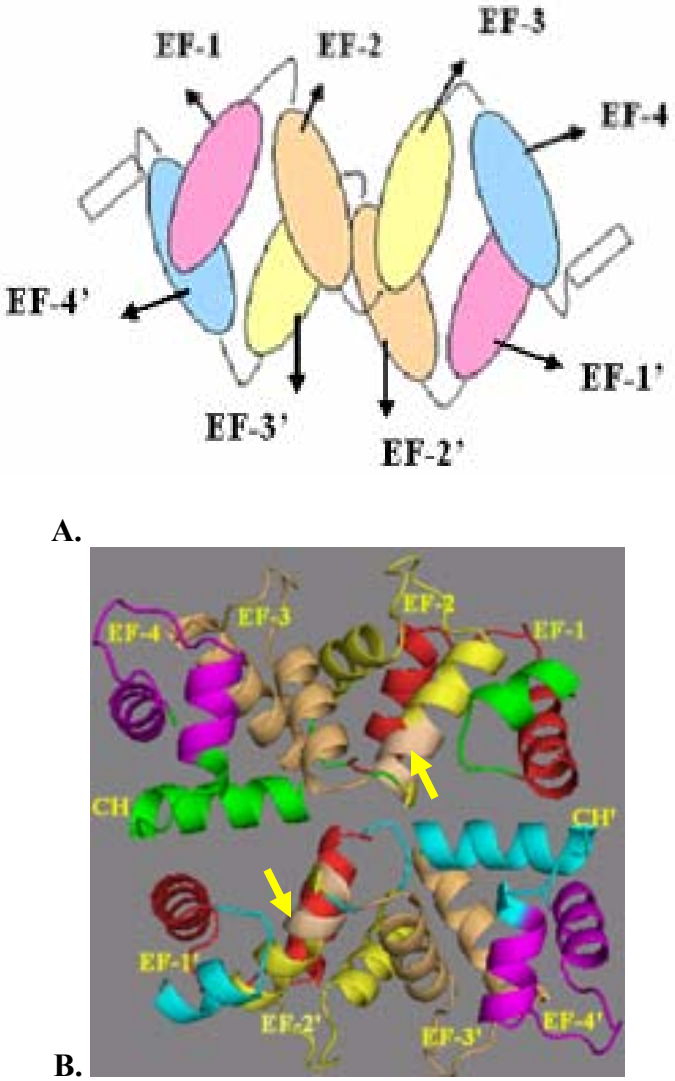

Figure 4-8: (A) Model for head-to-tail DREAM dimer in calcium bound state, based on KChIP1 crystal structure [128]. Each of the ellipses represents an EF-hand – Rose: EF-1, Tan: EF-2, light yellow: EF-3, pale blue: EF-4. Dimerization occurs via intermolecular interactions of EF-1 with EF-4 and EF-2 with EF-3. (B) Crystal structure of calcium bound KChIP1 [128] with EF hands colored- EF-1: red; EF-2: light yellow; EF-3: light orange; EF-4: magenta. Subunits are named by the color of N and C terminal helices (green and cyan). Metal coordinating loops are labeled. EF-1, EF-2, EF-3, EF-4 and CH (C-terminal helix) denote green subunit and EF-1', EF-2',EF-3', EF-4', CH' denote that of cyan subunit. Dark yellow arrows show leucine zipper present in EF-2 (L115-L119).

4.3.5 Recoverin does not bind DNA

Electrophoretic mobility shift assays were employed to probe whether recoverin exhibits calcium-sensitive binding to DRE similar to that of DREAM. The EMSA with recombinant recoverin in the presence and absence of calcium is shown in Fig.4-9. No detectable band shift was observed for recoverin (Fig.4-9) using the same conditions used to see a band shift with DREAM [74, 130]. Hence, recoverin does not bind DRE under the conditions of our experiments.

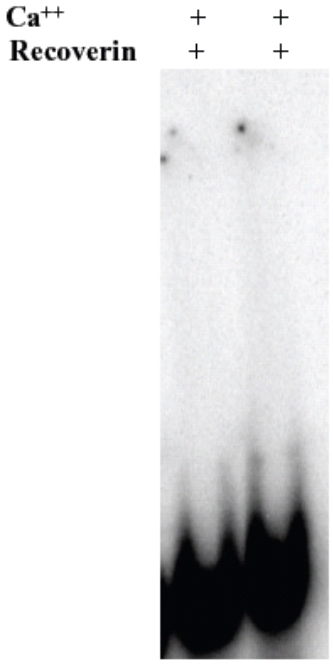

Figure 4-9: EMSA with recombinant recoverin incubated with 5nM of γ-P^{32} labeled dyn-DRE in the presence or absence of calcium as indicated. Protein concentration was ~90 μM.

4.3.6 DREAM co-purifies with nuclease activity

Initial EMSA experiments performed on wild type DREAM protein (referred interchangeably as DREAM-C, the C-terminal portion of DREAM comprising four EF hands) aimed at replicating previously published results [74, 130]. This was an essential

prerequisite, to ascertain DREAM's calcium-sensitive DNA binding behavior in my hands before we could proceed with analyzing the DREAM-Recoverin chimeras in more detail. Initial EMSA studies on DREAM protein by Carrion et al. (1999) used full length recombinant DREAM and 5'- P^{32} end-labeled DRE probe to characterize DREAM-DNA interaction. However, since the full-length recombinant protein was prone to aggregation (James Ames, personal communication) and very difficult to purify, a truncated protein comprising amino acids 65-256 (DREAM-C) was used in previous studies from the lab. DREAM-C binds functionally to DRE with about 2-fold lower affinity than full-length DREAM ([130], fig.1-9). The previous EMSA study using DREAM-C in Fig. 1-9 used a Cy5 flourophore to assay DNA binding. In the present study, 5'- P^{32} end-labeled DRE probe was used to perform EMSA with affinity-purified DREAM-C (see section 4.2.6). However, incubation of the DNA binding reactions at room temperature for 5 hours, similar to the previous studies in fig.1-9 [130], resulted in complete degradation of radio-labeled probe; as a result, no band shift was observable (fig.4-10A). This result was at odds with previously reported EMSA results for DREAM-DRE interaction [130].

The lack of band shift in my experiments (Fig. 4-10) could be due to non-availability of duplex DNA probe due to nuclease activity co-purifying with DREAM, as evidenced by the degraded probe at the bottom of the gel in Fig. 4-10. Since, earlier studies [130] were carried out using a fluorescent label (Cy5), the presence of the bulky fluorophore might have protected the labeled DRE from nuclease degradation.

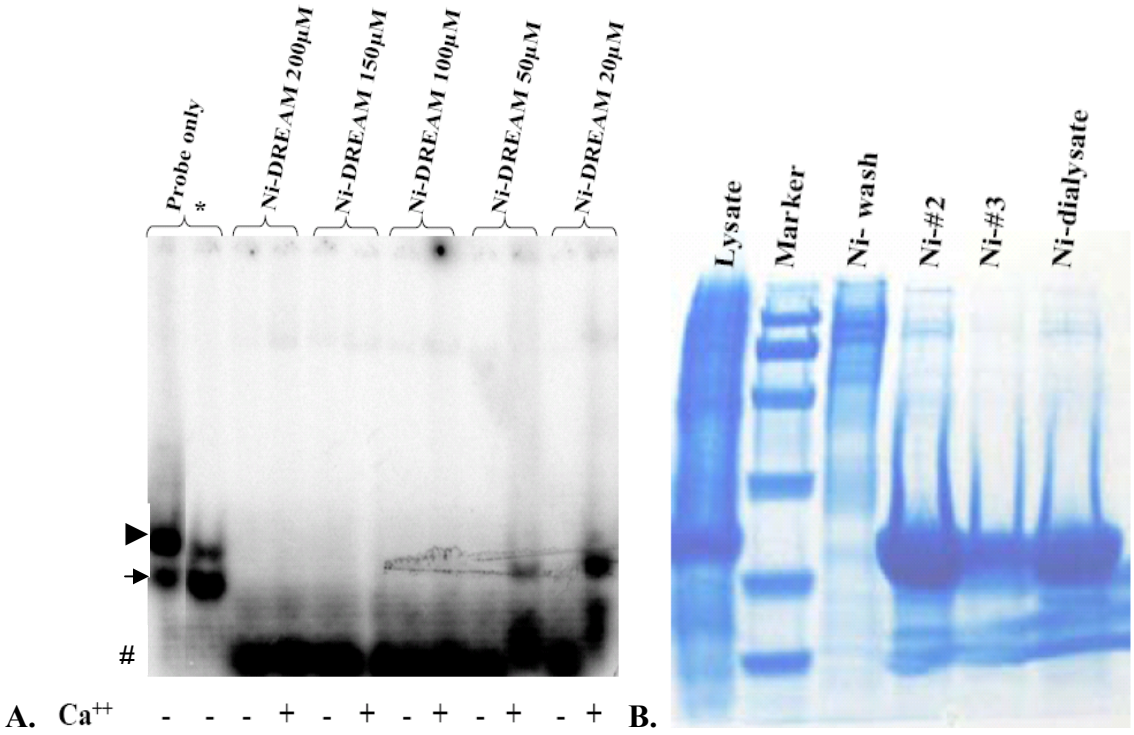

Figure 4-10: EMSA with Ni-affinity purified DREAM-C to test DREAM-DRE interaction. (A) EMSA with affinity (Ni-NTA chromatography) purified DREAM-C (Ni-DREAM) at indicated concentrations. Protein samples were diluted from Ni-dialysate (see 4.2.2). Protein concentration 285 μM. Asterisk indicates boiled probe to test the migration of single strand probe. Arrowhead indicates position of double stranded DNA, arrow points to the position of single strand probe. Degraded probe is found at the bottom from lane 3 onwards-position.indicated by '#'. (B) SDS-PAGE showing the steps in protein purification. Molecular weight markers from top represent 97, kda, 66, kda, 45 kda, 31 kda, 21 kda, and 14 kda.

In addition to nuclease degradation, other factors including protein denaturation and/or the presence of protein impurities might also have prevented the occurrence of a gel-shift. To overcome the nuclease problem, I added salmon sperm carrier DNA into the DNA binding reactions at different amounts (1 μg or 1.6 ng in 20 μl volume) and incubated the reactions at 4^{o}C instead of room temperature. The rationale is that carrier DNA and low temperature would prevent the nucleases in the reaction from acting on the radio-labeled probe. The reasoning behind 5-hour incubation in the earlier studies was that recombinant

DREAM protein tends to form aggregates and hence the long incubation time provided adequate time for the slow dissociation of aggregates into active free species that would then give rise to the band shift (James Ames personal communication). Thus, incubating overnight at 4^{o}C would serve a similar purpose. While this was successful in preventing the probe degradation, there still was no band shift detected (fig 4-11).

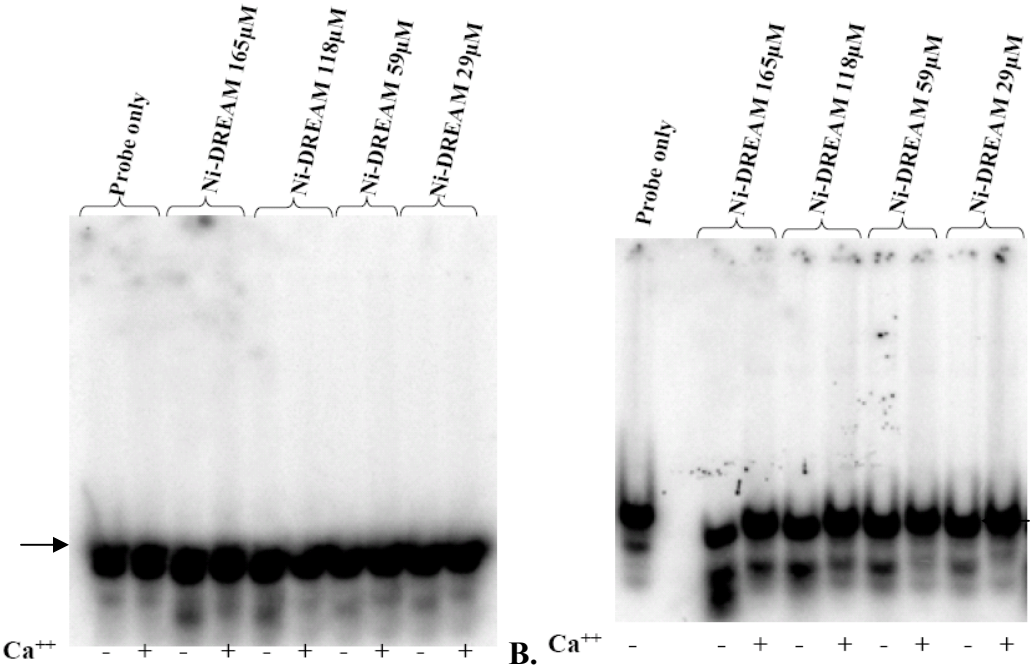

Figure 4-11: Effect of carrier DNA (salmon sperm DNA) on EMSA with DREAM-C. Carrier DNA addition prevents nuclease digestion of radio labeled probe but fails to promote DREAM-DRE interaction. Freshly prepared Ni-dialysate diluted to indicated protein concentrations was incubated with (A) 1µg (B) 1.6 ng amounts in 20 µl volume and incubated at 4oC overnight. Arrows indicate degradation products. Addition of calcium does not influence migration of probe (lane 2 in (A)).

The lack of a gel-shift in Fig. 4-11 is likely due to binding of DREAM protein to the carrier DNA. The core sequence recognized by DREAM was reported to be "GTCA" [179]. By probability, the occurrence of this sequence in a random double-stranded DNA is 4^4, or 1 in 256 bases. Thus, use of carrier DNA did not help in observing DREAM-DRE interaction. As an alternative approach, to remove the nuclease activity from

DREAM protein sample, I opted to use DEAE-anion exchange chromatography to purify recombinant DREAM (see section 4.2.2).

4.3.7 Heterogenous species of DREAM bind differentially to DNA

Further purification of recombinant DREAM-C protein samples was performed by applying the eluate from Ni-affinity column onto an anion exchange (DEAE) column. When each of the DEAE eluted fractions was assayed for DNA binding activity by EMSA, it was observed that the initial fraction (#14) (fig.4-12A, lanes 2 and 3, indicated by '*') exhibits calcium-sensitive DNA binding similar to the binding described in previous studies [74, 130].

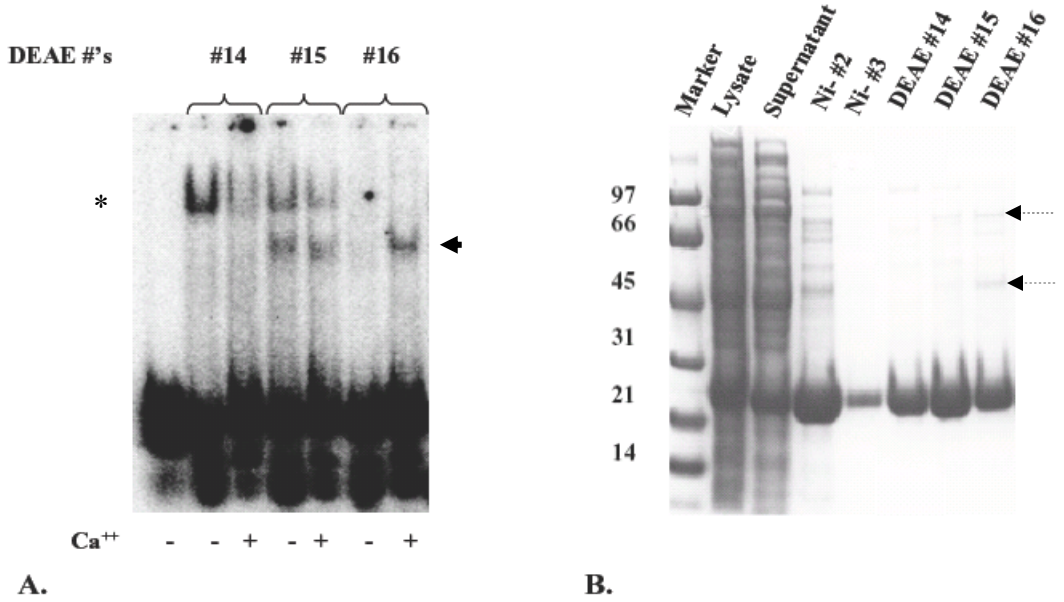

Figure 4-12: EMSA and SDS PAGE with DEAE purified fractions of DREAM-C. (A)EMSA: Lane 1 represents probe only without protein. Presence of 10mM calcium is indicated at the bottom. Protein concentrations are 58 µM, 77 µM, 46 µM for #14, #15, #16 respectively. Percentage of DNA bound (upper band only) was quantified to be 11.5% and 5.6% in lane numbers 2 and 3 respectively. Asterisk indicates band shift that is disrupted by calcium. Block arrow in (A) indicates position of band shift corresponding to DREAM's altered activity. (B) SDS PAGE showing the protein at the end of each purifcation step. Dashed arrows point to high molecular weight species in DEAE #16.

However, the later fractions (#15 and #16) show an additional band (indicated by arrow in fog.4-12A) that migrates faster and was also observed in the earlier published studies [74, 125, 130, 179] (also see fig.3-1). The second band shift shows enhanced signal in the presence of calcium (fig.4-12A, lanes 4-7).

Thus, the additional purification of DREAM-C restored its DNA binding activity as previously reported [74, 130]. However, it was indeed intriguing to observe that the later fractions, despite the presence of purified DREAM-C (as seen in the SDS PAGE, fig.4-12B) do not show the band shift similar to the initial fraction. The lack of band shift with protein from later fraction raises the question if the band shift obtained is DREAM-specific (which would be considered later in the study, section 4.3.11). Assuming that the band shift is due to DREAM, the simplest interpretation of segregation of the two different activities of the protein, upon DEAE purification, would be that recombinant DREAM protein exists in multiple conformational states that differentially recognize DNA. Before proceeding to characterize the later fractions further, I decided to check the specificity of the DNA binding activity from the initial fraction.

4.3.8 Recombinant DREAM-C binds specifically to DRE

To determine whether the DREAM-DRE interaction as seen in fig. 4-12A was sequence-specific, I performed competition experiments by adding unlabeled double-stranded probe oligos in excess to the DNA binding reactions, while performing EMSA of wild type DREAM-C. Specificity was determined by observing reduction (due to competition)

in observed band shift as a function of the addition of excess of unlabeled oligos corresponding to DRE, DREmut5 and c-AP-1.

The initial fraction behaved consistent with previously published results from the lab [130]. In the competition experiments using unlabeled probe DNA in EMSA, cold c-fos DRE abolished band shift as expected (fig.3-1). Likewise, the c-AP1 oligo, which contains the core DREAM binding element 'GTCA' in the anti-sense strand also abolishes the DREAM-DRE band shift in EMSA (fig.4-12). In contrast DRE-mut5, which has the critical single base, G → A, substitution (shown in fig.3-1), failed to abolish DNA binding as shown previously (fig.3-1, [179])

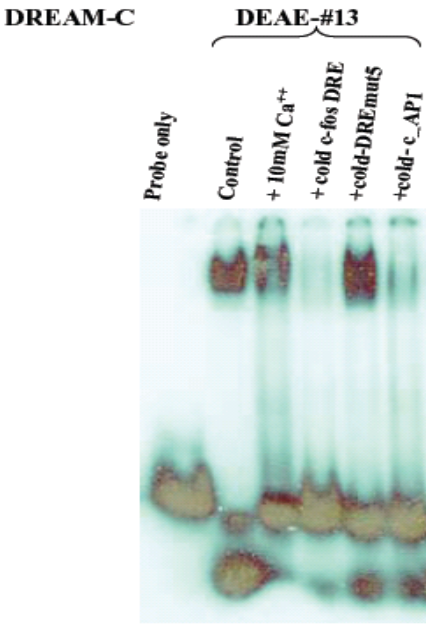

Figure 4-13: Test for the specificity of DREAM-DNA interaction EMSA of purified (DEAE fraction #13) DREAM-C with competition from 15 fold excess of cold probes, as indicated (c-fos DRE, DREmut5 or cAP-1). A quantified competition assay is presented below. Protein concentrations used are 49 μM. Control indicates DNA binding reaction with no calcium, or unlabeled probe. +10mMCa^{++}: control + calcium, cold-DNA (c-fos-DRE), m5: mut5 DRE (mutated dyn-DRE).

In summary, our initial attempt to reproduce the band shift indicating DREAM-DNA interaction as reported previously did not yield expected results. However, the inclusion

of an additional purification step resulted in the observation of a calcium-sensitive gel-shift consistent with the studies mentioned above. The band shift obtained was sequence specific as indicated by oligo competetion assays. Interestingly, EMSA analysis of individual DEAE eluted fractions of recombinant DREAM revealed, in addition to the previously characterized binding activity, a calcium-enhanced band shift that was exhibited only in the later fractions (#15 and #16 in fig.4-12A) from the DEAE column. This band shift might reflect a novel DNA binding activity of DREAM or might be explained by a contaminant protein from *E.coli*. Additional experiments were designed to determine the source of this new binding activity.

4.3.9 Recombinant DREAM exists in multiple conformational states

A fortuitous observation strongly suggests that the additional band shift is also due to DREAM-C activity. Figure 4-14A shows EMSA of freshly purified, DEAE eluted DREAM-C protein along with 6-month old DREAM protein sample stored at 4^{o}C. The freshly prepared protein sample shows a high molecular weight band shift that is calcium-sensitive (compare with fig.4-12A) in terms of recognizing DNA. While a calcium-enhanced, lower molecular weight band shift is observed in the fresh protein sample (fig.4-14A) similar to later fractions in fig.4-12A, it is present at much lower level. After 6 months, identical sample in fig.4-14A shows dramatically different binding properties resulting in a conversion from the high molecular weight, calcium-sensitive band shift to low molecular weight, calcium-enhanced band shift. The interconversion of one DNA binding activity to the other provides strong evidence for protein transformation with time.

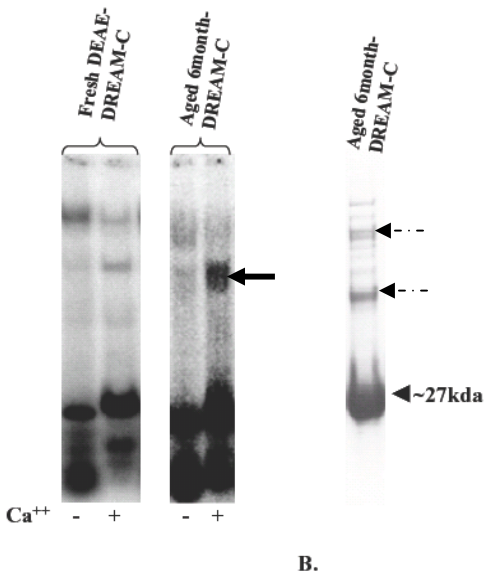

Figure 4-14: Transformation of DREAM protein activity with age. (A) EMSA of DREAM protein with DRE probe at two differnt time points. Left panel shows EMSA of freshly purifed protein. Right Panel shows the same sample as in the right stored for 6 months at 4^{o}C. Percentage DNA bound by the fresh sample was quantified to be 16% and 3%respectively (upper band only). Block arrow indicates position of band shift corresponding to DREAM's altered activity B) SDS PAGE of the protein sample of the aged protein. DREAM migrates at ~27 kda. Dashed arrows indicate high molecular weight species similar to those observed in fig.4-12B.

The 6-month-aged DREAM sample in fig.4-14 shows a calcium-enhanced lower band shift similar to the later fraction (#16 in fig.4-12A). SDS PAGE analysis of both samples [aged (fig.4-14B) and later fraction (fig.4-12B)] shows high molecular weight species that might represent oligomeric species of DREAM protein or DREAM protein complexed with a contaminant protein from *E.coli*. To ascertain the presence of DREAM protein, I performed western blot analysis with anti-DREAM antibody, on individual DEAE eluted DREAM protein fractions. The result shows that the high molecular weight species contain DREAM protein (fig.4-15). Furthermore, experiments using bacterial lysates, prepared from cells containing the empty expression vector (fig.4-17A) argue against the presence of a protein contaminant from *E.coli*.

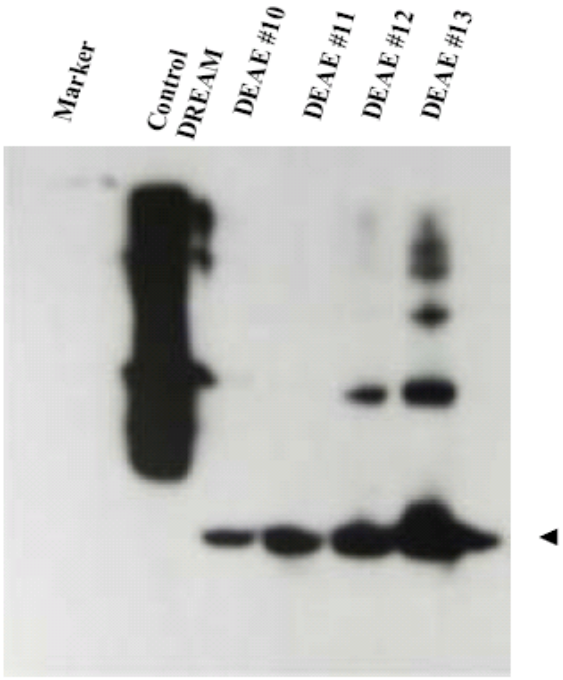

Figure 4-15: Western blot of DEAE fractions with Anti-DREAM antibody. Lanes from left to right are: Marker, control DREAM protein (51 kda GST-fusion DREAM protein purchased from Santacruz biotech. was used as positive control. Freshly purified DREAM-C-DEAE fraction #10, #11, # 12, # 13. High molecular weight bands were observed only in later DEAE fraction but NOT earlier DEAE fractions. Arrow head indicates recombinant DREAM protein migrating at ~27 kda.

Thus, the results from EMSA with individual DEAE fractions, comparison of freshly purified DREAM with aged sample, and western analysis consistently favor the existence of DREAM in multiple conformational states. While time can promote this transformation, another obvious possibility for the difference between each of the DEAE eluted fractions would be the concentration of salt. Recombinant protein bound to the DEAE column is eluted with a salt gradient from 0-100% across 150 ml with 0.6M KCl (see section 4.2.2). Therefore, I wished to test the effect of salt concentration on DREAM-DRE interaction.

4.3.10 Transformation of DREAM-DNA binding activity is not salt dependent

To examine the effect of salt on the EMSA band shifts, I performed EMSA experiments with separate DEAE fractions wherein I increased salt concentration of earlier fractions and decreased (by dialysis) the salt concentration of later fractions. The aim of this experiment was to test if salt concentration is responsible for the transformation of the DREAM-DNA binding activity from a calcium-sensitive DNA binding as seen in the case earlier fraction fig. 4-12A to calcium enhanced binding as observed in later fractions in fig.4-12A and aged sample in fig.4-14A.

Increasing the salt concentration did not perturb significantly, the DNA binding activity of initial fraction (#13, fig.4-16-lanes S1 and S2). However, since the later fractions do not show the second activity (the calcium enhanced DNA binding described above) in this experiment no conclusion can be made on the effect of salt on the calcium-enhanced lower band shift. It is also worth noting that decreasing the salt concentration in the later fractions (lanes under SS in fig.4-16) does not restore DNA binding similar to the initial fraction (lane 2, fig.4-16). Furthermore, the band shift observed in the case of initial fraction is sequence specific when competed with cold oligonucleotides as described in fig.4-13 lanes 3, 4, 5).

Thus, it was observed that salt concentration, by itself, is not the causative factor to transform DREAM-DNA binding activity from calcium sensitive binding as previously described (see fig.3-1, early fraction in fig.4-12A) to the calcium-enhanced DNA binding observed in this study (later fractions in fig.4-12A and aged sample in fig.4-14A)

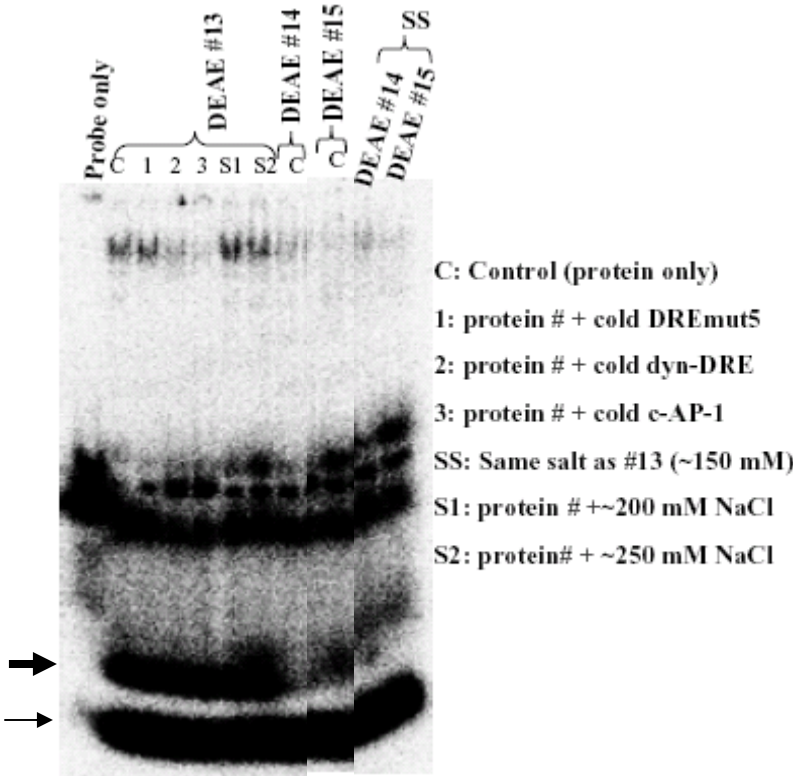

Figure 4-16: Effect of Salt on gel-shift exhibited by DEAE eluted fractions of DREAM-C. DEAE eluted fractions #13, #14, #15 with protein concentrations 49 μM, 87 μM and 72 μM respectively were incubated in the absence of Ca^{++} with radio labeled DRE probe. The figure shows EMSA of #13 in the absence and presence of unlabeled competitors in a 15 fold excess or with varying amounts of salt concentration. For fractions #14 and #15, the figure shows EMSA in the absence of unlabeled oligos, and with decreased salt concentration (SS). #13, #14 and #15 eluted at ~150 mM, ~200 mM and ~250mM salt respectively. Percentage of DNA bound in lane numbers 2,3,4,5,6,7,8,9,10,11 was quantified to be 29%, 31%, 11%, 7.3%, 29%, 20%, 18%, 24%, 13%, 6.5% respectively. Note that the probe only lane does not contain lower most bands that constitute products of exo and endo nuclease (shown by thin and dense arrows respectively) activity. The unbound probe consists of duplex, single strand and an endonuclease activity

4.3.11 DRE binding activity is associated with recombinant DREAM

To rule out the possibility of the band shift occurring due to an *E.coli* contaminant and to make sure that the observed DNA binding is indeed due to recombinant DREAM, I prepared bacterial lysates of strains containing the empty pET15b vector and performed EMSA with labeled dynorphin DRE after following the purification protocol for DREAM-C. The experiment was performed using a batch preparation (see section 4.2.2), with bacteria, containing empty vector and DREAM plasmid induced for protein expression. After inducing expression for 3 hours at 37^{o}C cells from both the cultures

(empty vector and pet15b-DREAM-C containing bacterial cultures) were harvested, and processed further, as described in the methods section. DNA binding reactions were prepared using the Ni^{++}- eluted protein samples for qualitative comparison. Not surprisingly, under identical purification and binding conditions, the bacterial lysate with empty vector did not show significant DNA binding but the lysates containing DREAM-C protein showed DNA binding (Fig 4-17A). Thus, the observed EMSA band shifts are definitely associated with the presence of DREAM-C, although presence of a contaminant *E.coli* protein along with DREAM cannot be ruled out. However, a far-Western analysis (that involves transfer of the protein-DNA complexes from EMSA-gel onto a membrane and probing with anti-DREAM antibody) should be performed to confirm that the radioactive band shift contains DREAM-C.

Figure 4-18 shows the SDS-PAGE analysis of the preparations of samples used in Fig 4-17. The purification steps in the case of empty vector lysates show that there‘s no detectable protein as observed by coomassie staining (fig.4-18A) consistent with the lack of band shift in fig.4-17A. Further, DREAM-C protein sample was free of impurities that can be detected by coomassie staining (fig.4-18B).

Supershift experiments were performed to confirm the presence of DREAM protein in the band shifts by adding anti-DREAM or anti-His antibodies to the DNA binding reactions. As a negative control, anti-HNF4 antibody was also tested. However, this experiment did not yield any retarded bands with anti-his antibody, and yielded a smear with anti-DREAM antibody (4-17B). The lack of supershift with anti-His antibody suggests that the His-tag may be inaccessible. A smear in the presence of anti-DREAM

antibody might indicate that DREAM does indeed interact with the antibody, but unfortunately, a negative control (antibody added without DREAM) was not performed. So, no clear conclusion can be made.

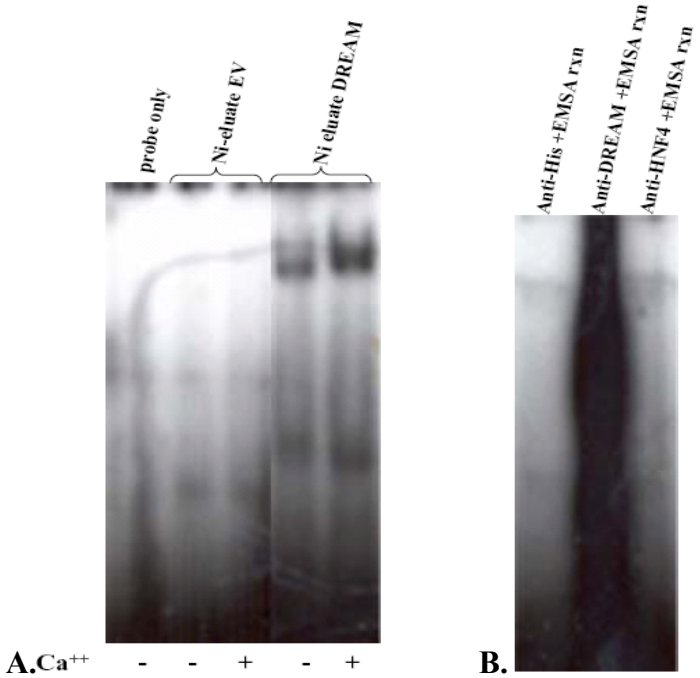

Figure 4-17: A) EMSA of Ni^{++}-eluates prepared from empty vector (EV) and DREAM-C plasmid containing bacterial lysates. Lanes: 1) probe only without protein 2, 3) Ni eluate EVTMg , 4, 5) Ni eluate EV, 6, 7) Ni eluate DREAM-C –TMg, 8,9) Ni eluate DREAM-C. TMg indicates presence of 0.2 % tween 20 and $MgCl_2$ in the sonication buffer. Arrowhead indicates position of specific DRE band retarded by DREAM protein. Protein concentrations of DREAM are 94 μM in lanes 2 & 3 and 100 μM in lanes 4 & 5. (B) Supershift experiment using 15 μg each of Anti-His antibody (Genscript) (lane 1), Anti-DREAM antibody (Santacruz) (lane 2) and Anti-HNF4 antibody (Santacruz) (lane 3). All supershift experiments were performed with DREAM-C protein sample in the absence of calcium.

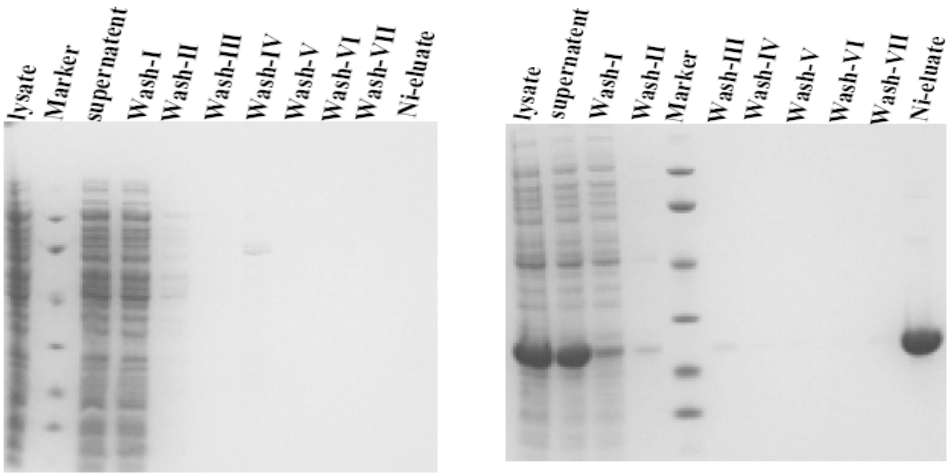

A. **B.**

Figure 4-18: SDS PAGE analysis indicating progress of purification steps of A) Empty vector and B) DREAM-C bacterial lysates by Ni^{++}-affinity chromatography using batch method. Excluding markers lanes from left to right show aliquots from lysate, supernatant, washes 1 through 7 and Ni- eluate. Of the eight washes described in the methods section aliquot from the last wash was omitted. Molecular weight markers from top represent 97, kda, 66, kda, 45 kda, 31 kda, 21 kda, and 14 kda.

4.3.12 Summary of DNA binding experiments

In summary, the EMSA gel-shift experiments with wild type DREAM protein in this study indicated considerable sample heterogeneity of DREAM protein. The early fraction from the DEAE elution exhibited sequence specific, Ca^{++}-sensitive DNA binding as observed before [74, 130]). However, the remainder of the protein (~90% of the total) showed either calcium-enhanced DNA binding or no binding at all. We currently do not understand why the multiple DNA bands with different calcium sensitivities were not seen in the previously published studies, which reported only one apparent species of DREAM that bound to DNA only in the absence of calcium [74, 130]. One possible explanation for the difference is that the extra purification step (DEAE chromatography) used in this study has resolved and uncovered multiple protein species that previously were either undetected or unresolved.

In the present study on DREAM-DRE interaction, a calcium-enhanced DREAM-DNA binding activity (by way of band shift position on EMSA) was observed and partially characterized, apart from the previously reported binding activity (fig.3-1). The puzzling nature of DREAM's dual mode of interaction with DRE (upper and lower bands on EMSA, figs.4-12A) is best explained by conformational heterogeneity of recombinant DREAM, which was inferred from the analysis of DEAE resolved fractions (fig. 4-12A), indicated by multiple bands in western blots (fig.4-15) and evidenced by the transformation of aged protein samples (fig.4-14). The sample heterogeneity was unfortunately found to be prep-dependent as later fractions from some protein preparations show enhanced binding on addition of calcium (fig.4-12A). However, the upper band shift seen in the early DEAE fraction was highly reproducible and shown to be sequence specific (figs.4-12, 4-13). In all cases, the later DEAE fractions were found to behave differently from the earlier eluted fractions, indicative of heterogeneous species. While the functional significance of the lower calcium-induced band shift in Fig. 4-12 is currently unclear, it is possible that it may be the result of an altered conformational state of the protein. Recently, D'Andrea et al. (2005) showed that thapsigargin treatment, which blocks endoplasmic reticulum Ca^{++} ATPase resulting in increased cytosolic calcium levels, leads to increased repression of thyroid genes Pax8 and TTF2/FoxE1 by DREAM correlated with increased binding to DRE [120]. Furthermore, the specificity of DREAM-DNA interaction was confirmed by the competition experiments that demonstrated DREAM's specificity towards DRE sequence as previously characterized [74, 130, 179]. Thus, DREAM binding to DNA under elevated calcium levels may be possible for which existence of DREAM in an alternative conformational state would be

a plausible explanation. Whether this binding is a result of DREAM-DRE interaction alone and not mediated by DREAM's interaction with other transcription factors remains to be established.

Heterogeneous DNA binding activities of DREAM could also be explained with an analogy to prion protein hypothesis wherein a small fraction of altered conformation may nucleate the conversion of native protein into its alternative form [212]. Future studies could test this hypothesis, by adding a small amount of protein sample from later eluted DEAE fractions into the earlier fractions and observe for any changes in its activity. In addition, to ascertain the functional nature of calcium enhanced binding to DNA (lower band shift) dominant negative mutants of DREAM that are completely disabled for metal-binding (refer section 2.1) could be used to perform EMSA. If the lower band is still observed with the mutants defective for calcium binding, then it could be deemed as a calcium-binding independent property of DREAM. Further, the specificity of this interaction could be tested by using unlabeled specific and non-specific probes for competition experiments.

4.3.13 EMSA analysis on DREAM-Recoverin Chimeras (DRC's)

In view of the apparent sample heterogeneity, all subsequent EMSA experiments on the chimeras were performed using two types of sample preparations: 1) pooled protein fractions eluted from DEAE chromatography to ascertain qualitative DNA binding and 2) individual and separated DEAE fractions to observe any calcium-induced effects. However, the interpretations of these results would be speculative, due to apparent uncertainity of multiple DREAM species and lack of knowledge on whether altered DNA

recognition of a chimera is due to disruption of binding site or due to its enhanced propensity to adopt alternative conformations.

When pooled DRC protein samples were used for EMSA experiments, all the chimera proteins except DRC-IV exhibited DNA binding similar to that of wild type (Fig 4-19). DRC-IV showed abolition of DNA binding upon addition of calcium, similar to that observed with wild type DREAM in previous reports [74, 130]. Collectively, since all the chimeras exhibit DNA binding, this would suggest that the DNA binding region in DREAM might be delocalized among the four EF-hands and not confined to a distinct structural region. However, given the variability and ambiguity of the EMSA results combined with circumstantial evidence that the observed EMSA band actually represents DNA binding to DREAM, it is certainly possible that the EMSA bands in this study will also represent some type of artificial binding to an E. coli contaminant protein. If this were the case, it could explain some of the prep-dependent artifacts in these studies such as the lower spurious bands as well as the calcium-insensitive EMSA bands. However, the uppermost EMSA band (associated with the early DEAE fractions: #14 in Fig. 4-12A) was shown in this study to be sequence specific and calcium sensitive, in the case of wild-type DREAM, as seen in previous studies [74, 123] (Fig.4-12), arguing that at least this band might represent functional DNA binding by DREAM.

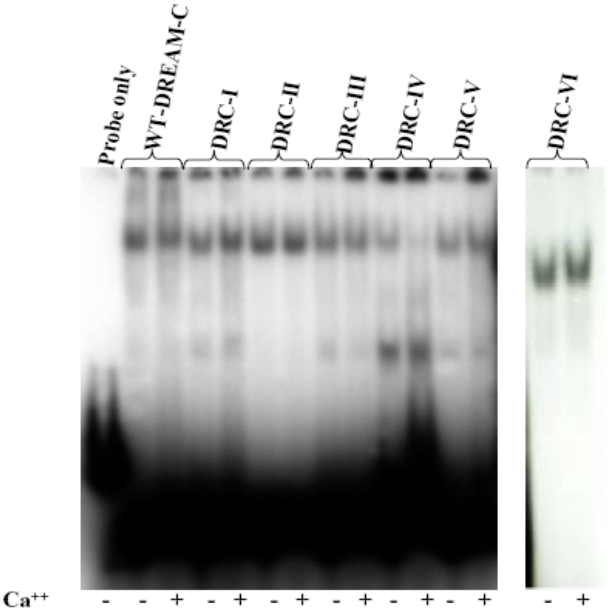

Figure 4-19: Electrophoretic mobility shift assay using pooled DEAE fractions of wild type DREAM-C and Dream-recoverin chimeras. Presence of 10 mM Ca^{++} is indicated at the bottom. In the case of DRC-VI, Ni-eluate was directly used for EMSA. Protein concentrations in all the lanes is ~65 μM.

Electrophoretic mobility shift assay of individual DEAE fractions of each of the chimeras and their SDS PAGE figures are shown in figures 4-20 through 4-25 respectively. The EMSA data for DRC-I (Fig. 4-20), -III (Fig. 4-22) and -VI (Fig. 4-25) are very similar to that described above for wild type (Fig. 4-12) and suggest that these chimeras exhibit at least some form of DNA binding, consistent with the EMSA data above on the pooled fractions in Fig. 4-19. However, the DEAE resolved EMSA data for DRC-II (Fig. 4-21) and DRC-IV (Fig. 4-23) both lack the calcium-responsive EMSA band associated with the early DEAE fraction (e.g. fraction #14 for wild type in Fig. 4-12; #10 for DRC-II; and #11 for DRC-IV). Recall, that this EMSA band for wild type was also shown to be sequence specific (Fig. 4-13). Since both DRC-II and DRC-IV lack the high affinity Mg^{++} binding at EF-2, perhaps Mg^{++} binding at EF-2 may be necessary for sequence-specific DNA binding to DREAM, consistent with a structural role for Mg^{++} as proposed and studied in Chapter II.

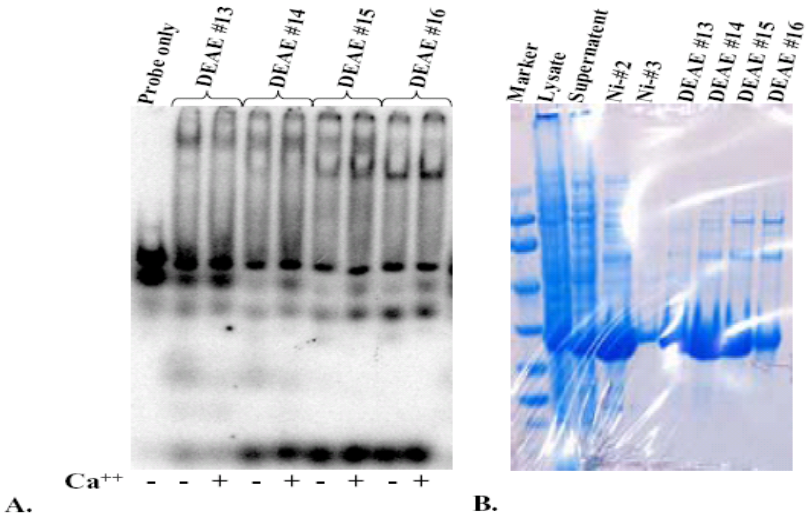

Figure 4-20: EMSA (A) and SDS-PAGE (B) diagrams of DRC-I. Presence of 10 mM Ca^{++} is indicated at the bottom in panel A. (B) Stages during the purification of recombinant DRC-I protein. Molecular weight markers from top represent 97, kda, 66, kda, 45 kda, 31 kda, 21 kda, and 14 kda.

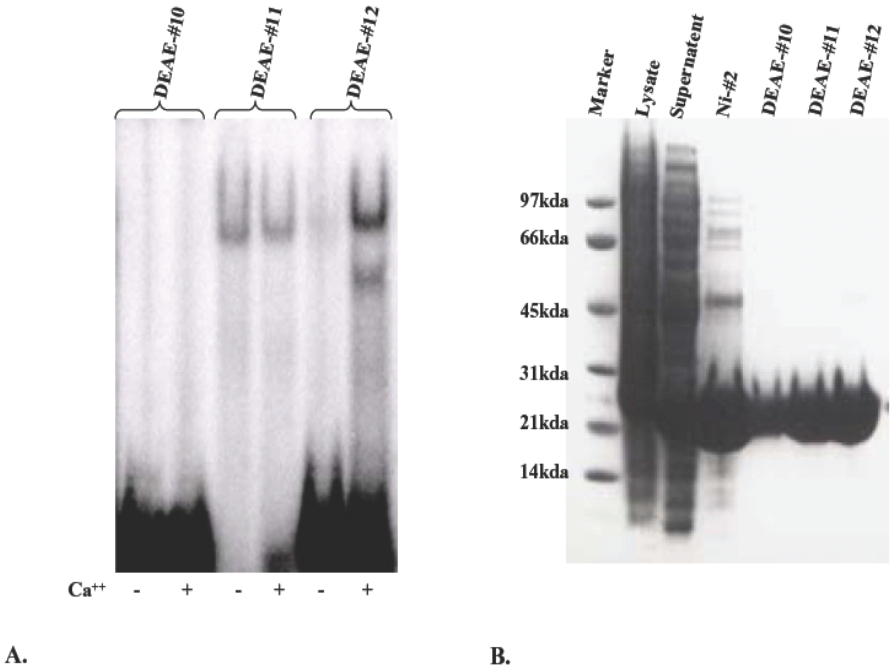

Figure 4-21: (A) EMSA and (B) SDS-PAGE diagrams of DRC-II. Presence of 10 mM Ca^{++} is indicated at the bottom in panel A.

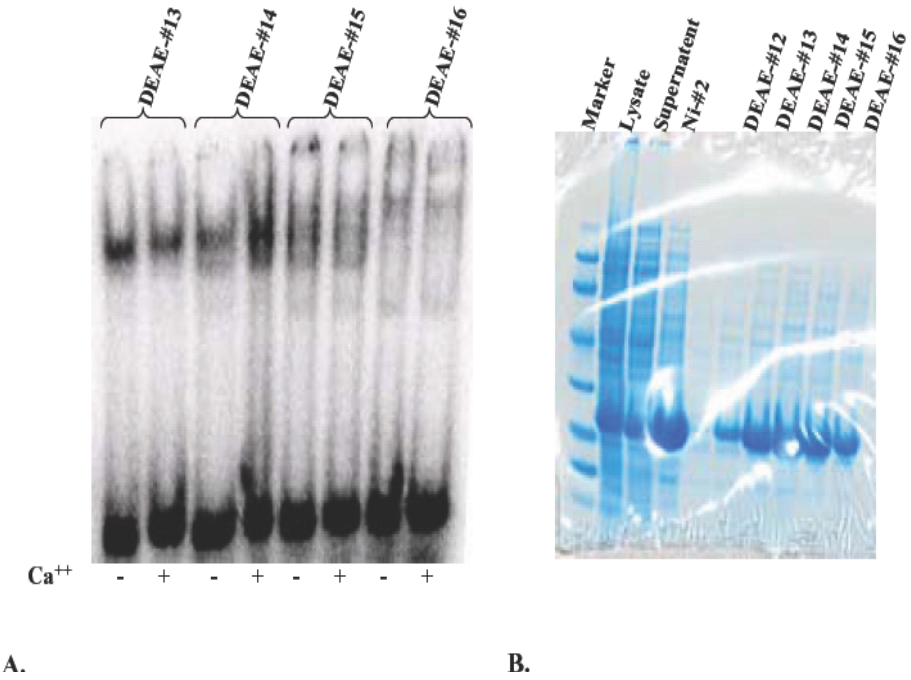

Figure 4-22: (A) EMSA and (B) SDS-PAGE of DRC-III. Presence of 10 mM Ca^{++} is indicated at the bottom in panel A. Molecular weight markers from top represent 97, kda, 66, kda, 45 kda, 31 kda, 21 kda, and 14 kda.

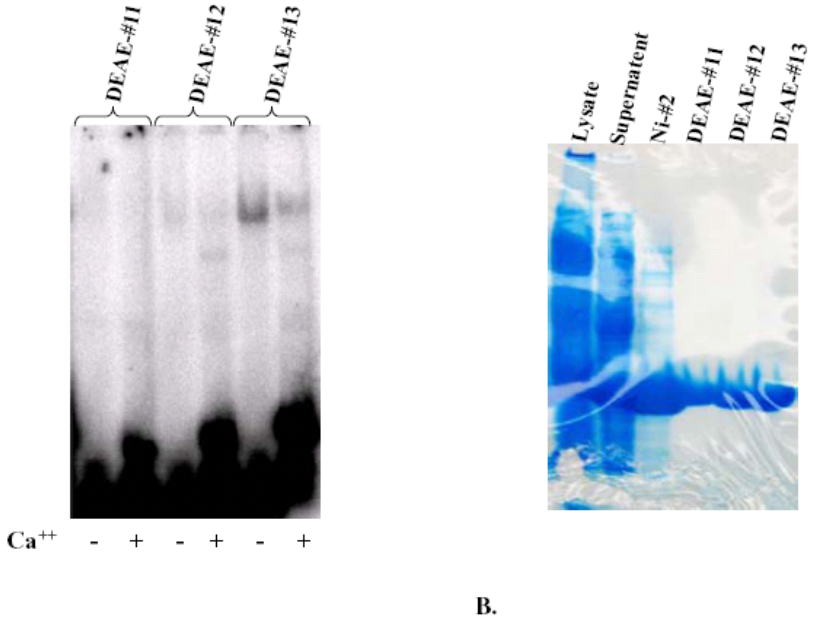

Figure 4-23: (A) EMSA and (B) SDS-PAGE of DRC-IV. Presence of 10 mM Ca^{++} is indicated at the bottom in panel A.

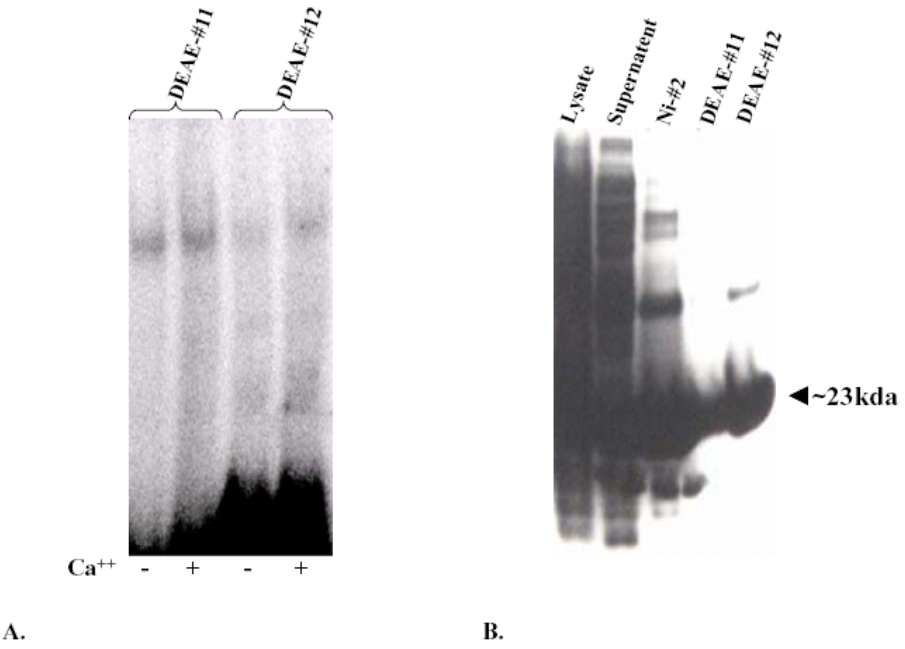

Figure 4-24: (A) EMSA and (B) SDS-PAGE of DRC-V. Presence of 10 mM Ca^{++} is indicated at the bottom in panel A.

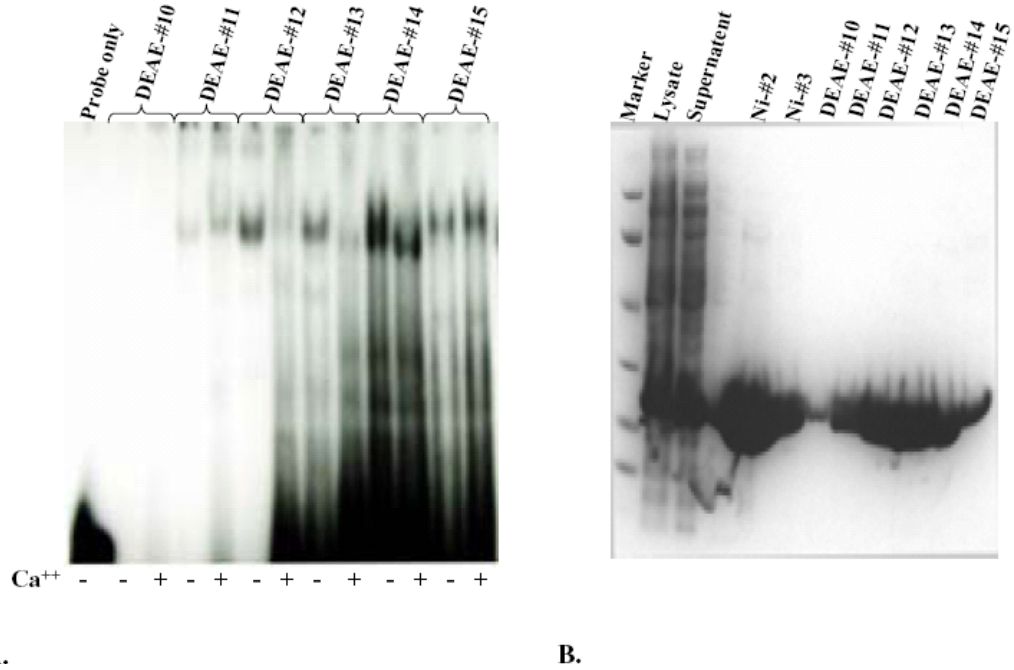

Figure 4-25: (A) EMSA and (B) SDS-PAGE of DRC-VI. Presence of 10 mM Ca^{++} is indicated at the bottom in panel A. (B) Lanes- M: Molecular weight markers from top represent 97, kda, 66, kda, 45 kda, 31 kda, 21 kda, and 14 kda.

4.3.14 Structural Model for DNA binding to DREAM

A structural model for DNA binding by DREAM can be proposed based on the x-ray crystal structure of calcium-bound KChIP1 and the data from this study (summarized in table 4-3). DREAM is thought to bind to DNA as a tetramer based on light scattering analysis of the DREAM-DNA complex [130] and apparent molecular mass on a Southwestern blot [74]. The Ca^{++}-bound form of DREAM was shown to be a dimer in solution based on the work in Chapter 2. The structure of the DREAM dimer can be estimated to have a head-to-tail orientation based on the x-ray structure of KChIP1 (Fig. 4-8). A head-to-tail dimer orientation is also consistent with the size chromatography studies on the chimeras showing that each EF-hand is essential for dimer formation. We speculate that two DREAM dimers may come together and bind to DNA on opposite sides, perhaps by encircling it (fig. 4-26). This orientation enables all four EF-hands in the DREAM protein to contact DNA and would explain the apparent DNA binding observed for all the chimeras (Fig. 4-19). Calcium binding to the DREAM tetramer causes conformational changes that promote its dissociation into dimers and abolishes its binding to DNA.

Protein	Mg^{++} sites	Ca^{++} sites	Oligomerization state		DNA binding	
			Ca^{++}-free	Ca^{++}-bound	Ca^{++}-free	Ca^{++}-bound
DREAM-C	1	2	Monomer	dimer	Yes	Yes
Recoverin	0	2	Monomer	Monomer	No	No
DRC-I	1	1	Monomer	Monomer	Yes	Yes
DRC-II	0	3	Aggregate/ monomer	Monomer	Yes	Yes
DRC-III	1	2	Monomer	Monomer	Yes	Yes
DRC-IV	0	2	Dimer	Aggregate	Yes	No
DRC-V	1	2	Tri/dimer	Tri/dimer	Yes	Yes
DRC-VI	1	1	Monomer	Monomer	Yes	yes

Table 4-3: Summary of SEC results of DREAM-C, Recoverin and DRC's I-VI.

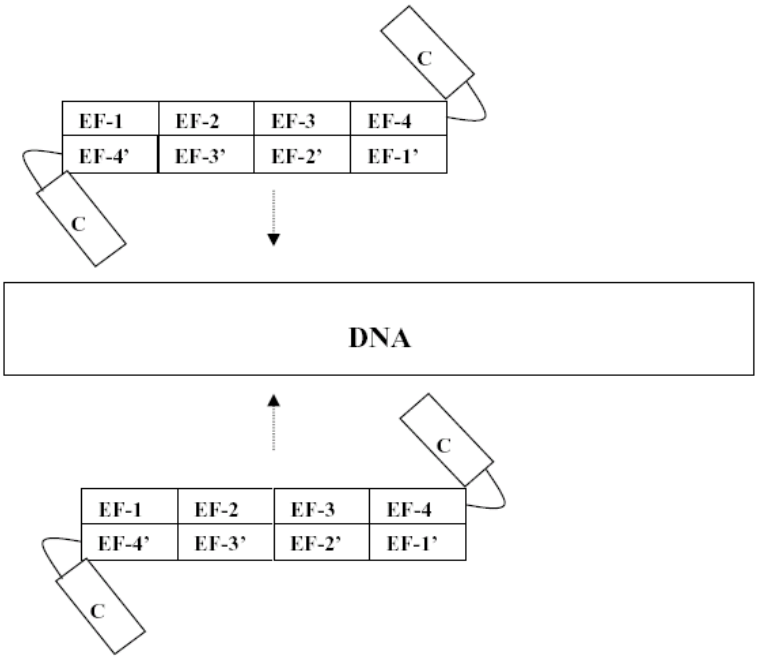

Figure 4-26: Model diagram showing potential assembly of a DREAM tetramer on the DNA. DREAM dimers, formed head-to-tail sideways similar to right and left hands joined with fingers against the palms of each other with the C-terminal helices projecting perpendicular to the plane of the palms, bind to DNA from either side thus assembling as a dimer of dimers formed head-to-tail again so that all the EF-hands make contact with the DNA.

4.4 Summary

In summary, the calcium insensitive DNA binding to DREAM not withstanding, this study points to a DNA binding region in DREAM that encompasses all four EF-hands. However, these results must be interpreted with extreme caution, in view of the heterogeneous behavior of wild type DREAM protein. Therefore, the possibility of a localized DNA binding site still cannot be entirely ruled out. In the future, it will be necessary to test more rigorously which of the observed EMSA bands represent functional DREAM binding to DRE and to completely rule out any possible binding that could be induced by E. coli proteins co-purifying with DREAM. Experiments aimed at observing specific antibody supershift of the EMSA bands would be fruitful in this regard. In addition, inclusion of an additional purification step, size exclusion chromatography, to isolate DREAM protein samples to homogeneity and testing for their DNA binding activity may address the issue of spurious band shift, due to co-purifying E.coli proteins, rigorously. The other important issue is to resolve the discrepancy with earlier studies regarding the calcium dependence of the EMSA shift. In this study, only a very small fraction of the protein (<10%) exhibits calcium-responsive DNA binding as was seen previously [74, 123]. The remainder of the protein in this study either binds DNA independent of calcium or in some cases binds DNA only in the presence of calcium. Clearly, the calcium-induced DNA binding is at odds with the earlier studies and is delineated from the calcium-sensitive binding, in this study. The possibility exists, however, that the calcium-induced DNA binding might be functionally relevant and might explain a recent study showing that DREAM potentiates the activation of gene

expression regulated by the Vitamin-D receptor only at high Ca^{++} levels [125] and also repression of thyroid specific transcription factors under elevated levels of calcium [120].

Bibliography

1. Lodish .H., B.A., Zipursky .S.L., Matsudaira P., Baltimore .D., Darnell .J.E., *Molceular Cell Biology*. 4 ed. 2000: W.H. Freeman and company.

2. Rasmussen, H., Kelley, G., and Douglas, J.S., *Interactions between Ca2+ and cAMP messenger system in regulation of airway smooth muscle contraction.* Am J Physiol, 1990. **258**(6 Pt 1): p. L279-88.

3. Pattni, K. and Banting, G., *Ins(1,4,5)P3 metabolism and the family of IP3-3Kinases.* Cell Signal, 2004. **16**(6): p. 643-54.

4. Berridge, M.J., Bootman, M.D., and Roderick, H.L., *Calcium signalling: dynamics, homeostasis and remodelling.* Nat Rev Mol Cell Biol, 2003. **4**(7): p. 517-29.

5. Brocard, J.B., Rajdev, S., and Reynolds, I.J., *Glutamate-induced increases in intracellular free Mg2+ in cultured cortical neurons.* Neuron, 1993. **11**(4): p. 751-7.

6. Listed, N.A., *Homeostasis*. 2006.

7. Medvedev, S.S., *Calcium signaling system in plants.* Russian Journal of Plant Physiology, 2005. **52**(2): p. 249 - 270.

8. Carafoli, E., *Calcium signaling: a tale for all seasons.* Proc Natl Acad Sci U S A, 2002. **99**(3): p. 1115-22.

9. Bailey, K., *Myosin and adenosinetriphosphatase.* Biochem J, 1942. **36**(1-2): p. 121-39.

10. Frank, G.B., *Evidence for an Essential Role for Calcium in Excitation-Contraction Coupling in Skeletal Muscle.* Proc R Soc Lond B Biol Sci, 1964. **160**: p. 504-12.

11. Weber, A., Herz, R., and Reiss, I., *The Regulation of Myofibrillar Activity by Calcium.* Proc R Soc Lond B Biol Sci, 1964. **160**: p. 489-501.

12. Hasselbach, W., *Atp-Driven Active Transport of Calcium in the Membranes of the Sarcoplasmic Reticulum.* Proc R Soc Lond B Biol Sci, 1964. **160**: p. 501-4.

13. Makinose, M. and Hasselbach, W., *ATP synthesis by the reverse of the sarcoplasmic calcium pump.* FEBS Lett, 1971. **12**(5): p. 271-272.

14. De Meis, L., Hasselbach, W., and Machado, R.D., *Characterization of calcium oxalate and calcium phosphate deposits in sarcoplasmic reticulum vesicles.* J Cell Biol, 1974. **62**(2): p. 505-9.

15. Rasmussen, H., *Cell Communication, Calcium Ion,and Cyclic Adenosine Monophosphate.* SCIENCE, 1970. **170**: p. 404-412.

16. Rasmussen H, J.P., Lake W, Goodman Db., *Calcium ion as second messenger.* Clinical Endocrinology (Oxf), 1976. **5 Suppl.**: p. 11S-27S.

17. Hafner, M., Petzelt, C., Nobiling, R., Pawley, J.B., Kramp, D., and Schatten, G., *Wave of free calcium at fertilization in the sea urchin egg visualized with fura-2.* Cell Motil Cytoskeleton, 1988. **9**(3): p. 271-7.

18. Steinhardt, R., Zucker, R., and Schatten, G., *Intracellular calcium release at fertilization in the sea urchin egg.* Dev Biol, 1977. **58**(1): p. 185-96.

19. Augustine, G.J., *How does calcium trigger neurotransmitter release?* Curr Opin Neurobiol, 2001. **11**(3): p. 320-6.

20. Schanne, F.A., Kane, A.B., Young, E.E., and Farber, J.L., *Calcium dependence of toxic cell death: a final common pathway.* Science, 1979. **206**(4419): p. 700-2.

21. Gangola, P. and Rosen, B.P., *Maintenance of intracellular calcium in Escherichia coli.* J Biol Chem, 1987. **262**(26): p. 12570-4.

22. Dominguez, D.C., *Calcium signalling in bacteria.* Mol Microbiol, 2004. **54**(2): p. 291-7.

23. Norris, V., Grant, S., Freestone, P., Canvin, J., Sheikh, F.N., Toth, I., Trinei, M., Modha, K., and Norman, R.I., *Calcium signalling in bacteria.* J Bacteriol, 1996. **178**(13): p. 3677-82.

24. Waditee, R., Hossain, G.S., Tanaka, Y., Nakamura, T., Shikata, M., Takano, J., and Takabe, T., *Isolation and functional characterization of Ca2+/H+ antiporters from cyanobacteria.* J Biol Chem, 2004. **279**(6): p. 4330-8.

25. Wayne, R. and Hepler, P.K., *Red Light Stimulates an Increase in Intracellular Calcium in the Spores of Onoclea sensibilis.* Plant Physiol, 1985. **77**(1): p. 8-11.

26. Knight, M.R., Smith, S.M., and Trewavas, A.J., *Wind-induced plant motion immediately increases cytosolic calcium.* Proc Natl Acad Sci U S A, 1992. **89**(11): p. 4967-71.

27. Liu, C.H., Ashton, G.C., and Catron, D.V., *The effect of intermittent consumption of calcium in rats.* J Nutr, 1956. **59**(2): p. 267-71.

28. White, P.J. and Broadley, M.R., *Calcium in plants.* Ann Bot (Lond), 2003. **92**(4): p. 487-511.

29. Berridge, M., Lipp, P., and Bootman, M., *Calcium signalling.* Curr Biol, 1999. **9**(5): p. R157-9.

30. Whitfield, J.F., Rixon, R.H., Macmanus, J.P., and Balk, S.D., *Calcium, cyclic adenosine 3',5'-monophosphate, and the control of cell proliferation: a review.* In Vitro, 1973. **8**(4): p. 257-78.

31. Sten Orrenius, B.Z.A.P.N., *Regulation of Cell death: The calcium- apoptosis link.* Nature Reviews Molecular Cell Biology, 2003. **4**: p. 552-565.

32. Gail, M.H., Boone, C.W., and Thompson, C.S., *A calcium requirement for fibroblast motility and prolifertion.* Exp Cell Res, 1973. **79**(2): p. 386-90.

33. Magee, A.I., Lytton, N.A., and Watt, F.M., *Calcium-induced changes in cytoskeleton and motility of cultured human keratinocytes.* Exp Cell Res, 1987. **172**(1): p. 43-53.

34. Penner, R. and Neher, E., *The role of calcium in stimulus-secretion coupling in excitable and non-excitable cells.* J Exp Biol, 1988. **139**: p. 329-45.

35. Lipp, P., Thomas, D., Berridge, M.J., and Bootman, M.D., *Nuclear calcium signalling by individual cytoplasmic calcium puffs.* Embo J, 1997. **16**(23): p. 7166-73.

36. Clapham, D.E., *Calcium signaling.* Cell, 1995. **80**(2): p. 259-68.

37. Iida, H., Yagawa, Y., and Anraku, Y., *Essential role for induced Ca2+ influx followed by [Ca2+]i rise in maintaining viability of yeast cells late in the mating pheromone response pathway. A study of [Ca2+]i in single Saccharomyces cerevisiae cells with imaging of fura-2.* J Biol Chem, 1990. **265**(22): p. 13391-9.

38. Miyawaki, A., Llopis, J., Heim, R., Mccaffery, J.M., Adams, J.A., Ikura, M., and Tsien, R.Y., *Fluorescent indicators for Ca2+ based on green fluorescent proteins and calmodulin.* Nature, 1997. **388**(6645): p. 882-7.

39. Schatzmann, H.J., *The calcium pump of the surface membrane and of the sarcoplasmic reticulum.* Annu Rev Physiol, 1989. **51**: p. 473-85.

40. Blaustein, M.P. and Lederer, W.J., *Sodium/calcium exchange: its physiological implications.* Physiol Rev, 1999. **79**(3): p. 763-854.

41. Favaron, M. and Bernardi, P., *Tissue-specific modulation of the mitochondrial calcium uniporter by magnesium ions.* FEBS Lett, 1985. **183**(2): p. 260-4.

42. Berridge, M.J., Lipp, P., and Bootman, M.D., *The versatility and universality of calcium signalling.* Nat. Rev. Mol. Cell Biol., 2000. **1**(1): p. 11-21.

43. Allbritton, N.L., Oancea, E., Kuhn, M.A., and Meyer, T., *Source of nuclear calcium signals.* Proc Natl Acad Sci U S A, 1994. **91**(26): p. 12458-62.

44. Leite, M.F., Thrower, E.C., Echevarria, W., Koulen, P., Hirata, K., Bennett, A.M., Ehrlich, B.E., and Nathanson, M.H., *Nuclear and cytosolic calcium are regulated independently.* Proc Natl Acad Sci U S A, 2003. **100**(5): p. 2975-80.

45. Echevarria, W., Leite, M.F., Guerra, M.T., Zipfel, W.R., and Nathanson, M.H., *Regulation of calcium signals in the nucleus by a nucleoplasmic reticulum.* Nat Cell Biol, 2003. **5**(5): p. 440-6.

46. Tsien, R.W. and Tsien, R.Y., *Calcium channels, stores, and oscillations.* Annu Rev Cell Biol, 1990. **6**: p. 715-60.

47. Hoshi, T. and Smith, S.J., *Large depolarization induces long openings of voltage-dependent calcium channels in adrenal chromaffin cells.* J Neurosci, 1987. **7**(2): p. 571-80.

48. Bezprozvanny, I., Watras, J., and Ehrlich, B.E., *Bell-shaped calcium-response curves of Ins(1,4,5)P3- and calcium-gated channels from endoplasmic reticulum of cerebellum.* Nature, 1991. **351**(6329): p. 751-4.

49. Kaftan, E.J., Ehrlich, B.E., and Watras, J., *Inositol 1,4,5-trisphosphate (InsP3) and calcium interact to increase the dynamic range of InsP3 receptor-dependent calcium signaling.* J Gen Physiol, 1997. **110**(5): p. 529-38.

50. Ghosh, T.K., Bian, J., and Gill, D.L., *Intracellular calcium release mediated by sphingosine derivatives generated in cells.* Science, 1990. **248**(4963): p. 1653-6.

51. Lee, H.C., Walseth, T.F., Bratt, G.T., Hayes, R.N., and Clapper, D.L., *Structural determination of a cyclic metabolite of NAD+ with intracellular Ca2+-mobilizing activity.* J Biol Chem, 1989. **264**(3): p. 1608-15.

52. Cancela, J.M., Van Coppenolle, F., Galione, A., Tepikin, A.V., and Petersen, O.H., *Transformation of local Ca2+ spikes to global Ca2+ transients: the combinatorial roles of multiple Ca2+ releasing messengers.* Embo J, 2002. **21**(5): p. 909-19.

53. Fabiato, A. and Fabiato, F., *Calcium-induced release of calcium from the sarcoplasmic reticulum of skinned cells from adult human, dog, cat, rabbit, rat, and frog hearts and from fetal and new-born rat ventricles.* Ann N Y Acad Sci, 1978. **307**: p. 491-522.

54. Itoh, T., Ueno, H., and Kuriyama, H., *Calcium-induced calcium release mechanism in vascular smooth muscles--assessments based on contractions evoked in intact and saponin-treated skinned muscles.* Experientia, 1985. **41**(8): p. 989-96.

55. Verkhratsky, A. and Shmigol, A., *Calcium-induced calcium release in neurones.* Cell Calcium, 1996. **19**(1): p. 1-14.

56. Saunders, C.M., Larman, M.G., Parrington, J., Cox, L.J., Royse, J., Blayney, L.M., Swann, K., and Lai, F.A., *PLC zeta: a sperm-specific trigger of Ca(2+) oscillations in eggs and embryo development.* Development, 2002. **129**(15): p. 3533-44.

57. Spat, A., Bradford, P.G., Mckinney, J.S., Rubin, R.P., and Putney, J.W., Jr., *A saturable receptor for 32P-inositol-1,4,5-triphosphate in hepatocytes and neutrophils.* Nature, 1986. **319**(6053): p. 514-6.

58. Spiegel, S. and Milstien, S., *Sphingosine-1-phosphate: an enigmatic signalling lipid.* Nat Rev Mol Cell Biol, 2003. **4**(5): p. 397-407.

59. Mao, C., Kim, S.H., Almenoff, J.S., Rudner, X.L., Kearney, D.M., and Kindman, L.A., *Molecular cloning and characterization of SCaMPER, a sphingolipid Ca2+ release-mediating protein from endoplasmic reticulum.* Proc Natl Acad Sci U S A, 1996. **93**(5): p. 1993-6.

60. Lee, H.C., *Physiological functions of cyclic ADP-ribose and NAADP as calcium messengers.* Annu Rev Pharmacol Toxicol, 2001. **41**: p. 317-45.

61. Lee, H.C., *Mechanisms of calcium signaling by cyclic ADP-ribose and NAADP.* Physiol Rev, 1997. **77**(4): p. 1133-64.

62. Lee, H.C. and Aarhus, R., *Structural determinants of nicotinic acid adenine dinucleotide phosphate important for its calcium-mobilizing activity.* J Biol Chem, 1997. **272**(33): p. 20378-83.

63. Dolmetsch, R.E., Lewis, R.S., Goodnow, C.C., and Healy, J.I., *Differential activation of transcription factors induced by Ca2+ response amplitude and duration.* Nature, 1997. **386**(6627): p. 855-8.

64. Dolmetsch, R.E., Xu, K., and Lewis, R.S., *Calcium oscillations increase the efficiency and specificity of gene expression.* Nature, 1998. **392**(6679): p. 933-6.

65. Michael J. Berridge, P.L.A.M.D.B., *THE VERSATILITY AND UNIVERSALITY OF CALCIUM SIGNALLING.* NATURE REVIEWS MOLECULAR CELL BIOLOGY, 2000. **1**: p. 11-21.

66. Philipson, K.D. and Nicoll, D.A., *Sodium-calcium exchange: a molecular perspective.* Annu Rev Physiol, 2000. **62**: p. 111-33.

67. Ishida, Y. and Paul, R.J., *Ca2+ clearance in smooth muscle: lessons from gene-altered mice.* J Smooth Muscle Res, 2005. **41**(5): p. 235-45.

68. Hoeflich, K.P. and Ikura, M., *Calmodulin in action: diversity in target recognition and activation mechanisms.* Cell, 2002. **108**(6): p. 739-742.

69. Ikura, M. and Ames, J.B., *Genetic polymorphism and protein conformational plasticity in the calmodulin superfamily: two ways to promote multifunctionality.* Proc Natl Acad Sci U S A, 2006. **103**(5): p. 1159-64.

70. Ebashi, S., *The Croonian lecture, 1979: Regulation of muscle contraction.* Proc R Soc Lond B Biol Sci, 1980. **207**(1168): p. 259-86.

71. Crabtree, G.R., *Calcium, calcineurin, and the control of transcription.* J Biol Chem, 2001. **276**(4): p. 2313-6.

72. Maurer, P., Hohenester, E., and Engel, J., *Extracellular calcium-binding proteins.* Curr Opin Cell Biol, 1996. **8**(5): p. 609-17.

73. An, W.F., Bowlby, M.R., Betty, M., Cao, J., Ling, H.P., Mendoza, G., Hinson, J.W., Mattsson, K.I., Strassle, B.W., Trimmer, J.S., and Rhodes, K.J., *Modulation of A-type potassium channels by a family of calcium sensors.* Nature, 2000. **403**(6769): p. 553-6.

74. Carrion, A.M., Link, W.A., Ledo, F., Mellstrom, B., and Naranjo, J.R., *DREAM is a Ca2+-regulated transcriptional repressor.* Nature, 1999. **398**(6722): p. 80-4.

75. Ames, J.B., Tanaka, T., Stryer, L., and Ikura, M., *Portrait of a myristoyl switch protein.* Curr Opin Struct Biol, 1996. **6**(4): p. 432-8.

76. Gerke, V., Creutz, C.E., and Moss, S.E., *Annexins: linking Ca2+ signalling to membrane dynamics.* Nat Rev Mol Cell Biol, 2005. **6**(6): p. 449-61.

77. Gerke, V. and Moss, S.E., *Annexins: from structure to function.* Physiol Rev, 2002. **82**(2): p. 331-71.

78. Bai, J. and Chapman, E.R., *The C2 domains of synaptotagmin--partners in exocytosis.* Trends Biochem Sci, 2004. **29**(3): p. 143-51.

79. Hui, E., Bai, J., and Chapman, E.R., *Ca2+ triggered simultaneous membrane penetration of the tandem C2 domains of synaptotagmin I.* Biophys J, 2006.

80. Pallanck, L., *A tale of two C2 domains.* Trends Neurosci, 2003. **26**(1): p. 2-4.

81. Bondon, A., Tiffoche, C., Simonneaux, G., Le Pennec, J.P., and Jego, P., *A possible calcium binding site in animal lectins: a 1H-NMR study of the interaction between lanthanides and a synthetic peptide from a highly conserved domain of Pleurodeles lectin.* Biochim Biophys Acta, 1992. **1135**(1): p. 19-26.

82. Weis, W.I., Taylor, M.E., and Drickamer, K., *The C-type lectin superfamily in the immune system.* Immunol Rev, 1998. **163**: p. 19-34.

83. Kretsinger, R.H. and Nockolds, C.E., *Carp muscle calcium-binding protein. II. Structure determination and general description.* J Biol Chem, 1973. **248**(9): p. 3313-26.

84. Favier-Perron, B., Lewit-Bentley, A., and Russo-Marie, F., *The high-resolution crystal structure of human annexin III shows subtle differences with annexin V.* Biochemistry, 1996. **35**(6): p. 1740-4.

85. Cheng, Y., Sequeira, S.M., Malinina, L., Tereshko, V., Sollner, T.H., and Patel, D.J., *Crystallographic identification of Ca2+ and Sr2+ coordination sites in synaptotagmin I C2B domain.* Protein Sci, 2004. **13**(10): p. 2665-72.

86. Chazin, M.N.A.W., *The EF hand calcium binding proteins data library*.

87. Lee, C.H., Jung, J.W., Yee, A., Arrowsmith, C.H., and Lee, W., *Solution structure of a novel calcium binding protein, MTH1880, from Methanobacterium thermoautotrophicum.* Protein Sci, 2004. **13**(4): p. 1148-54.

88. Honig, A.A.R.A.B., *Reevaluation of the Born Model of Ion Hydration.* The Journal of Physical Chemistry, 1985. **89**(26): p. 5588-93.

89. Sussman, F. and Weinstein, H., *On the ion selectivity in Ca-binding proteins: the cyclo(-L-Pro-Gly-)3 peptide as a model.* Proc Natl Acad Sci U S A, 1989. **86**(20): p. 7880-4.

90. Seaton, B.A. and Dedman, J.R., *Annexins.* Biometals, 1998. **11**(4): p. 399-404.

91. Swairjo, M.A. and Seaton, B.A., *Annexin structure and membrane interactions: a molecular perspective.* Annu Rev Biophys Biomol Struct, 1994. **23**: p. 193-213.

92. Nalefski, E.A. and Falke, J.J., *The C2 domain calcium-binding motif: structural and functional diversity.* Protein Sci, 1996. **5**(12): p. 2375-90.

93. Braunewell, K.H. and Gundelfinger, E.D., *Intracellular neuronal calcium sensor proteins: a family of EF-hand calcium-binding proteins in search of a function.* Cell Tissue Res, 1999. **295**(1): p. 1-12.

94. Burgoyne, R.D. and Weiss, J.L., *The neuronal calcium sensor family of Ca2+-binding proteins.* Biochem J, 2001. **353**(Pt 1): p. 1-12.

95. R, D.B., *The neuronal calcium-sensor proteins.* Biochim Biophys Acta, 2004. **1742**(1-3): p. 59-68.

96. Baumann, U., Wu, S., Flaherty, K.M., and Mckay, D.B., *Three-dimensional structure of the alkaline protease of Pseudomonas aeruginosa: a two-domain protein with a calcium binding parallel beta roll motif.* Embo J, 1993. **12**(9): p. 3357-64.

97. Kessin, R.H. and Franke, J., *Secreted adenylate cyclase of Bordetella pertussis: calmodulin requirements and partial purification of two forms.* J Bacteriol, 1986. **166**(1): p. 290-6.

98. Lin, Y.M., Liu, Y.P., and Cheung, W.Y., *Cyclic 3':5'-nucleotide phosphodiesterase. Purification, characterization, and active form of the protein activator from bovine brain.* J Biol Chem, 1974. **249**(15): p. 4943-54.

99. Teo, T.S., Wang, T.H., and Wang, J.H., *Purification and properties of the protein activator of bovine heart cyclic adenosine 3',5'-monophosphate phosphodiesterase.* J Biol Chem, 1973. **248**(2): p. 588-95.

100. Klee, C.B., Crouch, T.H., and Krinks, M.H., *Calcineurin: a calcium- and calmodulin-binding protein of the nervous system.* Proc Natl Acad Sci U S A, 1979. **76**(12): p. 6270-3.

101. Strynadka, N.C. and James, M.N., *Crystal structures of the helix-loop-helix calcium-binding proteins.* Annu Rev Biochem, 1989. **58**: p. 951-98.

102. Herzberg, O., Moult, J., and James, M.N., *Calcium binding to skeletal muscle troponin C and the regulation of muscle contraction.* Ciba Found Symp, 1986. **122**: p. 120-44.

103. Santamaria-Kisiel, L., Rintala-Dempsey, A.C., and Shaw, G.S., *Calcium-dependent and -independent interactions of the S100 protein family.* Biochem J, 2006. **396**(2): p. 201-14.

104. Yap, K.L., Ames, J.B., Swindells, M.B., and Ikura, M., *Diversity of conformational states and changes within the EF-hand protein superfamily.* Proteins, 1999. **37**(3): p. 499-507.

105. Hook, S.S. and Means, A.R., *Ca(2+)/CaM-dependent kinases: from activation to function.* Annu Rev Pharmacol Toxicol, 2001. **41**: p. 471-505.

106. Saijo, K., Mecklenbrauker, I., Santana, A., Leitger, M., Schmedt, C., and Tarakhovsky, A., *Protein kinase C beta controls nuclear factor kappaB activation in B cells through selective regulation of the IkappaB kinase alpha.* J Exp Med, 2002. **195**(12): p. 1647-52.

107. Spitaler, M. and Cantrell, D.A., *Protein kinase C and beyond.* Nat Immunol, 2004. **5**(8): p. 785-90.

108. Cruzalegui, F.H. and Bading, H., *Calcium-regulated protein kinase cascades and their transcription factor targets.* Cell Mol Life Sci, 2000. **57**(3): p. 402-10.

109. Sun, L., Youn, H.D., Loh, C., Stolow, M., He, W., and Liu, J.O., *Cabin 1, a negative regulator for calcineurin signaling in T lymphocytes.* Immunity, 1998. **8**(6): p. 703-11.

110. Saarikettu, J., Sveshnikova, N., and Grundstrom, T., *Calcium/calmodulin inhibition of transcriptional activity of E-proteins by prevention of their binding to DNA.* J Biol Chem, 2004. **279**(39): p. 41004-11.

111. Mayr, B. and Montminy, M., *Transcriptional regulation by the phosphorylation-dependent factor CREB.* Nat Rev Mol Cell Biol, 2001. **2**(8): p. 599-609.

112. Enslen, H., Tokumitsu, H., Stork, P.J., Davis, R.J., and Soderling, T.R., *Regulation of mitogen-activated protein kinases by a calcium/calmodulin-dependent protein kinase cascade.* Proc Natl Acad Sci U S A, 1996. **93**(20): p. 10803-8.

113. Cheng, H.Y., Pitcher, G.M., Laviolette, S.R., Whishaw, I.Q., Tong, K.I., Ikura, M., Salter, M.W., and Penninger, J.M., *DREAM is a critical transcriptional repressor for pain modulation.* Cell, 2002. **108**(1): p. 31-43.

114. Carrion, A.M., Mellstrom, B., and Naranjo, J.R., *Protein kinase A-dependent derepression of the human prodynorphin gene via differential binding to an intragenic silencer element.* Mol Cell Biol, 1998. **18**(12): p. 6921-9.

115. Link, W.A., Ledo, F., Torres, B., Palczewska, M., Madsen, T.M., Savignac, M., Albar, J.P., Mellstrom, B., and Naranjo, J.R., *Day-night changes in downstream regulatory element antagonist modulator/potassium channel interacting protein activity contribute to circadian gene expression in pineal gland.* J Neurosci, 2004. **24**(23): p. 5346-55.

116. Gilchrist, C.A., Leo, M., Line, C.G., Mann, B.J., and Petri, W.A., Jr., *Calcium modulates promoter occupancy by the Entamoeba histolytica Ca2+-binding transcription factor URE3-BP.* J Biol Chem, 2003. **278**(7): p. 4646-53.

117. Hamasaki-Katagiri, N., Molchanova, T., Takeda, K., and Ames, J.B., *Fission yeast homolog of neuronal calcium sensor-1 (Ncs1p) regulates sporulation and confers calcium tolerance.* J Biol Chem, 2004. **279**(13): p. 12744-54.

118. Sanz, C., Mellstrom, B., Link, W.A., Naranjo, J.R., and Fernandez-Luna, J.L., *Interleukin 3-dependent activation of DREAM is involved in transcriptional silencing of the apoptotic Hrk gene in hematopoietic progenitor cells.* Embo J, 2001. **20**(9): p. 2286-92.

119. Matsuda, M., Yamamoto, T.A., and Hirata, M., *Ca2+-Dependent Regulation of Calcitonin Gene Expression by the Transcriptional Repressor DREAM.* Endocrinology, 2006.

120. D'andrea, B., Di Palma, T., Mascia, A., Motti, M.L., Viglietto, G., Nitsch, L., and Zannini, M., *The transcriptional repressor DREAM is involved in thyroid gene expression.* Exp Cell Res, 2005. **305**(1): p. 166-78.

121. Jacobson, D.A., Cho, J., Landa, L.R., Tamarina, N.A., Roe, M.W., Buxbaum, J.D., and Philipson, L.H., *The Downstream Regulatory Element Antagonistic Modulator Regulates Islet Prodynorphin Expression.* Am J Physiol Endocrinol Metab, 2006.

122. Gomez-Villafuertes, R., Torres, B., Barrio, J., Savignac, M., Gabellini, N., Rizzato, F., Pintado, B., Gutierrez-Adan, A., Mellstrom, B., Carafoli, E., and Naranjo, J.R., *Downstream regulatory element antagonist modulator regulates Ca2+ homeostasis and viability in cerebellar neurons.* J Neurosci, 2005. **25**(47): p. 10822-30.

123. Osawa, M., Dace, A., Tong, K.I., Valiveti, A., Ikura, M., and Ames, J.B., *Mg2+ and Ca2+ differentially regulate DNA binding and dimerization of DREAM.* J Biol Chem, 2005. **280**(18): p. 18008-14.

124. Zaidi, N.F., Kuplast, K.G., Washicosky, K.J., Kajiwara, Y., Buxbaum, J.D., and Wasco, W., *Calsenilin interacts with transcriptional co-repressor C-terminal binding protein(s).* J Neurochem, 2006.

125. Scsucova, S., Palacios, D., Savignac, M., Mellstrom, B., Naranjo, J.R., and Aranda, A., *The repressor DREAM acts as a transcriptional activator on Vitamin D and retinoic acid response elements.* Nucleic Acids Res, 2005. **33**(7): p. 2269-79.

126. Flaherty, K.M., Zozulya, S., Stryer, L., and Mckay, D.B., *Three-dimensional structure of recoverin, a calcium sensor in vision.* Cell, 1993. **75**(4): p. 709-16.

127. Vijay-Kumar, S. and Kumar, V.D., *Crystal structure of recombinant bovine neurocalcin.* Nature Struct. Biol., 1999. **6**: p. 80-88.

128. Zhou, W., Qian, Y., Kunjilwar, K., Pfaffinger, P.J., and Choe, S., *Structural insights into the functional interaction of KChIP1 with Shal-type K(+) channels.* Neuron, 2004. **41**(4): p. 573-86.

129. Da Silva, A.C., Kendrick-Jones, J., and Reinach, F.C., *Determinants of ion specificity on EF-hands sites. Conversion of the Ca2+/Mg2+ site of smooth muscle myosin regulatory light chain into a Ca(2+)-specific site.* J Biol Chem, 1995. **270**(12): p. 6773-8.

130. Osawa, M., Tong, K.I., Lilliehook, C., Wasco, W., Buxbaum, J.D., Cheng, H.Y., Penninger, J.M., Ikura, M., and Ames, J.B., *Calcium-regulated DNA binding and oligomerization of the neuronal calcium-sensing protein, calsenilin/DREAM/KChIP3.* J Biol Chem, 2001. **276**(44): p. 41005-13.

131. Ledo, F., Kremer, L., Mellstrom, B., and Naranjo, J.R., *Ca2+-dependent block of CREB-CBP transcription by repressor DREAM.* EMBO J., 2002. **21**(17): p. 4583-4592.

132. Buxbaum, J.D., Choi, E.K., Luo, Y., Lilliehook, C., Crowley, A.C., Merriam, D.E., and Wasco, W., *Calsenilin: a calcium-binding protein that interacts with the presenilins and regulates the levels of a presenilin fragment.* Nat Med, 1998. **4**(10): p. 1177-81.

133. Jo, D.G., Kim, M.J., Choi, Y.H., Kim, I.K., Song, Y.H., Woo, H.N., Chung, C.W., and Jung, Y.K., *Pro-apoptotic function of calsenilin/DREAM/KChIP3.* Faseb J, 2001. **15**(3): p. 589-91.

134. Jo, D.G., Lee, J.Y., Hong, Y.M., Song, S., Mook-Jung, I., Koh, J.Y., and Jung, Y.K., *Induction of pro-apoptotic calsenilin/DREAM/KChIP3 in Alzheimer's disease and cultured neurons after amyloid-beta exposure.* J Neurochem, 2004. **88**(3): p. 604-11.

135. Bourne, Y., Dannenberg, J., Pollmann, V., Marchot, P., and Pongs, O., *Immunocytochemical localization and crystal structure of human frequenin (neuronal calcium sensor 1).* J Biol Chem, 2001. **276**(15): p. 11949-55.

136. Zaidi, N.F., Berezovska, O., Choi, E.K., Miller, J.S., Chan, H., Lilliehook, C., Hyman, B.T., Buxbaum, J.D., and Wasco, W., *Biochemical and immunocytochemical characterization of calsenilin in mouse brain.* Neuroscience, 2002. **114**(1): p. 247-63.

137. Choi, E.K., Zaidi, N.F., Miller, J.S., Crowley, A.C., Merriam, D.E., Lilliehook, C., Buxbaum, J.D., and Wasco, W., *Calsenilin is a substrate for caspase-3 that preferentially interacts with the familial Alzheimer's disease-associated C-terminal fragment of presenilin 2.* J Biol Chem, 2001. **276**(22): p. 19197-204.

138. Morgan, D.O., *Principles of CDK regulation.* Nature, 1995. **374**(6518): p. 131-4.

139. Shah, S., Pishvaian, M.J., Easwaran, V., Brown, P.H., and Byers, S.W., *The role of cadherin, beta-catenin, and AP-1 in retinoid-regulated carcinoma cell differentiation and proliferation.* J Biol Chem, 2002. **277**(28): p. 25313-22.

140. Damalas, A., Kahan, S., Shtutman, M., Ben-Ze'ev, A., and Oren, M., *Deregulated beta-catenin induces a p53- and ARF-dependent growth arrest and cooperates with Ras in transformation.* Embo J, 2001. **20**(17): p. 4912-22.

141. Zaidi, N.F., Thomson, E.E., Choi, E.K., Buxbaum, J.D., and Wasco, W., *Intracellular calcium modulates the nuclear translocation of calsenilin.* J Neurochem, 2004. **89**(3): p. 593-601.

142. Ledo, F., Carrion, A.M., Link, W.A., Mellstrom, B., and Naranjo, J.R., *DREAM-alphaCREM interaction via leucine-charged domains derepresses downstream regulatory element-dependent transcription.* Mol Cell Biol, 2000. **20**(24): p. 9120-6.

143. Eferl, R. and Wagner, E.F., *AP-1: a double-edged sword in tumorigenesis.* Nat Rev Cancer, 2003. **3**(11): p. 859-68.

144. Focking, M., Holker, I., and Trapp, T., *Chronic glucocorticoid receptor activation impairs CREB transcriptional activity in clonal neurons.* Biochem Biophys Res Commun, 2003. **304**(4): p. 720-3.

145. Lilliehook, C., Bozdagi, O., Yao, J., Gomez-Ramirez, M., Zaidi, N.F., Wasco, W., Gandy, S., Santucci, A.C., Haroutunian, V., Huntley, G.W., and Buxbaum, J.D., *Altered Abeta formation and long-term potentiation in a calsenilin knock-out.* J Neurosci, 2003. **23**(27): p. 9097-106.

146. Wickenden, A.D., Lee, P., Sah, R., Huang, Q., Fishman, G.I., and Backx, P.H., *Targeted expression of a dominant-negative K(v)4.2 K(+) channel subunit in the mouse heart.* Circ Res, 1999. **85**(11): p. 1067-76.

147. Kuo, H.C., Cheng, C.F., Clark, R.B., Lin, J.J., Lin, J.L., Hoshijima, M., Nguyen-Tran, V.T., Gu, Y., Ikeda, Y., Chu, P.H., Ross, J., Giles, W.R., and Chien, K.R., *A defect in the Kv channel-interacting protein 2 (KChIP2) gene leads to a complete loss of I(to) and confers susceptibility to ventricular tachycardia.* Cell, 2001. **107**(6): p. 801-13.

148. Malenka, R.C. and Nicoll, R.A., *Long-term potentiation--a decade of progress?* Science, 1999. **285**(5435): p. 1870-4.

149. Amberg, G.C., Koh, S.D., Imaizumi, Y., Ohya, S., and Sanders, K.M., *A-type potassium currents in smooth muscle.* Am J Physiol Cell Physiol, 2003. **284**(3): p. C583-95.

150. Przewlocki, R. and Przewlocka, B., *Opioids in chronic pain.* Eur J Pharmacol, 2001. **429**(1-3): p. 79-91.

151. Costigan, M. and Woolf, C.J., *No DREAM, No pain. Closing the spinal gate.* Cell, 2002. **108**(3): p. 297-300.

152. Zachariou, V. and Goldstein, B.D., *Dynorphin-(1-8) inhibits the release of substance P-like immunoreactivity in the spinal cord of rats following a noxious mechanical stimulus.* Eur J Pharmacol, 1997. **323**(2-3): p. 159-65.

153. Brodersen, D., *Understanding the structure and regulation of the S100-proteins*, in *Institute of Molecular and Structural Biology*. 1999, University of Aarhus.

154. Rupp, B., *Protein Structure Basics*, in *http://ruppweb.dyndns.org/Xray/tutorial/protein_structure.htm*, E. hand, Editor. August 09, 2000.

155. Moncrief, N.D., Kretsinger, R.H., and Goodman, M., *Evolution of EF-hand calcium-modulated proteins. I. Relationships based on amino acid sequences.* J Mol Evol, 1990. **30**(6): p. 522-62.

156. Olshevskaya, E.V., Ermilov, A.N., and Dizhoor, A.M., *Dimerization of guanylyl cyclase-activating protein and a mechanism of photoreceptor guanylyl cyclase activation.* J Biol Chem, 1999. **274**(36): p. 25583-7.

157. Muralidhar, D., Kunjachen Jobby, M., Jeromin, A., Roder, J., Thomas, F., and Sharma, Y., *Calcium and chlorpromazine binding to the EF-hand peptides of neuronal calcium sensor-1.* Peptides, 2004. **25**(6): p. 909-17.

158. Drake, S.K., Zimmer, M.A., Kundrot, C., and Falke, J.J., *Molecular tuning of an EF-hand-like calcium binding loop. Contributions of the coordinating side chain at loop position 3.* J Gen Physiol, 1997. **110**(2): p. 173-84.

159. Drake, S.K., Zimmer, M.A., Miller, C.L., and Falke, J.J., *Optimizing the metal binding parameters of an EF-hand-like calcium chelation loop: coordinating side chains play a more important tuning role than chelation loop flexibility.* Biochemistry, 1997. **36**(32): p. 9917-26.

160. Blumenschein, T.M. and Reinach, F.C., *Analysis of affinity and specificity in an EF-hand site using double mutant cycles.* Biochemistry, 2000. **39**(13): p. 3603-10.

161. Cates, M.S., Teodoro, M.L., and Phillips, G.N., Jr., *Molecular mechanisms of calcium and magnesium binding to parvalbumin.* Biophys J, 2002. **82**(3): p. 1133-46.

162. Finley, N.L., Howarth, J.W., and Rosevear, P.R., *Structure of the Mg2+-loaded C-lobe of cardiac troponin C bound to the N-domain of cardiac troponin I: comparison with the Ca2+-loaded structure.* Biochemistry, 2004. **43**(36): p. 11371-9.

163. Fujise, H., Cruz, P., Reo, N.V., and Lauf, P.K., *Relationship between total magnesium concentration and free intracellular magnesium in sheep red blood cells.* Biochim Biophys Acta, 1991. **1094**(1): p. 51-4.

164. Cox, J.A., Durussel, I., Comte, M., Nef, S., Nef, P., Lenz, S.E., and Gundelfinger, E.D., *Cation binding and conformational changes in VILIP and NCS-1, two neuron-specific calcium-binding proteins.* J Biol Chem, 1994. **269**(52): p. 32807-13.

165. Wingard, J.N., Chan, J., Bosanac, I., Haeseleer, F., Palczewski, K., Ikura, M., and Ames, J.B., *Structural analysis of Mg2+ and Ca2+ binding to CaBP1, a neuron-specific regulator of calcium channels.* J Biol Chem, 2005. **280**(45): p. 37461-70.

166. Pauls, T.L., Durussel, I., Cox, J.A., Clark, I.D., Szabo, A.G., Gagne, S.M., Sykes, B.D., and Berchtold, M.W., *Metal binding properties of recombinant rat*

parvalbumin wild-type and F102W mutant. J Biol Chem, 1993. **268**(28): p. 20897-903.

167. Haiech, J., Derancourt, J., Pechere, J.F., and Demaille, J.G., *Magnesium and calcium binding to parvalbumins: evidence for differences between parvalbumins and an explanation of their relaxing function.* Biochemistry, 1979. **18**(13): p. 2752-8.

168. Peshenko, I.V. and Dizhoor, A.M., *Ca2+- and Mg2+-binding properties of GCAP-1: Evidence that Mg2+-bound form is the physiological activator of photoreceptor guanylyl cyclase.* J Biol Chem, 2006.

169. Peshenko, I.V. and Dizhoor, A.M., *Guanylyl cyclase-activating proteins (GCAPs) are Ca2+/Mg2+ sensors: implications for photoreceptor guanylyl cyclase (RetGC) regulation in mammalian photoreceptors.* J Biol Chem, 2004. **279**(17): p. 16903-6.

170. Hutschenreiter, S., Neumann, L., Radler, U., Schmitt, L., and Tampe, R., *Metal-chelating amino acids as building blocks for synthetic receptors sensing metal ions and histidine-tagged proteins.* Chembiochem, 2003. **4**(12): p. 1340-4.

171. Wiseman, T., Williston, S., Brandts, J.F., and Lin, L.N., *Rapid measurement of binding constants and heats of binding using a new titration calorimeter.* Anal Biochem, 1989. **179**(1): p. 131-7.

172. Schwarz, F.P., Puri, K.D., Bhat, R.G., and Surolia, A., *Thermodynamics of monosaccharide binding to concanavalin A, pea (Pisum sativum) lectin, and lentil (Lens culinaris) lectin.* J Biol Chem, 1993. **268**(11): p. 7668-77.

173. Craig, T.A., Benson, L.M., Venyaminov, S.Y., Klimtchuk, E.S., Bajzer, Z., Prendergast, F.G., Naylor, S., and Kumar, R., *The metal-binding properties of DREAM: evidence for calcium-mediated changes in DREAM structure.* J Biol Chem, 2002. **277**(13): p. 10955-66.

174. Ames, J.B., Hamasaki, N., and Molchanova, T., *Structure and calcium-binding studies of a recoverin mutant (E85Q) in an allosteric intermediate state.* Biochemistry, 2002. **41**(18): p. 5776-87.

175. Gilli, R., Lafitte, D., Lopez, C., Kilhoffer, M., Makarov, A., Briand, C., and Haiech, J., *Thermodynamic analysis of calcium and magnesium binding to calmodulin.* Biochemistry, 1998. **37**(16): p. 5450-6.

176. Maune, J.F., Klee, C.B., and Beckingham, K., *Ca2+ binding and conformational change in two series of point mutations to the individual Ca(2+)-binding sites of calmodulin.* J Biol Chem, 1992. **267**(8): p. 5286-95.

177. Yamniuk, A.P., Nguyen, L.T., Hoang, T.T., and Vogel, H.J., *Metal ion binding properties and conformational states of calcium- and integrin-binding protein.* Biochemistry, 2004. **43**(9): p. 2558-68.

178. Henzl, M.T., Larson, J.D., and Agah, S., *Estimation of parvalbumin Ca(2+)- and Mg(2+)-binding constants by global least-squares analysis of isothermal titration calorimetry data.* Anal Biochem, 2003. **319**(2): p. 216-33.

179. Ledo, F., Link, W.A., Carrion, A.M., Echeverria, V., Mellstrom, B., and Naranjo, J.R., *The DREAM-DRE interaction: key nucleotides and dominant negative mutants.* Biochim Biophys Acta, 2000. **1498**(2-3): p. 162-8.

180. Raumann, B.E., Rould, M.A., Pabo, C.O., and Sauer, R.T., *DNA recognition by beta-sheets in the Arc repressor-operator crystal structure.* Nature, 1994. **367**(6465): p. 754-7.

181. Mclure, K.G. and Lee, P.W., *How p53 binds DNA as a tetramer.* Embo J, 1998. **17**(12): p. 3342-50.

182. White, A., Ding, X., Vanderspek, J.C., Murphy, J.R., and Ringe, D., *Structure of the metal-ion-activated diphtheria toxin repressor/tox operator complex.* Nature, 1998. **394**(6692): p. 502-6.

183. Fields, S. and Song, O., *A novel genetic system to detect protein-protein interactions.* Nature, 1989. **340**(6230): p. 245-6.

184. Pugh, B.F. and Gilmour, D.S., *Genome-wide analysis of protein-DNA interactions in living cells.* Genome Biol, 2001. **2**(4): p. REVIEWS1013.

185. Brickwood, S.J., Myers, F.A., and Chandler, S.P., *Methods for the analysis of protein-chromatin interactions.* Mol Biotechnol, 2002. **20**(1): p. 1-15.

186. Guille, M.J. and Kneale, G.G., *Methods for the analysis of DNA-protein interactions.* Mol Biotechnol, 1997. **8**(1): p. 35-52.

187. Potier, N., Donald, L.J., Chernushevich, I., Ayed, A., Ens, W., Arrowsmith, C.H., Standing, K.G., and Duckworth, H.W., *Study of a noncovalent trp repressor: DNA operator complex by electrospray ionization time-of-flight mass spectrometry.* Protein Sci, 1998. **7**(6): p. 1388-95.

188. Geyer, H., Geyer, R., and Pingoud, V., *A novel strategy for the identification of protein-DNA contacts by photocrosslinking and mass spectrometry.* Nucleic Acids Res, 2004. **32**(16): p. e132.

189. Tang, Y., Chen, Y., Lichti, C.F., Hall, R.A., Raney, K.D., and Jennings, S.F., *CLPM: a cross-linked peptide mapping algorithm for mass spectrometric analysis.* BMC Bioinformatics, 2005. **6 Suppl 2**: p. S9.

190. Beyaert., W.V.C.A.R., *Yeast Two-Hybrid: State of the Art.* Biol. Proced. Online, 1999. **2**: p. 1-38.

191. Drees, B.L., *Progress and variations in two-hybrid and three-hybrid technologies.* Curr Opin Chem Biol, 1999. **3**(1): p. 64-70.

192. Coates, P.J. and Hall, P.A., *The yeast two-hybrid system for identifying protein-protein interactions.* J Pathol, 2003. **199**(1): p. 4-7.

193. Adam, P.J., Regan, C.P., Hautmann, M.B., and Owens, G.K., *Positive- and negative-acting Kruppel-like transcription factors bind a transforming growth factor beta control element required for expression of the smooth muscle cell differentiation marker SM22alpha in vivo.* J Biol Chem, 2000. **275**(48): p. 37798-806.

194. Gonzalez, A., Bazaldua-Hernandez, C., West, M., Woytek, K., and Wilson, V.G., *Identification of a short, hydrophilic amino acid sequence critical for origin recognition by the bovine papillomavirus E1 protein.* J Virol, 2000. **74**(1): p. 245-53.

195. Clontech, *MATCHMAKER Vectors*. 2006.

196. Listed, N.A., in *http://proteome.wayne.edu/vectorsandstrains/pJG4-5.jpg*, pJG4-5, Editor.

197. Manual, U., *Yeast protocols handbook*. 2001: Clontech.

198. Roodyn, D.B. and Wilkie, D., *A characteristic pattern of respiratory enzymes in cytoplasmic 'petite' strains of Saccharomyces cerevisiae as revealed by multiple enzyme analysis.* Biochem J, 1967. **103**(1): p. 3contd-5c.

199. Manfredi, J., *Yeast two-hybrid system and use thereof*. 2003, Myriad Genetics, Inc. (Salt Lake City, UT): United States.

200. Klopotowski, T. and Wiater, A., *Synergism of aminotriazole and phosphate on the inhibition of yeast imidazole glycerol phosphate dehydratase.* Arch Biochem Biophys, 1965. **112**(3): p. 562-6.

201. Mattanovich, D., Gasser, B., Hohenblum, H., and Sauer, M., *Stress in recombinant protein producing yeasts.* J Biotechnol, 2004. **113**(1-3): p. 121-35.

202. Van Criekinge, W. and Beyaert, R., *Yeast Two-Hybrid: State of the Art.* Biol Proced Online, 1999. **2**: p. 1-38.

203. Murre, C., Mccaw, P.S., and Baltimore, D., *A new DNA binding and dimerization motif in immunoglobulin enhancer binding, daughterless, MyoD, and myc proteins.* Cell, 1989. **56**(5): p. 777-83.

204. Wintjens, R. and Rooman, M., *Structural classification of HTH DNA-binding domains and protein-DNA interaction modes.* J Mol Biol, 1996. **262**(2): p. 294-313.

205. Struhl, K., *Helix-turn-helix, zinc-finger, and leucine-zipper motifs for eukaryotic transcriptional regulatory proteins.* Trends Biochem Sci, 1989. **14**(4): p. 137-40.

206. Takeda, Y., Sarai, A., and Rivera, V.M., *Analysis of the sequence-specific interactions between Cro repressor and operator DNA by systematic base substitution experiments.* Proc Natl Acad Sci U S A, 1989. **86**(2): p. 439-43.

207. Travers, A., *DNA-protein interactions: IHF--the master bender.* Curr Biol, 1997. **7**(4): p. R252-4.

208. Chen, S., Gunasekera, A., Zhang, X., Kunkel, T.A., Ebright, R.H., and Berman, H.M., *Indirect readout of DNA sequence at the primary-kink site in the CAP-DNA complex: alteration of DNA binding specificity through alteration of DNA kinking.* J Mol Biol, 2001. **314**(1): p. 75-82.

209. Ray, S., Zozulya, S., Niemi, G.A., Flaherty, K.M., Brolley, D., Dizhoor, A.M., Mckay, D.B., Hurley, J., and Stryer, L., *Cloning, expression, and crystallization of recoverin, a calcium sensor in vision.* Proc Natl Acad Sci U S A, 1992. **89**(13): p. 5705-9.

210. Ames, J.B., Tanaka, T., Stryer, L., and Ikura, M., *Secondary structure of myristoylated recoverin determined by three-dimensional heteronuclear NMR: implications for the calcium-myristoyl switch.* Biochemistry, 1994. **33**(35): p. 10743-53.

211. Retzer, M.D., Kabani, A., Button, L.L., Yu, R.H., and Schryvers, A.B., *Production and characterization of chimeric transferrins for the determination of the binding domains for bacterial transferrin receptors.* J Biol Chem, 1996. **271**(2): p. 1166-73.

212. Prusiner, S.B., *Prions.* Proc Natl Acad Sci U S A, 1998. **95**(23): p. 13363-83.